

**Innate immune genes in the zebrafish,
*Danio rerio***

Inaugural-Dissertation

zur

Erlangung des Doktorgrades
der Mathematisch-Naturwissenschaftlichen Fakultät
der Universität zu Köln

vorgelegt von

Cornelia Stein

aus Köln

Köln, 2011

Berichterstatter: Prof. Dr. rer. nat. M. Leptin

und

Prof. Dr. rer. nat. S. Roth

Tag der mündlichen Prüfung: 01.02.2010

Table of Contents

ABBREVIATIONS	V
1 INTRODUCTION	1
1.1 INNATE AND ADAPTIVE IMMUNITY	1
1.1.1 Evolution of immune genes in vertebrates	1
1.2 CELLS OF THE IMMUNE SYSTEM IN ZEBRAFISH	2
1.2.1 Development of immune cells in the zebrafish	4
1.3 THE INNATE IMMUNE SYSTEM IN ZEBRAFISH EMBRYOS	6
1.4 CELLULAR INNATE IMMUNE MECHANISMS	7
1.4.1 TLR mediated signaling	8
1.4.2 RLR mediated signaling	10
1.4.3 NLR mediated signaling	12
1.4.3.1 The NACHT domain	12
1.4.3.2 Ligand sensing mediated by LRRs	14
1.4.3.3 Effector domains and downstream signaling	15
1.4.4 Interferon signaling	17
1.5 AIMS	18
2 MATERIAL AND METHODS	19
2.1 MATERIAL	19
2.1.1 Solutions and buffers	19
2.1.2 Cells and Plasmids	20
2.1.3 Oligonucleotides	21
2.1.3.1 Oligos to generate PCR products for UTR-GFP morpholino controls	23
2.1.4 Morpholino oligonucleotides	23
2.1.5 Software	23
2.1.6 Sequences used in the phylogenetic analysis	24
2.2 METHODS	24
2.2.1 Zebrafish methods	24
2.2.1.1 Keeping and raising zebrafish	24
2.2.1.1.1 Origin of zebrafish	24
2.2.1.1.2 Growth conditions	24
2.2.1.1.3 Zebrafish embryos	25
2.2.1.1.4 Staging of embryos and larvae	25

TABLE OF CONTENTS

2.2.1.2	Anesthetization of embryos, larvae and adults	25
2.2.1.3	PTU treatment to prevent pigmentation	25
2.2.1.4	Lateral line labeling with 4-di-2-Asp	25
2.2.1.5	Mechanical dechorionisation of embryos.....	26
2.2.1.6	Fixation and storage of zebrafish embryos.....	26
2.2.1.7	In situ hybridization of whole embryos.....	26
2.2.1.7.1	Prehybridisation	26
2.2.1.7.2	Hybridisation	26
2.2.1.7.3.	Washing Steps.....	26
2.2.1.7.4	Antibody incubation.....	27
2.2.1.7.5	Color substrate reaction.....	27
2.2.1.7.6	Analyzing whole-mount embryos	27
2.2.1.8	Infection assays	27
2.2.1.8.1	Incubation method	27
2.2.1.8.2	Infection method	27
2.2.2	Molecular biology protocols	28
2.2.2.1	Polymerase chain reaction (PCR).....	28
2.2.2.2	PCR with double stranded (ds) DNA as template.....	28
2.2.2.3	PCR with first strand synthesis as template.....	28
2.2.2.4	PCR with genomic DNA as template	29
2.2.3	Agarose gel electrophoresis	29
2.2.4	Extraction of PCR fragments from agarose gels (Gelextraction).....	29
2.2.5	Restriction enzyme digestion of DNA.....	29
2.2.6	Phenol-Chloroform Extraction and Ethanol precipitation.....	30
2.2.7	Ligation	30
2.2.8	Transformation of bacteria cells	30
2.2.9	Growing of Escherichia coli	31
2.2.10	Minipreparation of plasmid DNA.....	31
2.2.11	DNase-free RNase	31
2.2.12	Sequencing of DNA.....	31
2.2.13	in vitro transcription to produce in situ probes.....	32
2.2.14	Injection of morpholino oligonucleotides and mRNA into zebrafish embryos.....	32
2.2.14.1	Preparation of capped mRNA for zebrafish injections	32
2.2.14.2	Morpholino design.....	32
2.2.14.3	Injection of zebrafish embryos	33
2.2.14.4	Isolation of genomic DANN.....	33

2.2.14.5	RNA isolation and first-strand synthesis (RT).....	33
2.2.14.6	Quantification of DNA or RNA by spectrophotometric determination ...	34
2.2.14.7	Bacterial strains used for infections	34
2.3	PHYLOGENETIC ANALYSIS.....	34
3	RESULTS	36
3.1	<i>IN SILICO</i> ANALYSIS OF INNATE IMMUNE GENES IN THE ZEBRAFISH	36
3.1.1	Conserved protein families in mammals and fish	37
3.1.1.1	Adaptor proteins.....	37
3.1.1.2	Kinases	38
3.1.1.3	Interferon regulatory factors (IRFs).....	41
3.1.1.4	Signal transducers and activators of transcription (STATs).....	43
3.1.1.5	TNF-receptor associated factors (TRAFs).....	45
3.1.2	Divergent protein families: the class II cytokines.....	47
3.1.3	Divergent protein families: the class II cytokine receptors.....	52
3.1.4	Divergent protein families: the NLR proteins	56
3.1.4.1	NLR protein families in mammals and fish.....	59
3.1.4.2	Fish-specific NLR proteins	62
3.2	<i>IN VIVO</i> ANALYSIS OF INNATE IMMUNE GENES IN THE ZEBRAFISH	70
3.2.1	Infection of zebrafish embryos.....	70
3.2.1.1	Infection of zebrafish embryos by co-incubation.....	70
3.2.1.2	Infection of zebrafish embryos by microinjection	76
3.2.2	Functional characterization of <i>ifnγ</i> genes and potential target genes.....	77
3.2.2.1	<i>Ifnγ</i> target genes in the zebrafish.....	78
3.2.2.2	Effects of altered <i>ifnγ</i> expression during bacterial infection.....	80
3.2.3	Analysis of genes encoding putative IFN γ receptor chains.....	83
3.2.3.1	Sequence analysis of putative IFN γ receptor chains	83
3.2.3.2	Morpholino mediated knockdown of putative IFN γ receptor chains.....	84
3.2.3.3	<i>crfb13</i> knockdown during bacterial infection	92
3.2.4	Conserved NLR proteins in the zebrafish.....	95
3.2.4.1	Characterization of the <i>nwd1/NACHT-P1</i> gene.....	96
4	DISCUSSION.....	101
4.1	<i>IN SILICO</i> ANALYSIS OF INNATE IMMUNE GENES	101
4.1.1	Protein families with largely conserved orthology.....	101
4.1.2	Divergent protein families	104
4.2	<i>IN VIVO</i> ANALYSIS OF INNATE IMMUNE GENES.....	106

TABLE OF CONTENTS

4.2.1	Infection assays.....	106
4.2.2	Functional characterization of ifny genes and potential target genes.....	106
4.2.3	Putative Ifny receptor genes.....	107
4.2.4	The <i>nwd1/NACHT-P1</i> gene.....	109
5	ABSTRACT	110
6	ZUSAMMENFASSUNG.....	112
7	REFERENCES	114
8	APPENDIX	132
	DANKE	136
	ERKLÄRUNG UND TEILPUBLIKATIONEN.....	137
	LEBENS LAUF	138

Abbreviations

aa	amino acid
AGM	aorta-gonad-mesonephros
ALM	anterior lateral mesoderm
Amp	ampicillin
AP-1	activator protein-1
APAF1	apoptotic protease activating factor 1
ASC	apoptosis-associated speck-like protein containing a CARD
BCR	B cell antigen receptor
BIR	baculoviral inhibitor of apoptosis repeat
Birc1	BIR-containing protein 1
BMP	bone morphogenetic protein
bp	base pairs
C2 domain	Ca ²⁺ -dependent membrane-targeting domain
CIITA	major histocompatibility complex, class II, transactivator
CARD	caspase recruitment domain
Cardif	CARD adaptor inducing IFN β , also called IPS-1
cDNA	copy DNA
cfu	colony forming unit
CHOP	C/EBP-homologous protein
CHT	caudal hematopoietic tissue
CRF2	class II cytokine receptor family
CRFB	piscine class II cytokine receptor family
CUE domain	coupling of ubiquitin conjugation to ER degradation domain
DAP	DNAX-activation protein
dpf	days post fertilization
dpi	days post infection
Dr	<i>Danio rerio</i>
dsDNA	double-stranded DNA
dsRNA	double-stranded RNA
ER	endoplasmic reticulum
ERK1/2	extracellular signal-regulated kinase 1/2
EST	expressed sequence tag
F3	coagulation factor III, also known as tissue factor
FADD	Fas-associated death domain protein

Fgf	fibroblast growth factor
GBP	guanylate-binding protein
Fisna	Fish-specific NACHT associated domain
FNIII	fibronectin type III domain
Fr	<i>Takifugu rubripes</i>
GRC	Genome Reference Consortium
HMM	hidden markov model
HSC	hematopoietic stem cell
hpf	hours post fertilization
hpi	hours post infection
Hs	<i>Homo sapiens</i>
ICM	intermediate cell mass
IFN	interferon
IFNR	interferon receptor
Ig	immunoglobulin
IKAP	IKK complex associated protein
IκB	inhibitor of NFκB
IKI3	insensitive to killer toxin domain
IKK	IκB kinase
IL	interleukin
IL22BP	interleukin 22 binding protein
IL-R	interleukin receptor
IPAF	IL-1β-converting enzyme protease-activating factor
IPS-1	IFNβ promoter stimulator-1
IRAK	IL-1R-associated kinase
IRG	immunity-related GTPase
IRF	IFN regulatory factor
ISRE	IFN-stimulated response element
JAK	Janus kinase
JNK	c-jun N-terminal kinase
KIR	killer immunoglobulin-like receptors
LGP2	laboratory of genetics and physiology 2
LRR	leucine-rich repeats
LPS	lipopolysaccharide
MAL	MyD-adaptor-alike, also called TIRAP
MAP	mitogen-activated protein
MAPK	mitogen-activated protein kinase

MAVS	mitochondrial antiviral signaling protein, also called IPS-1
MATH	meprip and TRAF homology domain
MEKK3	mitogen-activated protein kinase kinase kinase 3
MDA5	melanoma differentiation associated gene 5
MITA	mediator of IRF3 activation
MHC	major histocompatibility complex
Mm	<i>Mus musculus</i>
mRNA	messenger RNA
Mo	antisense morpholino oligonucleotide
MyD88	myeloid differentiation primary response gene 88
Mx	myxovirus resistant protein
NAIP	neuronal apoptosis inhibitory protein
NALP	NACHT-LRR-PYD-containing protein
NACHT	NTPase domain found in Naip, CIITA, HET-E and TP1
NB-ARC	nucleotide-binding domain shared by Apaf1, certain plant R gene products and nematode CED-4
NB-LRR	plant nucleotide binding site, leucine-rich repeat protein
NCC	non-specific cytotoxic cells
NEMO	NFκB essential modifier
NFκB	nuclear factor kappa B
NITR	novel immune-type receptors
NK cell	natural killer cell
NKGD2	natural killer (NK) receptor group 2D
NLK	NFκB essential modulator-like kinase
NLR	nucleotide-binding domain, leucine-rich repeat containing family of proteins
NOD	nucleotide-binding oligomerization domain containing protein
ORF	open reading frame
PAMPs	pathogen-associated molecular patterns
PBS	phosphate buffered saline
PCR	polymerase chain reaction
PFA	paraformaldehyd
PGE2	prostaglandin E2
PGN	peptidoglycan
PLM	posterior lateral mesoderm
PRR	pattern recognition receptor
poly IC	polyinosinic-polycytidylic acid

PTU	phenylthiourea
<i>rag</i>	recombination activating gene
RD	repressor domain
RIG-I	retinoic acid-inducible gene-I
RING	really interesting new gene
RING finger	zinc-finger domain of the C3HC4 type found in RING and other proteins
RIPK	receptor-interacting protein kinase
RLR	RIG-I-like receptor
RT	reverse transcriptase
Runx-1	runt-related transcription factor 1
SAM	SARM-interacting domain
SARM1	sterile α and HEAT/armadillo motif containing protein 1
SPRY	splA/ryanodine receptor domain
ssRNA	single-stranded RNA
STAT	signal transducer and activator of transcription
STING	stimulator of IFN genes
TAB	TAK1-binding protein
TAK1	TGF- β activated kinase 1
TANK	TRAF family member associated NF κ B activator
TBK1	TANK-binding kinase 1
TCR	T cell antigen receptor
TF	tissue factor, also called coagulation factor III
TGF	transforming growth factor
TICAM	TIR domain-containing adapter molecule
TIR	Toll/IL-1R
TIRAP	TIR domain-containing adapter protein, also called MAL
TIRP	TIR domain-containing protein, also called TICAM-2
TLR	Toll-like receptor
Tn	<i>Tetraodon nigroviridis</i>
TNF	tumor necrosis factor
TNFR	TNF receptor
TOLLIP	Toll interacting protein
TRADD	TNFR-associated death domain protein
TRAF	TNFR-associated factor
TRAM	TRIF-related adapter molecule, also called TICAM2
TRIF	TIR-domain containing adaptor inducing IFN β , also called TICAM1
TRIM	tripartite motif protein

TYK2	Non-receptor tyrosine-protein kinase 2
VEGF	vascular endothelial growth factor
VISA	virus-induced signaling adaptor, also called IPS-1
VLIG	very large inducible GTPase protein
VLR	variable lymphocyte receptor
WD40	repeat of ~40 aa, often terminating in a Trp-Asp (W-D) dipeptide
WGS	whole genome shotgun project
WISH	whole mount <i>in situ</i> hybridization
WNT	wingless-type MMTV integration site family
wpf	weeks post fertilization

1 Introduction

1.1 Innate and adaptive immunity

In vertebrates the innate and adaptive immune systems both contribute to defend the organism against pathogenic infections. The adaptive immune system has been the subject of scientific research for a number of decades, whereas the specific response strategies employed by the innate immune system have only recently been started to be uncovered.

The innate immune response forms the first line of the hosts' defense against pathogens. After invasion of infectious agents, such as viruses, bacteria, fungi, or parasites, the innate immune response seeks to prevent their dissemination and thereby to limit the detriment to the infected host. The main components mediating innate immune responses are the complement system, phagocytes, and natural killer cells (NK cells) (for details see section 1.3).

In vertebrates, the adaptive immune response becomes activated as a consequence of complement activation and the release of proinflammatory cytokines by phagocytes or natural killer cells. The subsequent clonal response of the adaptive immune system is specific for the invading pathogen and leads to the development of memory B-cells.

1.1.1 Evolution of the immune systems in vertebrates

More primitive life forms, like flowering plants or insects, rely solely on innate immune defense strategies and have developed intricate mechanisms to fight off pathogenic infections.

The adaptive immune system seems to be an invention of the gnathostome lineage (jawed vertebrates) within the vertebrate clade, as it is absent in agnathans (jawless vertebrates represented by lampreys and hagfishes). The evolution of the jaw presumably led to dietary changes accompanied by a higher degree of injuries and infections. This might have resulted in a selective constraint leading to the development of the thymus, the central organ of the adaptive immune system (Matsunaga and Rahman 2001).

To date, there is ongoing controversy about the temporal origin of the adaptive immune system. One model is the "big bang" hypothesis (Abi Rached et al. 1999), proposing that the adaptive immune system emerged in association with the postulated two rounds of genome-wide duplications, one of which is thought to have occurred before and the other after the split of agnathans and gnathostomes. The other model postulates that the adaptive immune system arose by gradual accumulation of small

changes over an extended period, arguing that the evolution of the adaptive immune system started long before the divergence of those two lineages (Klein and Nikolaidis 2005).

Indeed, earlier studies in jawless vertebrates showed that these are capable of producing specific agglutinins against antigens and rejecting skin allografts with immunological memory suggesting that agnathans are equipped with adaptive immune systems (Finstad and Good 1964; Fujii et al. 1979a; Fujii et al. 1979b; Hildemann 1970; Linthicum and Hildemann 1970; Litman et al. 1970; Marchalonis and Edelman 1968; Pollara et al. 1970). However, subsequent attempts to identify T cell receptors (TCRs), B cell receptors (BCRs), or major histocompatibility (MHC) molecules have been unsuccessful. This apparent paradox was resolved by the discovery that jawless vertebrates have a unique form of adaptive immunity that does not rely on TCR, BCR, or MHC molecules (Alder et al. 2005; Cooper and Alder 2006; Pancer and Cooper 2006). The identification of variable lymphocyte receptors (VLRs) in lampreys suggests that different types of antigen receptor systems emerged during vertebrate evolution (Pancer et al. 2004). Although VLRs and TCRs/BCRs both generate diversity by combinatorial joining of gene segments, they are structurally and evolutionary unrelated. But in general it appears that the acquisition of antigen receptors capable of generating diversity by somatic recombination was indispensable for the survival of the emerging vertebrates.

From an evolutionary perspective the cartilaginous fish (Chondrichthyes) and the bony fish (Osteichthyes) are among the earliest vertebrate groups in which the main components of the adaptive immune system (MHC genes and B/T cells) are present. The zebrafish, *Danio rerio*, belongs to the infraclass Teleostei of the ray-finned fish class (Actinopterygii). As a model organism it can therefore be used to explore the immune system of jawed vertebrates.

1.2 Cells of the immune system in zebrafish

The immune system of the zebrafish resembles that of higher vertebrates in many aspects. Since the essential features of a multi-lineage myeloid system have been retained, the zebrafish has proven itself to be a robust and highly conserved model for studying vertebrate hematopoiesis (for review see (Amatruda and Zon 1999; Berman et al. 2005; Crowhurst et al. 2002; Traver 2004).

The obvious differences are that zebrafish lack bone marrow and lymph nodes. Hematopoiesis takes place in the kidney of adult zebrafish, as is the case in all teleosts (Zapata 1979). Immune and blood cells arise from hematopoietic, pluripotent stem cells

in the whole kidney marrow (Fig. 1.1). These stem cells differentiate either into the myeloid lineage (giving rise to monocytes, neutro-, eosino-, and basophilic granulocytes, thrombocytes, and erythrocytes) or the lymphoid lineage (B-, T-, and NK-cells). The early progenitors of T-cells migrate from the kidney to the thymus, where they mature to immunocompetent T-cells (Trede and Zon 1998; Willett et al. 1999). The presence of mast cells and dendritic cells in zebrafish has been unclear, but recent results indicate that both cell types are present (Dobson et al. 2008; Lin et al. 2009). In contrast to mammals, fish additionally possess melanomacrophages, which contain heterogeneous inclusions of mostly melanin, hemosiderin, and lipofuscin (Agius 1984; Herraez and Zapata 1991). Melanomacrophages are found as aggregates in the hematopoietic tissues of spleen and kidney and in the periportal areas of the liver (Roberts 1975; Wolke 1992). It has been suggested that these aggregates represent the primitive analogues to germinal centers of lymph nodes in mammals (Ferguson 1976; Roberts 1975).

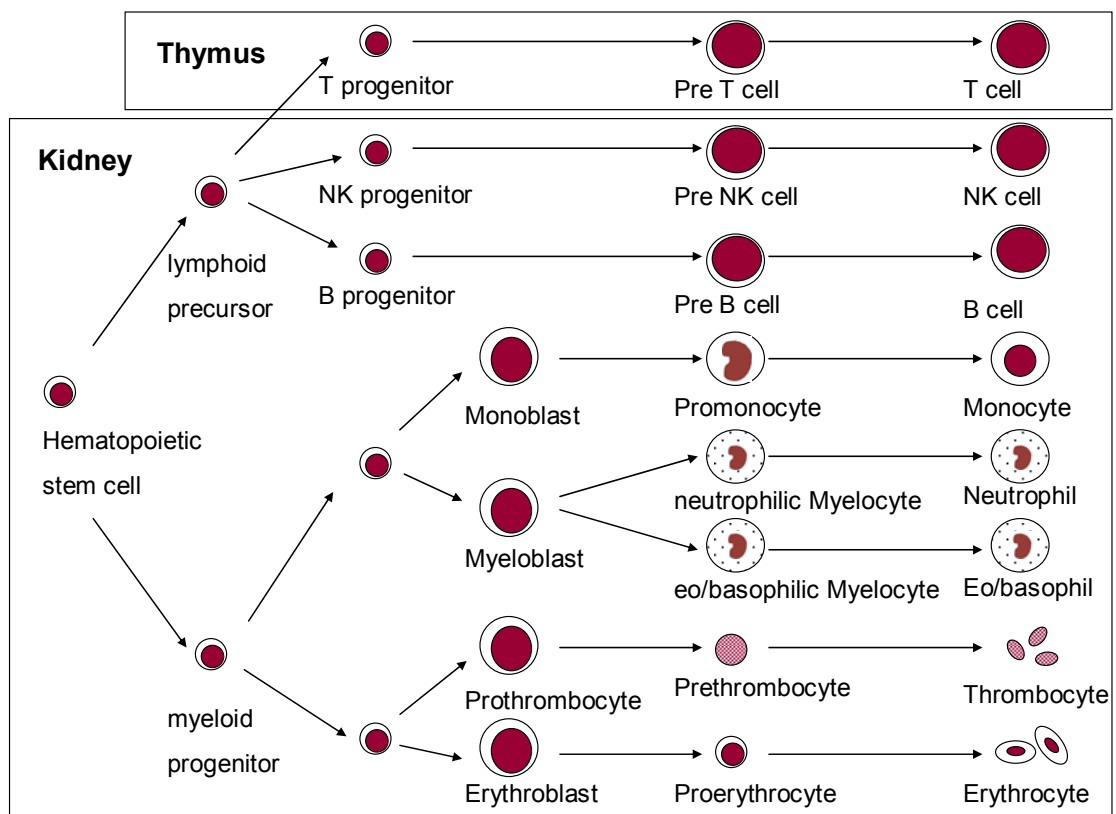


Figure 1.1: Model of the definitive hematopoiesis in adult zebrafish.

All definitive blood and immune cells derive from hematopoietic pluripotent stem cells (HSCs) located in the kidney. The HSCs give rise to two cell lineages, the myeloid and lymphoid cell types. The myeloid progenitor cells develop into monocytes, granulocytes, thrombocytes, and erythrocytes. Note that erythrocytes are nucleated in most fish species. The lymphoid precursors give rise to T and B lymphocytes as well as NK cells. The T cell precursors migrate to the thymus, where they mature to immunocompetent T cells (modified after (Traver et al. 2003).

1.2.1 Development of immune cells in the zebrafish

The zebrafish is an excellent model to study the development of immune and blood cells due to its external development with optically transparent embryos. A diverse collection of described blood mutants provides a rich source for the study of genetic components of human blood and immune disorders (reviewed in (Barut and Zon 2000)). The development of immune and blood cells in vertebrate embryos occurs in two temporally overlapping phases, which are called primitive and definitive hematopoiesis. The primitive hematopoiesis in mammals initiates in the extraembryonic yolk sac, while in zebrafish it takes place within the embryo at two distinct sites: the anterior lateral mesoderm (ALM) and the posterior lateral mesoderm (PLM), which later forms the intermediate cell mass (ICM). Primitive erythrocytes derive from the ICM (Al-Adhami and Kunz 1977; Detrich et al. 1995; Thompson et al. 1998) and primitive macrophages are formed in the ALM and migrate subsequently onto the yolk (Herbomel et al. 1999). Both primitive cell subsets arise between the 13- to 30-somite stages. Since the primitive wave of hematopoiesis is transient, it lasts only for less than 24 hours.

With the onset of circulation at about 24 hours post fertilization (hpf) the first progenitors of the second, definitive wave of hematopoiesis can be found (Burns et al. 2002; Gering and Patient 2005; Kalev-Zylinska et al. 2002). Similar to the primitive wave, also the definitive hematopoiesis occurs at independent sites within the zebrafish embryo.

At first, erythromyeloid progenitors develop in the posterior blood island (PBI). Studies in mammals, where they are also formed in the yolk sac, have shown that these cells have a limited differentiation program, giving rise only to erythroid and myeloid cells (Palis et al. 2001; Palis et al. 1999). Furthermore, they seem to constitute a transient population, due to their lack of self-renewal properties (Cumano et al. 2001). By fate-mapping studies similar results have been obtained in the zebrafish (Bertrand et al. 2007).

These findings led to the speculation that these cells evolved to provide innate immune protection before the first hematopoietic stem cells (HSCs) are produced (Palis et al. 2001). This seems indeed likely, since mature cells derived from the HSCs are not yet present for several days in mammalian as well as in zebrafish development.

In mammals and in the zebrafish the HSCs arise predominantly in the ventral wall of the dorsal aorta in a region known as the aorta-gonad-mesonephros (AGM). The development of HSCs and blood cells in the zebrafish is initiated and regulated by signal transduction pathways including the vascular endothelial growth factor (Vegf), bone morphogenetic protein (Bmp), Hedgehog, prostaglandin E2 (Pge2) – wingless-type MMTV integration site family (Wnt), and Notch - runt-related transcription factor

(Runx) pathways. Wilkinson and colleagues just recently demonstrated that Bmp4 is required for HSC formation in the developing zebrafish embryo (Wilkinson et al. 2009). By 26 hpf, genes involved in specifying definitive HSCs, *c-myb* and *runx1*, start to be expressed in the AGM (Burns et al. 2005; Gering and Patient 2005). A subset of the *runx1*⁺ cells in the AGM express CD41, the earliest known surface marker of nascent HSCs, at 33 hpf (Bertrand et al., 2008; Kissa et al., 2008).

Fate mapping and cell tracing studies revealed that HSCs leave the AGM and migrate through the blood to the pronephros at 48-56 hpf (Bertrand et al. 2008; Kissa et al. 2008). In addition, HSCs populate the caudal hematopoietic tissue (CHT), which has formed as a consequence of extensive remodeling of the PBI region (Murayama et al. 2006). In the CHT the HSCs give rise to erythroid, myeloid, and thromboid cells at around 3 dpf. Similar to the fetal liver in mammals, the CHT represents an intermediate site of hematopoietic differentiation, so that subsequently erythropoiesis, myelopoiesis, and thrombopoiesis shift to the kidney at around 5 dpf (Lin et al. 2005). From the larval stage into adulthood the kidney marrow is the primary site of hematopoiesis. B lymphocytes have been found at 19 dpf in the kidney and the pancreas, although the latter is still discussed as a site for B cell maturation (Danilova and Steiner 2002; Langenau et al. 2004; Willett et al. 1999). Secreted immunoglobulin (Ig) was only detectable by Western blotting at 4 weeks post fertilization (wpf) onwards (Lam et al. 2004).

A different subset of HSCs from the AGM has been observed to colonize the developing thymus at around 54-56 hpf (Kissa et al. 2008). By day 4, the expression of lymphoid genes like *recombination activating gene (rag) 1* and *2* and *ikaros* have been observed in thymocytes within the developing thymus (Willett et al. 1997). Mature lymphocytes are found in thymic epithelium by 7 dpf (Trede et al. 2001). However, during the first three weeks of development functional T cells could not be identified outside the thymus (Langenau et al. 2004) and the thymus itself does not seem morphologically mature until 3 weeks post fertilization (wpf) (Lam et al. 2002), although individual T cells have been found to be present in peripheral organs already at 9 dpf (Danilova et al. 2004). By assaying the acquired immune response to T cell dependent and independent antigens, it has been shown that immunocompetence is first achieved at 4-6 weeks of development (Lam et al. 2004).

For the first three weeks of development the zebrafish is therefore entirely dependent on innate immune defense mechanisms to fend off invading pathogens. In contrast to mice, which have circulating T cells at 7 days *post partum* (reviewed in (Adkins 1999), the zebrafish offers the opportunity to examine the defense strategies employed by the innate immune system independently of the acquired immune response.

1.3 The innate immune system in zebrafish embryos

Pathogens are recognized by three different components of the innate immune system: the complement system, NK cells, and phagocytes.

The complement system is highly developed in fish. Components of the classical (antibody-dependent), the alternative, and the mannose-binding lectin pathways have been identified in fish (reviewed in (Zarkadis et al. 2001a). Furthermore, zebrafish possess additional complement components compared to mammals, e.g. three genes encoding C3 convertase, two factor B genes, and at least three mannose-binding lectin genes (Gongora et al. 1998; Zarkadis et al. 2001b). However, not all of these extra components have been functionally evaluated.

In adult zebrafish complement factors are produced by the liver. Although in the embryo the liver primordium begins to develop at 32 hpf (Korzhan et al. 2001), vascularization, which is critical for liver function, is not completed until 3 dpf (Field et al. 2003). In order to activate the mainly macrophage-based immune response in the embryo, different sources of complement have been discussed, like the yolk syncytial layer or the macrophage itself. Indeed, early hepatic cells that appear in the endoderm of the yolk sac have been observed (Korzhan et al. 2001). However, using *in vitro* and *in vivo* approaches Wang and colleagues demonstrated that maternal complement components of the alternative pathway protect the early zebrafish embryo against bacterial infection (Wang et al. 2009; Wang et al. 2008). Additionally it was shown by this group, that complement gene transcripts of the alternative pathway were markedly increased by challenge with lipopolysaccharide (LPS) soon after hatching, which occurs at around 3 dpf.

The presence of NK-like cells has been shown in various fish species. Based on structural relationships to mammalian NK receptors, two multigene families identified in the zebrafish have been proposed to be the functional orthologs of mammalian NK receptors. One large gene family, the novel immune-type receptors (NITRs), encode Ig-like receptors of the KIR-type (Hawke et al. 2001; Litman et al. 2001; Yoder et al. 2001). The other family has been proposed to be orthologous to the mammalian NK receptor group 2D (NKGD) genes, which encode Lectin-type NK cell receptors (Sato et al. 2003). Although the receptor genes have been found to be highly divergent, the adaptor molecules like DNAX-activation protein (DAP) 12 and DAP10 have been shown to be conserved between mammals and fish (Yoder et al. 2007).

In addition to NK-like cells, fish possess non-specific cytotoxic cells (NCCs) (Evans et al. 1984b; Greenlee et al. 1991; Le Morvan et al. 1996). They are found predominantly in the kidney. Morphologically they appear similar to monocytes, but their mode of action resembles mammalian NK cells. It has been suggested, that NCCs represent

the evolutionary precursor to NK cells (Evans et al. 1984c; Jaso-Friedmann et al. 2001). However, the classification of NCCs as NK cells has remained in question, mainly because the NCCs used for functional studies were composed of a mixture of cell types or subpopulations that targeted different yet unknown antigens. Furthermore, in the channel catfish a NK cell line has been cloned from peripheral blood leukocytes that has been proven to be distinct from NCCs (Evans et al. 1984a; Evans et al. 1987). As of now, it is still unclear if these NCCs are the evolutionary progenitors to mammalian NK cells or if they rather represent a fish specific cell type.

The first primitive macrophages in the developing zebrafish embryo have been observed before the onset of circulation (Herbomel et al. 1999). Immature granulocytes start to circulate in the blood by 48 hpf, whereas eosinophilic granulocytes could first be detected at 5 dpf (Lieschke et al. 2001; Willett et al. 1999).

As in mammals, the first cells to arrive at the site of infection are the resident macrophages. Upon release of proinflammatory signals by these macrophages, granulocytes will arrive within 6 hours to 4 days. These are followed by monocytes from the blood circulation, which will differentiate into macrophages. The phagocytotic uptake of pathogens by activated leukocytes leads to degradation and subsequent antigen presentation by MHC molecules. The presented antigens can be recognized by CD8 or CD4 T cells. The mechanisms of pathogen recognition by phagocytes resulting in their activation have only partially been resolved in the zebrafish and will be discussed therefore based on signal transduction pathways known from mammals.

1.4 Cellular innate immune mechanisms

A primary challenge to the innate immune system is the discrimination of a wide variety of potential pathogens from self, with the use of a restricted number of germline-encoded receptors. These receptors recognize highly conserved microbial structures, so called pathogen-associated molecular patterns (PAMPs). Pathogen-associated motifs include mannans in the yeast cell wall, various bacterial cell-wall components such as LPS, peptidoglycans (PGN) and lipoproteins, as well as viral components, such as double-stranded RNA (dsRNA), single-stranded RNA (ssRNA), and DNA.

There are three major groups of pattern recognition receptors (PRRs): the Toll-like receptors (TLRs), the nucleotide-binding domain and leucine-rich repeat containing proteins (NLRs), and the retinoic acid-inducible gene I (RIG-I)-like receptors (RLRs).

Recognition of PAMPs is mediated in almost all TLRs and NLRs by leucine-rich repeats (LRRs) and the downstream signal is generally transduced by protein-protein interaction domains. This leads to the activation of signaling cascades resulting in the

induction of proinflammatory cytokines, cytokine processing or cell death. Furthermore, the responses elicited by the PRRs are important not only to eliminate pathogens but also to develop a pathogen-specific acquired immune response.

1.4.1 TLR-mediated signaling

TLRs are highly conserved from *Drosophila* to humans and share structural and functional similarities (Lemaitre et al. 1995; Lemaitre et al. 1996; Medzhitov et al. 1997). There are now at least 10 TLRs known in humans and 13 in mice, which differ in regard to their ligand specificity, expression pattern and induction of target genes (for review see (Aderem and Ulevitch 2000; Beutler 2009; Kumar et al. 2009; Medzhitov and Janeway 2000). TLRs can be classified into two groups on the basis of their subcellular localization. TLR1, 2, 4, 5, 6, and 11 are present at the plasma membrane and recognize pathogen components in the extracellular space. The second group is made up by TLR3, 7, 8, and 9, which localize to intracellular compartments, such as the endoplasmic reticulum (ER), endosomes, or lysosomes.

The additional TLRs present in human and mice appear to be the product of species-specific expansions. TLR10, which exists in humans and is most closely related to TLRs 1, 2, and 6, has been lost from the mouse genome. The TLRs 11, 12, and 13 are non-functional in or lost from the human genome. Of these, only TLR11 has been characterized so far, indicating that TLR11-mediated recognition of PAMPs is necessary for the regulation of interferon (IFN) γ and the subsequent responses it induces (Yarovinsky et al. 2008; Yarovinsky et al. 2005).

TLRs elicit cellular responses by signaling through their cytoplasmic Toll-interleukin-1 receptor (TIR) domain, which recruits TIR-containing adaptors. These adaptors include: myeloid differentiation factor 88 (MyD88) (Lord et al. 1990); TIR domain-containing adaptor protein (TIRAP), also called MyD-adaptor-alike (MAL) (Fitzgerald et al. 2001; Horng et al. 2001); TIR-domain-containing adaptor molecule-1 (TICAM-1), also referred to as TIR-domain-containing adaptor inducing interferon- β (TRIF) (Oshiumi et al. 2003a; Yamamoto et al. 2003a); TICAM-2, also called TRIF-related adaptor molecule (TRAM) or TIR-containing protein (TIRP) (Bin et al. 2003; Oshiumi et al. 2003b; Yamamoto et al. 2003b); and sterile α and HEAT/armadillo motif containing protein 1 (SARM1) (Mink et al. 2001).

The signaling cascade induced by TLRs will be described using TLR1 and TLR2 signaling as an example (Fig. 1.2): Heterodimerization of the receptors upon ligand sensing leads to the recruitment of the adaptors MyD88 and TIRAP. MyD88, which has been shown to be the essential adaptor for all TLRs besides TLR3, subsequently interacts with the IL-1R-associated kinase 4 (IRAK4) via their Death domains. IRAK4

then in turn recruits IRAK1 and IRAK2 to the complex, by which these become phosphorylated and thereby activated (Janssens and Beyaert 2003; Suzuki et al. 2002). The kinases dissociate from the receptor complex and interact with tumor necrosis factor receptor (TNFR) associated factor 6 (TRAF 6), an E3 ligase. This leads to the recruitment of transforming growth factor β (TGF β) activated kinase 1 (TAK1) binding protein 1 and 2 (TAB1 and TAB2), by TRAF6. Upon activation by phosphorylation of TAK1, which is bound by the TAB proteins, the inhibitory κ B (I κ B) kinase (IKK) complex becomes activated. The IKK complex comprises the two catalytic subunits IKK1 and IKK2 as well as the regulatory subunit, referred to as NF κ B essential modulator (NEMO). Next, the IKK complex phosphorylates I κ B, thereby marking it for ubiquitination and releasing the transcription factor NF κ B (Deng et al. 2000). Subsequently, NF κ B translocates into the nucleus, where it activates the expression of target genes encoding proinflammatory cytokines and chemokines. Negative regulators like IRAK3 or Toll interacting protein (TOLLIP) influence the signal intensity and duration (Kobayashi et al. 2002; Zhang and Ghosh 2002).

TLR1 and TLR2 signaling also leads to the activation of activator protein-1 (AP-1) induced target genes via the mitogen-activated protein (MAP) kinase cascades p38, extracellular signal-regulated kinase (ERK) 1/2, and Jun N-terminal kinase (JNK). Additional signal transduction pathways activate interferon regulatory factor (IRF) 3 or 7, which induce the expression of type I interferons.

Most TLRs are thought to be functional multimers. They are either heteromeric, like the TLR2 complexes with TLR 1 or 6, homomeric, or complexed with non-TLR subunits, like CD14, MD-2, or Dectin-1. For example, TLR4 seems not to detect LPS directly, but only as a complex with MD2 (Kim et al. 2007). While the majority of TLRs utilize more than one adaptor, certain adaptor molecules have been shown to be essential for individual TLR signaling, e.g. TLR4 signaling is dependent on TICAM-2 expression (Oshiumi et al. 2003b).

The diverse set of TLRs and the distinct signaling pathways proximal to the receptors ensure not only the recognition of various pathogens but also allow for a fine-tuned first-line response without damage to the host.

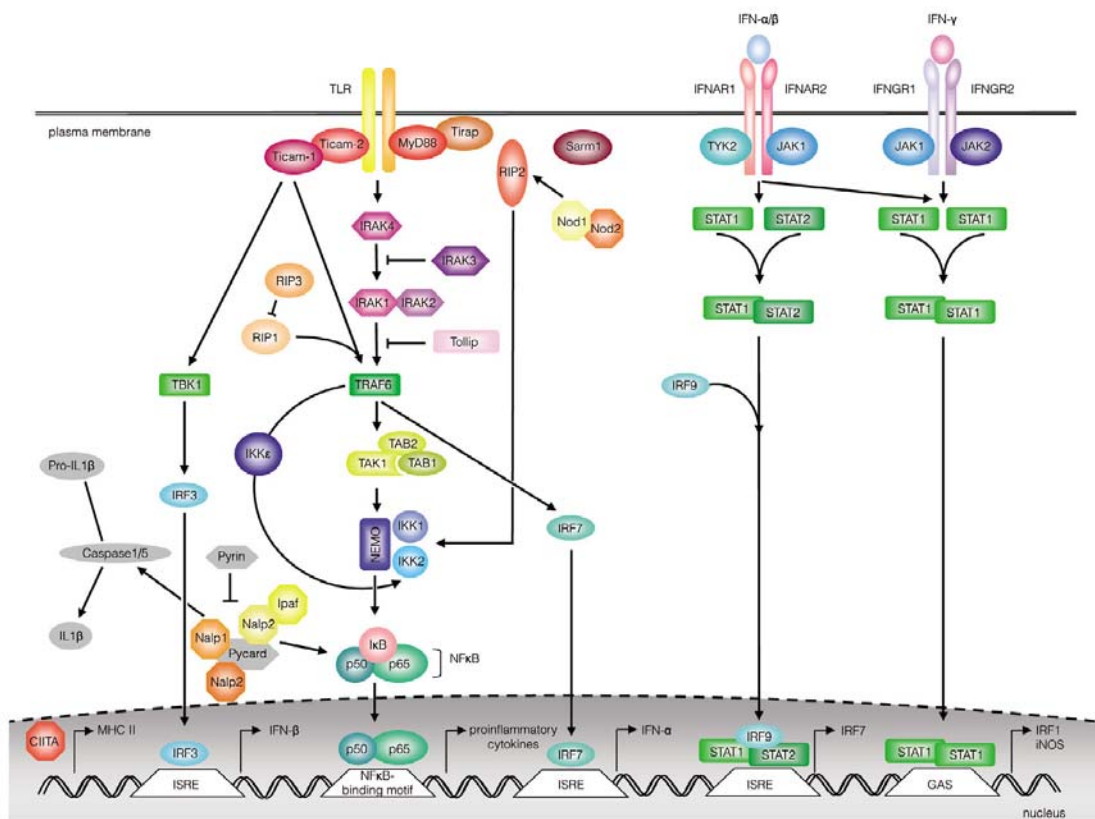


Figure 1.2: Components of the TLR, NLR and IFN signaling pathways.

Recognition of microbial motifs by TLRs or NLRs leads to the activation of adaptor molecules, which in turn activate downstream signaling proteins, like kinases that amplify the signal, or to the activation of caspases, which proteolytically activate interleukin 1 β (IL1 β). Subsequent activation of intracellular signaling proteins ultimately results in the induction or suppression of genes that orchestrate the inflammatory response. Binding of interferon (IFN) to its cognate receptor activates the classical Janus tyrosin kinase (JAK) - signal transducer and activator of transcription (STAT) pathway leading to the expression of further antiviral or proinflammatory cytokines and chemokines.

The molecules analyzed in this work are shown in color. For simplicity, not all members of each protein family are shown.

1.4.2 RLR-mediated signaling

The RLR family of cytoplasmic RNA helicases comprises three members: retinoic acid-inducible gene-1 (RIG-I), melanoma differentiation associated gene 5 (MDA5) and laboratory of genetics and physiology 2 (LGP2). RIG-I and MDA5 contain N-terminal tandem caspase recruitment domains (CARDs), a central DExD/H helicase domain and a C-terminal repressor domain. LGP2 is similar in domain structure, but lacks the CARDs.

A number of studies have shown that both RIG-I and MDA5 detect RNA viruses and the synthetic dsRNA analogue polyinosine-polycytidylic acid (poly(I:C)) in the

cytoplasm (Andrejeva et al. 2004; Kang et al. 2002; Kovacsovics et al. 2002; Yoneyama et al. 2005; Yoneyama et al. 2004). Subsequent *in vivo* studies revealed that RIG-I and MDA recognize different groups of RNA viruses (Gitlin et al. 2006; Kato et al. 2006). This distinction is based on nonself RNA patterns generated by the viruses over the course of their replication. Biochemical studies have shown that RIG-I preferentially recognizes short dsRNA or ssRNA with a non-capped 5' triphosphate moiety, whereas MDA5 senses long dsRNA (Cui et al. 2008; Kato et al. 2008; Takahasi et al. 2008).

The viral RNA patterns are sensed by the repressor domain (Cui et al. 2008; Takahasi et al. 2008). In the absence of viral RNA, however, the repressor domain is proposed to autorepress the RLRs by masking the CARDS and the helicase domain. Binding of nonself RNA by the repression domain may then induce conformational changes releasing the CARDS for downstream signaling and the helicase domain for multimerization using ATP hydrolysis (Saito et al. 2007).

Although the repressor domain shows only limited conservation among the RLR family members, the repressor domain of LGP2 has been shown to bind to RIG-I, thereby negatively regulating RIG-I mediated antiviral signaling (Saito et al. 2007). However, results from a different study using LGP2-deficient mice suggest that depending on the type of RNA virus, the LGP2 protein can both negatively and positively regulate RIG-I and MDA5 responses (Venkataraman et al. 2007).

Both RIG-I and MDA5 initiate the antiviral response by binding to IFN β promoter stimulator-1 (IPS-1) (Kawai et al. 2005), which has also been referred to as CARD adaptor inducing IFN β (Cardif) (Meylan et al. 2005), mitochondrial antiviral signaling protein (MAVS) (Seth et al. 2005), and virus-induced signaling adaptor (VISA) (Xu et al. 2005). Activated RIG-1 and MDA5 interact via their CARDS with the CARD of IPS-1. IPS-1 relays the signal to the TNFR-associated death domain protein (TRADD), which forms a complex with the Fas-associated death domain protein (FADD) and the receptor-interacting protein kinase 1 (RIPK1) (Kawai et al. 2005; Michallet et al. 2008). FADD in turn recruits caspase 8 and caspase 10 to the complex, where these become processed and activate NF κ B (Takahashi et al. 2006). TRADD also recruits TRAF3 to activate the kinases TRAF family member associated NF κ B activator (TANK) binding kinase 1 (TBK1) and IKK ϵ , which leads to the activation of IRF3 and IRF7 (Schroder et al. 2008; Soulat et al. 2008). Furthermore, FADD has also been implicated in IRF3 activation (Balachandran et al. 2004).

Additional factors contributing to RLR mediated antiviral signaling have been identified in the recent past. The mediator of IRF3 activation (MITA), also called stimulator of IFN genes (STING), for example, has been demonstrated to form a complex with IPS-1,

RIG-I, and TBK1, suggesting that it functions as an adaptor to link IPS-1 to TBK (Ishikawa and Barber 2008; Zhong et al. 2008). A further factor identified is TRIM25, a member of the tripartite motif (TRIM) protein family, which contains a cluster of a RING-finger domain, a B box/coiled-coil domain and a splA/ryanodine receptor (SPRY) domain. As an E3 ubiquitin ligase, TRIM25 has been shown not only to be essential for RIG-I ubiquitination, which facilitates the recruitment of IPS-1, but also for an increase in RIG-1 downstream signaling activity (Gack et al. 2007).

Thus, recognition of viral RNA in the cytosol by RIG-1 and MDA5 leads to the expression of type I interferons and inflammatory cytokines via different signaling cascades. RIG-I itself is inducible by IFN. An increase of RIG-I levels observed during the IFN response might therefore promote RIG-1 self-assembly and potentiate signaling to drive an IFN amplification loop (Saito et al. 2007).

1.4.3 NLR-mediated signaling

Many different names have been given to this family, but in 2008 a standardized nomenclature has been proposed (Ting et al. 2008), which will be used in the following. The nucleotide-binding domain and leucine-rich repeat containing proteins (NLRs) constitute a large family of intracellular PRRs involved in the sensing of pathogenic products and the regulation of cell signaling and cell death. Mutations within several NLR encoding genes have been linked to human autoimmune and autoinflammatory diseases (reviewed in (McGonagle et al. 2007).

The NLR family members share a common tripartite domain architecture consisting of a variable N-terminal effector domain, a central nucleotide-binding domain and C-terminal repeats, which are in most cases LRRs.

1.4.3.1 The NACHT domain

Initially, members of this protein family were identified by the presence of the nucleotide-binding domain, which has NTPase activity. This NTPase domain shows similarities to motifs of an ATPase domain termed NB-ARC, because its nucleotide-binding domain (NB) has been found in different pro-apoptotic proteins like the mammalian apoptotic protease activating factor 1 (APAF1), the plant resistance (R) proteins involved in disease and stress response, and the cell death protein 4 (CED-4) from *C. elegans*. (van der Biezen and Jones 1998b). Moreover, proteins harboring a NB-ARC or the NTPase domain found in NLRs share an analogous domain structure, characterized by the presence of protein-protein interaction modules C-terminal to the nucleotide-binding domain, like WD40 repeats or LRRs.

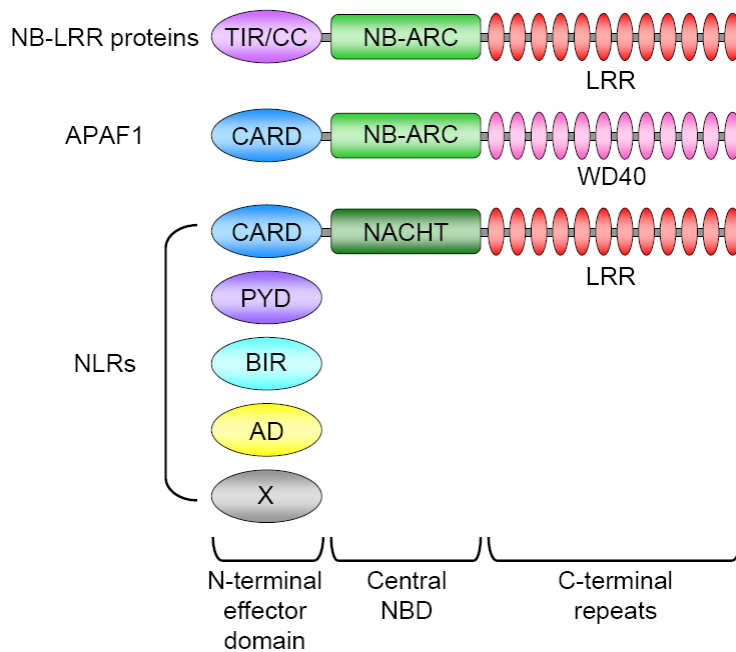


Figure 1.3: Conserved protein architecture in mammalian NLRs and plant NB-LRR proteins.

Nucleotide binding and leucine-rich repeat containing (NLR) proteins have a tripartite structure: an N-terminal effector domain, a central nucleotide-binding domain (NBD, referred to as NACHT), and C-terminal leucine-rich repeats (LRRs). The N-terminal effector domain consists of either a caspase recruitment domain (CARD), a pyrin domain (PYD), baculoviral inhibitor of apoptosis (BIR) repeats, or a transactivation domain (AD). One NLR protein has an undefined effector domain (X). Apoptotic-protease activating factor 1 (APAF1) and plant nucleotide binding site, leucine-rich repeat (NB-LRR) proteins contain a related nucleotide-binding domain, called NB-ARC. APAF1 also has an N-terminal CARD, whereas NB-LRR proteins are characterized by Toll/Interleukin-1 receptor (TIR) or coiled-coil (CC) N-terminal effector domains. APAF-1 has C-terminal WD40 repeats, NLRs and NB-LRRs have LRRs instead.

The founding members of the NLRs also include animal, fungal, plant, and bacterial proteins and thus the individual names were also used to generate an acronym for this emerging new family of NTPases. These founding proteins were neuronal apoptosis inhibitor protein (NAIP), MHC class II transactivator (CIITA), plant *het* gene product involved in vegetative compatibility (HET-E), and telomerase-associated protein 1 (TP-1), which led to the term NACHT describing this particular domain found in a variety of proteins (Koonin and Aravind 2000). As evident from these early observations, the NACHT domain in NLR proteins is evolutionary highly conserved and closely related to the NB-ARC domain found in plant NB-LRR proteins (Leipe et al. 2004); for review on the NB-ARC domain containing plant NB-LRRs see (DeYoung and Innes 2006; Jones and Dangl 2006).

The NACHT domain has been implicated to be essential for the biological function of the NLRs, because NLR activation by microbial ligands leads to the oligomerization of

NACHT domains, resulting in large multiprotein complexes serving as signaling platforms for the activation of adaptor molecules or effector proteins. These multiprotein scaffolds have also been referred to as inflammasomes (Martinon et al. 2002). *In vitro* studies suggest that the underlying mechanistic principles leading to this assembly are similar to those observed for the apoptosome formation by APAF-1, which has been resolved by electron cryo-microscopy (Faustin et al. 2007; Yu et al. 2005; Yu et al. 2006).

1.4.3.2 Ligand sensing mediated by LRRs

Various PAMPs with diverse structures have been shown to induce a NLR-mediated response (reviewed in (Kawai and Akira 2009). According to the current paradigm, NLR signaling is believed to be initiated by the C-terminal LRR region through the recognition of PAMPs, a property the NLRs share with members of the TLR family. Several studies have demonstrated that the LRRs of NLR proteins are required for PAMP sensing (Inohara et al. 2001; Inohara et al. 2003; Tanabe et al. 2004). However, there is no clear evidence of a physical interaction between the PAMPs and the LRRs and it has also been speculated that additional linker proteins are involved. Recently, some insight into the possible mechanism of ligand-receptor binding was obtained by the analysis of crystal structures of TLR1:TLR2 and TLR4:MD2 interacting with agonistic ligands. For the TLR1:TLR2 heterodimer a ligand-binding site at the concave surface of the LRR domain was proposed, whereas the ligand sensing by the MD2:TLR4 complex seemed to be primarily mediated by MD-2 (Jin et al. 2007; Kim et al. 2007). Although it is tempting to speculate that a similar mechanism operates for the LRRs of NLRs, the fact that the cytoplasmic NLRs are not attributed to intracellular compartments raises the question of how the cytoplasmic LRRs can come into proximity to their designated ligands.

To date, only in plant NB-LRRs direct PAMP-LRR interactions have been observed (Dodds et al. 2006). The intracellular NBS-LRRs proteins have also been found to indirectly recognize PAMPs. During infection, bacterial type III secretion systems translocate effector proteins into host cells. The NB-LRRs have been shown to recognize the host cell proteins targeted by these type III effector proteins (reviewed in (van der Biezen and Jones 1998a). Analogous to the mechanism identified in plants, it has been suggested that some of the mammalian NLRs react to the bacterial type III secretion system, e.g. detect pore formation. There is no direct evidence for this, but it appears that NLR family members react to membrane perturbation or its downstream consequences, e.g. potassium efflux (Franchi et al. 2007; Kanneganti et al. 2007;

Mariathasan et al. 2006; Pelegrin and Surprenant 2007; Petrilli et al. 2007; Sutterwala et al. 2007). These signals are also released by damaged or dying cells and have been referred to as danger signals or danger associated molecular patterns (DAMPs), with reference to PAMPs. Various DAMPs, like ATP, uric acid, or UV irradiation, have been shown to induce a NLR-mediated response (Feldmeyer et al. 2007; Mariathasan et al. 2006; Martinon et al. 2006; Sutterwala et al. 2007).

Similar to the repressor domain of RLRs, the LRRs are also implicated to autorepress the effector and the NACHT domain in the absence of a stimulus. Upon ligand sensing the induced conformational changes unmask the NACHT for oligomerization and the effector domain to transduce the signal to further adaptors or effector proteins.

1.4.3.3 Effector domains and downstream signaling

At present, there are 22 NLR family members known in humans, whereas in mice 33 NLRs have been identified. The mammalian NLRs can be divided into four subfamilies, based on different N-terminal effector domains. The effector domains found in NLRs are CARDs, pyrin domains (PYDs), baculoviral inhibitor of apoptosis repeat (BIR) domains, or the transactivator domain (AD) (Fig. 1.3). The designated subfamilies are (based on the initial of the domain name): NLRC (formerly known as NODs), NLRP (formerly known as NALPs), NLRB (formerly known as NAIP or Birc) and NLRA.

The sole member of the NLRA subgroup is the MHC class II transactivator (CIITA). CIITA does not directly interact with DNA, but supposedly coordinates the assembly of transcription factors and histone-modifying acetylases and methylases on MHC class II promoters (Zika et al. 2005; Zika and Ting 2005). In humans, defects in CIITA result in an autosomal recessive hereditary immunodeficiency, termed bare lymphocyte syndrome (BLS) (Steimle et al. 1993). BLS patients are extremely sensible to a variety of infections (reviewed in (Reith and Mach 2001), which is probably due to reduced numbers of peripheral CD4 T cells (DeSandro et al. 1999).

A further subfamily, designated as NLRX, groups NLR family members that do not share any of the other known effector domains.

The majority of NLRs found in mammals harbor a CARD or a PYD, which both belong to the death-fold domain superfamily. As the name suggests, they were originally identified in proteins involved in apoptosis, but have also been found in proteins participating in immune and inflammatory response pathways. The recruitment and activation of NLR interaction partners is mediated by homotypic interactions between these domains (CARD-CARD or PYD-PYD). The mammalian NLRP1 (NALP1) and NLRP3 (NALP3) as well as NLRC4 (IPAF) have been shown to assemble upon activation into an inflammasome, acting as a molecular scaffold for caspase-1

activation (Boyden and Dietrich 2006; Franchi et al. 2006; Mariathasan et al. 2006; Martinon et al. 2002; Miao et al. 2006). In PYD-containing NLRPs the activation of caspase-1 is mediated by the apoptosis-associated speck-like protein containing a CARD (ASC) adaptor protein. This protein has a bimodular structure, containing both a PYD and a CARD. NLRC4 directly interacts with CARD domain of caspase-1, as does NLRP1, which has a unique CARD at its C-terminus. Caspase-1 is a cysteine protease that cleaves proteins at specific sequences following aspartyl residues and is produced as catalytically inactive zymogen. The current view is that the scaffold of activated, oligomerized NLRs leads to an arrangement of tightly packed caspases, allowing their crossprocessing, which is essential for activation. *In vitro* studies have shown that the interaction of procaspase-1 molecules with the CARDS of oligomerized NLRP1 proteins is sufficient to achieve protease activation (Faustin et al. 2007). Caspase activation by scaffold activated homotypic interactions was initially observed in the apoptosome, by which the caspases 8 and 9 become activated and initiate a proteolytic cascade resulting in apoptosis (Acehan et al. 2002; Shiozaki et al. 2002).

The proinflammatory caspase-1, however, processes the inactive prointerleukin-1 β (proIL-1 β) to produce the active cytokine IL1 β , which is a major mediator of inflammation in mammals (Cerretti et al., 1992; Thornberry et al., 1992). Active caspase-1 also cleaves other cytokines like IL18, IL17b and IL33 (Nadiri et al., 2006). The secreted cytokines bind to their ubiquitously expressed cognate receptors, which belong to the TLR-IL-1R superfamily. Activation of these receptors and subsequent interaction of their TIR domains with downstream signaling components leads to activation of NF κ B and MAPK, as well as to the induction of additional cytokines, such as IL6, IFN γ , or IL4. In addition to the induced inflammatory response, this will also lead to activation of the acquired immune system.

The most intensively studied members of the NLRC subfamily are nucleotide-binding oligomerization domain containing protein 1 (NOD1) and NOD2, which have retained their names. Upon activation by bacterial peptidoglycan derivatives they transduce the signal via CARD-containing adaptors like RIPK2 to downstream signaling components, resulting in the activation of NF κ B and MAPK and the induction of proinflammatory cytokines and chemokines (Chamaillard et al. 2003; Girardin et al. 2003a; Girardin et al. 2003b; Girardin et al. 2003c; Inohara et al. 2003; Viala et al. 2004).

Members of the NLRB subgroup are called NAIP proteins. The NAIP proteins are unusual in that they contain three BIR repeats at their N-terminus. NAIP proteins have been shown to be activated by Legionella flagellin protein (Wright et al. 2003). Subsequent activation of caspase-1 has also been described, but the exact interaction mechanisms have not been fully resolved (Ren et al. 2006). It has been proposed that

activated NAIP interacts with NLRPC4 via their NACHT domains, leading to caspase activation (Zamboni et al. 2006). However, it was also found that NAIP5 mediates caspase-independent restriction of *Legionella pneumophila* pathogenesis, hence the signaling pathways downstream of NAIP remain a question of further studies (Lamkanfi et al. 2007; Lightfield et al. 2008; Molofsky et al. 2006).

In addition to inducing an inflammatory response, NLRs have also been implicated in cell death. In particular, they seem to induce two different modes of cell death, pyroptosis and pyronecrosis. Both differ from apoptosis, in that they elicit a substantial inflammation, which affects neighboring cells. The morphological features of the dying cell are also more similar to necrosis than apoptosis, like an intact mitochondrial membrane or a lack of chromatin condensation. In contrast to necrosis, pyroptosis and pyronecrosis require the adaptor ASC. Pyroptosis has been shown to be inducible by NLRC4, NAIP, and NLRP1, which results in caspase-1 mediated cell death (Cervantes et al. 2008; Fernandes-Alnemri et al. 2007; Miao et al. 2008). Pyronecrosis, on the other hand, is caspase-1 independent and induced by NLRP3, which activates a cathepsin B-mediated lysosomal pathway leading to cell death (Fujisawa et al. 2007; Huang et al. 2009; Willingham et al. 2007). This is intriguing, since NLRP3 interacts with ASC within the inflammasome leading to caspase-1 activation and an inflammatory response.

Several recent studies reported interactions of different NLR signaling pathways (Hsu et al. 2008; Pan et al. 2007) and also crosstalk between TLR, RLR, and NLR signaling (Kim et al. 2008; Moore et al. 2008; van Heel et al. 2005). Additional components involved in NLR-induced inflammation and cell death have been identified, ranging from a diverse set of pathogenic elicitors (reviewed in (Geddes et al. 2009) to positive or negative regulators (Moore et al. 2008; Saitoh et al. 2008; Tattoli et al. 2008) and additional signaling targets (Willingham et al. 2009). These findings have broadened the view on the complex interplay in innate immune signaling pathways. However, molecular details of NLR signaling like the mode of ligand sensing or the temporal and spatial regulation of NLRs within the cell remain unresolved.

1.4.4 Interferon signaling

Vertebrate interferon (IFN) proteins are widely expressed cytokines that play an important role in the defense against viral and microbial infections. They have also been recognized for their antiproliferative and immunomodulatory effects.

The IFNs are classified into three types (type I-III) (Kotenko 2003, Pestka 2004) according to receptor specificity, gene structure, and sequence homology. The IFNs

belong to the class II cytokine family, which also includes IL10-related cytokines (reviewed in (Renauld 2003). Type I (IFN α , β , ϵ , κ , ω) and type III IFNs (IFN λ 1-3) are induced in many cell types by viral or bacterial products. In addition to their strong antiviral effects, they modulate many aspects of immune and inflammatory responses (for review see (Li et al. 2009; Stetson and Medzhitov 2006). In contrast to type I and type III IFNs, the sole type II IFN, IFN γ , is a more potent pro-inflammatory than antiviral cytokine and a key endogenous activator of macrophages. IFN γ is mainly secreted by T cells, NK cells and macrophages.

The members of each IFN type bind to a type-specific receptor complex. These receptors consist of heterologous receptor chains, which are thought to dimerize upon ligand binding. The ligand-receptor interaction activates the classical Janus tyrosine kinase (JAK) – signal transducer and activator of transcription (STAT) pathway (Fig. 1.1) together with additional signaling cascades. IFN signaling results in the transcriptional induction of a large number of target genes (IFN-stimulated genes; ISGs) to evoke versatile biological activities. (Boehm et al. 1998; Der et al. 1998; Ehrh et al. 2001).

Further characteristics of the interferons and their receptors are described in detail in regard to the results obtained during this work.

1.5 Aims

The zebrafish is increasingly used as a model to genetically address immunological problems. However, there has been a paucity of information concerning the repertoire of innate immune components and the complexity of the signaling mechanisms. The first aim of this work was therefore to conduct a thorough phylogenetic analysis to identify orthologs of known innate immune signaling components in the genome of the zebrafish. A second aim was to investigate the physiological functions of the Ifn γ signaling system during the innate immune response to bacterial infection in zebrafish embryos. Suitable infection assays should be tested and used in combination with morpholino-mediated knockdown approaches to analyze potential Ifn γ receptor chains and target genes. An additional aim was to analyze a novel *nlr* gene, which was identified during the phylogenetic analysis.

2 Materials and Methods

2.1 Materials

The chemicals and enzymes used in this study had at least the quality standard *pro analysi* and were bought, if not stated otherwise, from the following companies: Biozym (Oldendorf), Sigma-Aldrich (Deisenhofen), NEB (New England Biolabs; Beverly, USA), GibcoBRL/Life Technologies (Paisley, Schottland), Roth (Karlsruhe).

Buffers and solutions, which are not mentioned separately, have been prepared according to (Sambrook et al. 2001).

2.1.1 Solutions and buffers

Block I	0.2 % (w/v) BSA (Bovine Serum Albumine) in PBST
Block II	0.2 % (w/v) BSA / 5 % sheep serum (heat inactivated) in PBST
DEPC-H ₂ O	0.1% (v/v) DEPC in H ₂ O
DNA loading dye (6x)	0.25% (w/v) Bromphenol Blue or Xylene Cyanol 70% (v/v) Glycerol
DNA-extractionbuffer	10 mM Tris pH 8.2 10 mM EDTA 200mM NaCl 0.5% SDS
Embryo media	40 mM NaCl 1 mM KCl 1.5 mM HEPES 2.5 mM CaCl ₂ pH 7.21
Hybridisation-Mix	50% (v/v) Formamid 5x SSC 1% (w/v) Boehringer Block (Roche) 5 mg/ml <i>torula</i> yeast RNA (Roche) 50 µg/ml Heparin 1x Denhards 0.1% (v/v) Tween-20 0.1% (w/v) Chaps 5 mM EDTA

2 MATERIAL AND METHODS

P1	50 mM Tris-HCl (pH 8.0) 10 mM EDTA 100 µg/ml DNase-free RNase
P2	200 mM NaOH 1% (w/v) SDS
P3	3 M NaOAc (pH 5.5)
PBS	140 mM NaCl 10 mM KCl 8 mM Na ₂ HPO ₄ 2 mM KH ₂ PO ₄ pH 7.4
PBT	0.1% (v/v) Tween-20 in PBS
SSC (20x)	3 M NaCl 0.3 Na-citrate pH 7.4
TAE	40 mM Tris 20 mM acetic acid 1 mM EDTA
TBE	45 mM Tris 25 mM boric acid 1 mM EDTA
TE	10 mM Tris-HCl pH 8.0 1mM EDTA
low TE	10 mM Tris-HCl pH 8.0 0.1mM EDTA
Xpho	100 mM Tris-HCl pH 9.5 50 mM MgCl ₂ 0.1% (v/v) Tween-20

2.1.2 Cells and Plasmids

For overexpression studies the pCS2+ vector was used, which is the standard vector for misexpression experiments in zebrafish and *Xenopus* (Turner and Weintraub 1994). As control for these functional studies and for GFP-morpholino control experiments, a

modified pCS2+eGFP was used (kindly provided by the members of the former Campos-Ortega lab). Standard transformations were done using competent DH5 α (Invitrogen).

2.1.3 Oligonucleotides

The used oligonucleotides were synthesized by the companies Metabion or Invitrogen. The lyophilized oligo was dissolved in an appropriate volume of H₂O to obtain a concentration of 100 μ M. All used primers are listed below in 5' – 3' orientation.

Tab. 2.1: Oligonucleotides

Dr ifny1 SP	GCGCATACAGATTTGACGG
Dr ifny1 ASP	TTTTTCTGTGGAGGCCCGAT
Dr ifn- γ 2 SP	ATGATTGCGCAACACATGAT
Dr ifn- γ 2 ASP	AAAGCCTTTGCTGGACGAT
Dr crfb1 SP1	AGTGAACCGGGTGTAGTGACGT
Dr crfb1 ASP1	AGCAGAGTCACACTTTAGCAAT
Dr crfb1 SP2	CACGACTTCATCATTGCTAA
Dr crfb1 ASP2	TATCGTCTTTCCTTGATTCA
Dr crfb6 SP	GAACGACGCTTTCTCAACTC
Dr crfb6 ASP	GACTCGATTTGAAATGGCCC-3'
Dr crfb7 SP	ATGTGGAAGAGAAGTATGA
Dr crfb7 ASP	TTTAGCCTTACTCTCCTGTC
Dr crfb7 SP1 e2	CGACATATGGGAGGGAAATG
Dr crfb7 ASP1 i4	TCAAGGTGTCCATTGGGTTT
Dr crfb7 SP2 i6	TGCTGCTTCACAATTTGTTTG
Dr crfb7 ASP2 e7	ATGGTTGTTTCGGTTTCAGC
Dr crfb13 SP e1:	TGATCATTATGTGGTGTGCGGTGACGG
Dr crfb13 ASP e5 :	GCGATTGATCCACAGAGAATAGCTGC
Dr crfb13 SP e4:	AGCTGTGGATGCGTCTGT
Dr crfb13 ASP i4:	ACAGACTGCCACTGCTCA
Dr crfb13 ASP e4	GGATGGGTTAAGGATGATGG
Dr crfb13 ASP e6	TCATCTCCAGCAGGCATTTAGGACTGTCGT
Dr crfb15 SP e1:	CCTCAGAACGTGAAGGTGGTCTCC
Dr crfb15 ASP e4 :	CAGGAGTGCTGTACTGTCCCCTTC
Dr crfb15 SP2	TGGTCTCCATCAACATGGGTG
Dr crfb15 ASP2	GATCCACCTTTGCCTGAACACA
Dr crfb15 SPi3e4	GATGCTCAGTCCTTGCGATT
Dr crfb15 ASPi5	GAAGGCATGACCCAAATGTC
Dr nwd1 SP1 e5	CTCTTGACTGACCTGAAGCAACGCAT
Dr nwd1 ASP1 e5	AAGACAAACACCTCGAAGAACAGAATCG
Dr nwd1. ATG SP2	ATGGATGTGGTGGAGATGAGAGAG
Dr nwd1. ATG ASP2	GCGTTGCTTCAGGTCAGTCAAG
Dr nwd1 SP3	GATGGAGCATGGCTTTCTCAG
Dr nwd1 ASP3	CGTTGCTTCAGGTCAGTCAA
Dr nwd1 e4 SP4	TATATCCTCCTGCCAATCACG
Dr nwd1 e4 ASP4	GCAACCTCAGCAGAACAACCTC

Dr nwd1 SP5	TCAAATGTGGAATGCGTGAC
Dr nwd1 ASP5	CAGTGAAATCCCCGTCTCTC
Dr nwd1 SP6	ACAATCGGGGAGTTGTTCTG
Dr nwd1 ASP6	TTCAGATGCAAAGGGTTTCC
Dr nwd1 SP7	AACACACAGCCCTACACACATC
Dr nwd1 SP8	GGAAACCCTTTGCATCTGAA
Dr nwd1 ASP8	TGCGTGAGCAAGGTGATAAG
Dr nwd1 SP9 e6/7	TTCACTCACAGGCAGTTTGC
Dr nwd1 ASP9 e10/11	CAACAGCCTTCACCCCTTTA
Dr nwd1 SP10	GGATCCCTCGCTGTTAGTGACA
Dr nwd1 ASP10	TGCGGTCAGCTCAAACAGAG
Dr nwd1 SP11	TTTGGGGAAAGCCGTCTACATTC
Dr nwd1 ASP11	GAGTACCTTTCAAATGGTCCATCG
Dr nwd1 SP12	CTTTATCCCAGAAACCTTGTGC
Dr nwd1 ASP12	GATGCCAATGAAGTTGAACTGA
Dr nwd1 SP13 e1	GGCCTTCTGATCTCAGTGG
Dr nwd1 ASP13 e2	CAAACCTTTGGCAGTGGGTCT
Dr nwd1 SP14 e19	GATGATGCCACACAAGGATG
Dr nwd1 ASP14 e19	CGGTCGTTGAGTGTGTGAAG
Mm nwd1 SP e8	GACGTGGAGGAACAACAGGT
Mm nwd1 ASP e12	TTCAGAAACCACCAGGAACC
Mm nwd1 SP2	GCCCTTAGCCACTACAGCAG
Mm nwd1 ASP2	CCTGCTTCAACTCCTCCAAG
Dr nod1 SP e1	AACTCTTACCTGAAGCTGCTGACTGTTC
Dr nod1 ASP e3:	TGGTCCAGATTCTGTAAATATCCCAAACCTC
Dr nod2 SP e1:	CAGGTTCGAAGACTGTTAGACCAAGTAA
Dr nod2 ASP e1:	AAATGAGGGTGGTCTAGGATGAATTG
Dr nod3 SP e1:	CTGTTACCAGGGGCAACACT
Dr nod3 ASP e3:	TAATAGAGAGCGCCCAGGAA
Dr nod9 SP e1:	CTCAGATCCCATTGAGATCCACAGGC
Dr nod9 ASP e1:	CGCTGCATAACTCAGTGGAGCTGA
Dr apaf1 SP e2:	AAAGCCACTCTGGAGCAGGACATCAA
Dr apaf1 ASP e4:	TGAGTGAACGATCTCGAACAACCTCG
Dr irge1 SP	GACGCTAAGCCTAAAGAAAAACAAGGAAACT
Dr irge1 ASP	TAGACATCATGTCTATCAGAATACGGTCAGTG
Dr irge2 SP	ATGAAGATACAGAAGCAGAAGCAGGAATTG
Dr irge2 ASP	TCAACTGGCTGTTTCAGCAAGATCCT
Dr irge3 SP	GGCCACAGCAAAAGCCAAAGAAAGTT
Dr irge3 ASP	CTGAAAGCCTCGCCAGTGATCCATC
Dr irge4 SP	GGAAAAGGCCACAGCAAAAGCCAAAG
Dr irge4 ASP	GTTTTATTTTTCTGAAAGCCTCGCCAGTGA
Dr irge5 SP	CATTTGTCAATGCCCTGCGAGGC
Dr irge5 ASP	CAGTGACACTCCTGGGATTGGAGCAA
Dr irge6 SP	ATGGAATGTGTGATTGAGCAAAACAAGC
Dr irge6 ASP	TTAATAGACACCAGTCACTCCTGCAGCTT
Dr irgf1 SP	GACTATTGTGTAATAACCCAGGAGGACCTG
Dr irgf1 ASP	CAGCAGATTTAAATCATACTTGCTGAGC
Dr irgf2 SP	ATCTGCCAACAGCATTTGGCACAAT
Dr irgf2 ASP	TTATCACATTTCTGATGTCTTCTGCTATGACATTC
Dr irgf3 SP	GCTGAAACTGGGGTTGTAGAAACCACC
Dr irgf3 ASP	CTAGACTTCAGTCTCCAGTGAAGCATTTAGCA

Dr irgf4 SP	GCTGAGGAGATTGTAAGATTGAGGAAAACC
Dr irgf4 ASP	CTTCCCTGATACATCACAGAGCCTCTG
Dr irgg1 SP	ATGTTTTTTTCTAGATTATGCATGCCAGCA
Dr irgg1 ASP	TCACCTTGCTTTTAGCCATCCACCA
Dr irgq1 SP	ACACAGCACGTCCAGCAGACTGAGAAAC
Dr irgq1 ASP	GCGATATAATATGCAAAAGCACTTGTCTCTG
Dr irgq2 SP	ATGGCTGACGTGATAAAGGGTCTCAACC
Dr irgq2 ASP	CTACTGTCGCTCTCCAGTCACCATAGCAAC
Dr irgq3 SP	ATGAGAGCTCGAAAGCTGGAGTTGCA
Dr irgq3 ASP	TTACATAAATTTGCAAGAATCTGATCTTTTCCA
Dr β -actin SP	ATGGATGATGAAATTGCCGCAC
Dr β -actin ASP	ACCATCACCAGAGTCCATCACG
T3	AATTAACCCTCACTAAAGGG
T7	GCCCTATAGTGAGTCGTATTAC

2.1.3.1 Oligos to generate PCR products for UTR-GFP morpholino controls

Tab. 2.2: Oligos for UTR-GFP constructs

Dr crfb1 Mo con UTR SP	GACTGGATCCGAACCGGGTGTAGTGACGTT	BamH1
Dr crfb1 Mo con UTR ASP	CTAGGAATTCCACAAACAAAAGCAGAGTCACA	Eco R1
Dr crfb6 Mo con UTR SP	GACTGGATCCGCCGATGGGATTTAAACGTA	BamH1
Dr crfb6 Mo con UTR ASP	CTAGATCGATTACCACATCTTTCACCAAACCA	Clal + Stop
Dr crfb7 Mo con UTR SP	GACTGGATCCCTGCTTGGGTGCTACAGATG	BamH1
Dr crfb7 Mo con UTR ASP	CTAGGAATTCTGTCAGTTCAGCATCATATCCA	Eco R1

2.1.4 Morpholino oligonucleotides

The following morpholino oligonucleotides (Mo) were used (synthesized by Gene Tools).

Tab. 2.3: Morpholinos

Mo crfb1	GAGTCACACTTTAGCAATGATGAAG
Mo crfb6	TCTTTCACCAAACCATTTGCGAGAG
Mo crfb7	TCAGTTCAGCATCATATCCAACAAC
Mo crfb15 1	AACATAAGCATTTTCATACCTCATC
Mo crfb15 2	TCCTATGATAGCTACAAGGGAGCAA
Mo crfb13	TCTAAATGGTTTGTAGTTACCTGAG
Mo ifny1	TTTCTGTGCTGTGAACCAAGTGATG
Mo ifny2	TGAAGGCGTTCGCTAAAGTTAGAGT
Mo nwd1	TAACATGACTGACCTTGATAACAGG
Mo pu.1	GATATACTGATACTCCATTGGTGGT

2.1.5 Software

Adobe Acrobat Reader 9

Adobe Photoshop CreativeSuite2

Adobe Acrobat Reader 9

AxioVision 4.6, Zeiss

ClustalW

Informax Vector NTI 10

Jalview

Leica Application Suite 2.8.1

MEGA 3.1

Microsoft Office 2003

Furthermore the services of PubMed, Blast, Zebrafish EST-Database, ZFIN, Ensembl, Bioinformatics, Primer3, HMMer, LogoMatM, Pfam, Swissprot, Smart, and Prosite have been used.

2.1.6 Sequences used in the phylogenetic analysis

The protein sequences analyzed in the phylogenetic study are available at <http://genomebiology.com/2007/8/11/R251#IDAMU5GP>.

2.2 Methods

2.2.1 Zebrafish methods

2.2.1.1 Keeping and raising zebrafish

2.2.1.1.1 Origin of zebrafish

The zebrafish *Danio rerio* is a three to four centimetres long fresh water fish from the Ganges that belongs to the family *Cyprinidae*. Animals kept in the facility were obtained from the Tautz and Campos-Ortega labs (Cologne strain) and were further bred. The fish originally derive from pet shops in Cologne and Göttingen.

2.2.1.1.2 Growth conditions

Starting with day 6, zebrafish were kept in an aquarium, consisting of several serial 12 l tank units, at a water temperature between 26 and 28°C (Mullins et al., 1994). The maximum extent of utilization of a unit amounted to 10 fish per liter. The aquarium was supplied continuously with fresh water, whereby daily 1/10 of the liquid volume was replaced by fresh water. One half of the fresh water was adjusted by means of an ion exchange resin to a total hardness between 6-10 degrees of hardness units; the other half was transmitted from a reverse osmosis plant. Within the aquarium, the water was circulated by a pump system. Suspended particles were sieved by integrated filter units

from the water and the filtered water was sterilized afterwards by UV irradiation. The accumulation of toxic substances (e.g. nitrite) was prevented by using a bacterial filter. Fish were fed twice daily. Beside the usual fodder (Tetramin), Artemia and Bosmina were fed, in order to ensure balanced nutrition. The light and darkness rhythm was adjusted to 14 hours light and 10 hours darkness.

2.2.1.1.3 Zebrafish embryos

The collection of embryos for various experiments took place in the morning starting with the light phase, which is the trigger for spawning. In the evening before, the adult male and female fish were put into a plastic box, divided by a separator. The bottom of the box was filled with marbles with the aim to prevent the adult fish feeding their own eggs. In the morning the divider was removed at the designated time point, allowing the fish to mate and 20-30 minutes later the embryos were collected. Embryos and young larvae were kept in petri-dishes with embryo medium before and after the experiments and were allowed to develop until the desired stage in an incubator at 28.5°C. The embryo medium was exchanged daily.

2.2.1.1.4 Staging of embryos and larvae

Staging of the embryos and larvae during development was performed according to (Kimmel et al. 1995).

2.2.1.2 Anesthetization of embryos, larvae and adults

For anesthetization tricaine (ethyl-4-aminobenzoate, Sigma-Aldrich) was used. The stock-solution containing 0.4% (w/v) tricaine in 50mM Tric-HCl (pH 7.5) was kept at 4°C in the dark and was diluted to 0.02% (w/v) in embryo media for anesthetization of the fish.

2.2.1.3 PTU treatment to prevent pigmentation

Embryos were incubated starting at 6 hpf in 0.2mM phenylthiourea (PTU) to prevent pigmentation. The stock solution containing 0.06% (w/v) (4mM) PTU (Sigma-Aldrich) was kept at -20°C and was diluted to 0.003% (w/v) (1:20) in embryo media for usage.

2.2.1.4 Lateral line labeling with 4-di-2-Asp

Neuromast hair cells of embryos or larvae were labeled by incubating the fish in 5 mM 4-(4-diethylaminostyryl)-N-methylpyridiniumiodide (4-di-2-Asp, Sigma D-3418) (Collazo et al. 1994) in embryo medium for five minutes. Labeled embryos or fish were rinsed in fresh embryo medium and were anaesthetised with tricaine for observation.

2.2.1.5 Mechanical dechorionisation of embryos

Embryos of the desired growth stage were manually dechorinated using fine-pointed watch-makers forceps.

2.2.1.6 Fixation and storage of zebrafish embryos

Embryos or larvae were fixed in 4% paraformaldehyd (PFA) in PBS. The fixation was performed either for two hours at room temperature or overnight at 4°C. After fixation embryos were transferred to PBT (PBS + 0.1 % Tween-20) and washed in PBT 3 x 5min. After subsequent washing steps in methanol (3 x 5min), the embryos or larvae were kept at -20°C in methanol until further use.

2.2.1.7 In situ hybridization of whole embryos

In situ hybridization by means of Digoxigenin labeled probes is a non-radioactive procedure, which makes it possible, to determine the spatial expression of mRNA (Tautz and Pfeifle 1989). The embryos were incubated with digoxigenin labeled anti-sense RNA probes. The hybridized probes were then detected immunochemically, by means of alkaline phosphatase (AP) conjugated anti-digoxigenin Fab fragments, whereby the enzymatic conversion of specific substrates resulted in the production of colored precipitates.

For in situ hybridisation of zebrafish embryos the protocol by Schulte-Merker and colleagues (Schulte-Merker et al. 1992) was followed with slight modifications.

2.2.1.7.1 Prehybridisation

Embryos were first incubated in a solution of 50% PBST / 50% Hybridisation solution (Hybmix), which was replaced after 5 min by 100% Hybmix. The incubation in Hybmix was 1 hour at 65°C.

2.2.1.7.2 Hybridisation

The RNA probes were dissolved in a small volume of Hybmix (250µl). After the prehybridisation the pure Hybmix was replaced by the prepared probe/Hybmix solution, in which the embryos were incubated for 16h at 65°C.

2.2.1.7.3 Washing steps

After hybridisation the embryos were incubated for 30 min in Hybmix at 65°C. Subsequently and successively the embryos were washed 2 times for 30 min with a solution of 50% hybmix/50% 2xSSCT and 2times for 30 min with 0.2xSSCT at 65°C.

2.2.1.7.4 Antibody incubation

The embryos were first washed twice for 5 min and later once for 20 min with PBST at room temperature. Then the embryos were incubated for 10 min in Block I and subsequently in Block II for 60 min. Block II was afterwards replaced by an 1:2000 dilution of anti-Digoxigenin-AP Fab fragments (Roche) in Block II. The incubation was carried out for 6h at room temperature, followed by eight times washing for 15 min with PBST.

2.2.1.7.5 Color substrate reaction

Embryos were incubated 2 times for 5 min in AP buffer and subsequently transferred to 24 well plates, in which the AP buffer was replaced by *BM-Purple*-solution (Roche). The color substrate reaction took place in the dark and was carried out from 30 min to several hours, depending on the target RNA. To stop the reaction *BM-Purple* was removed, the embryos were washed twice in PBST and afterwards fixed in 4% PFA.

2.2.1.7.6 Analyzing whole-mount embryos

The embryos were transferred into 4% methylcellulose (sigma), on a hollow grinding slide and brought into a suitable position using a fine needle. The embryos were then analysed using a stereomicroscope (MZ16; Leica) and photographed with a digital camera (Leica).

2.2.1.8 Infection assays

2.2.1.8.1 Incubation method

PTU-treated embryos were dechorionized at 26-28 hpf. Bacterial suspensions were diluted in embryo media to a final volume of 5ml. The embryos were incubated with the bacteria in petri-dishes at 28.5°C. By serial dilution and plating on LB-agar or Middlebrook-Cohn-7H10 agar the cfu/ml was determined. For each bacterial concentration tested (see Fig. 3.20) 20 embryos were used. The survival rate of the embryos was measured from 1 day post infection (dpi) up to 6 dpi. Control embryos were grown in embryo media.

2.2.1.8.2 Infection method

At 24-32 hpf dechorionized embryos were anesthetized using tricaine and arranged on agarose plates for infection. Infection was achieved by injecting the bacteria into the embryonic blood island or the caudal vein. To determine the amount of injected bacteria, control injections were performed in 100 µl of sterile PBS and plated on LB-

Amp plates to count the colonies. After infection, embryos were washed in embryo media and incubated further at 28.5 °C to score survival or for RNA isolation.

2.2.2 Molecular biology protocols

2.2.2.1 Polymerase chain reaction (PCR)

2.2.2.2 PCR with double stranded (ds) DNA as template

To perform the PCR the Biometra UNO-Thermoblock (Biotron) was used.

Components for the PCR:

For one reaction 1-100ng template DNA were used. Furthermore 100nM sense Primer, 100nM antisense Primer, 100µM Desoxynucleotidtriphosphate (dNTP)-mixture (Sigma) and 1 × reactionbuffer were added. The end volume of the reaction was 50µl. 1µl of the Red Taq DNA Polymerase (1unit/µl) (Sigma) were required for each reaction.

PCR conditions:

- (1) 2 min at 95°C for Denaturation
- (2) 15 sec at 95°C
- (3) 30 sec at 55°C for primer annealing (temperature depending on the used primer)
- (4) 1 min at 72°C for DNA synthesis (time depending on product length; 1 min for 1kb)
- (5) 29 repeats of steps 2-4
- (6) 5 min at 72°C for elongation
- (7) hold at 16°C

The obtained PCR products were then run on an agarose gel (2.2.3) and extracted following the protocol of the Rapid GFX PCR DNA Purification Kit (Amersham Biosciences).

2.2.2.3 PCR with first strand synthesis as template

The used first strand synthesis was produced with RNA from embryos of different developmental stages. RNA was isolated from up to 100 embryos using the µMac mRNA isolation kit (Miltenyi Biotec) according to the protocol. The *SuperScript III First-Strand Synthesis System for RT-PCR* (Invitrogen) and oligo dT-primer or random

hexamers were used for the first strand reaction (set up according to kit protocol). PCRs were performed as described in 2.2.2.2 with 7.5ng template cDNA.

2.2.2.4 PCR with genomic DNA as template

To amplify the 5'UTR of *crfb1*, *crfb6*, and *crfb7* for the morpholino control experiments, as well as for the validation of the *irg* Primer and to analyze intron/exon boundaries for splice-morpholino design, genomic DNA was used as template for the PCR (PCR conditions see 2.2.2.2; primer seq. see materials table 1 and 2). Genomic DNA was isolated from embryos or adults. The obtained PCR product, and in parallel the *eGFP-pCS2+* vector for the morpholino control experiments, was digested with the indicated restriction enzymes (see table 2), purified as described (2.2.4) and extracted using the Rapid GFX PCR DNA Purification Kit (Amersham Biosciences). Afterwards the digested product and the plasmid were ligated (ligation see 2.2.7). The ligation was then used to transform DH5 α (Invitrogen) (transformation see 2.2.8).

2.2.3 Agarose gel electrophoresis

To separate nucleic acids depending on their size agarose gels were used. The amount of agarose was between 0.8 % und 2 % in 1 \times Tris-Acetate Electrophoresis (TAE)-buffer. 1/6 6 \times loading-dye was added to the samples. The 1kb hyperladder (Bioline) was used as DNA standard. and the gel was run in a horizontal flat bed gel chamber filled with 1 \times TAE. To visualize nucleic acids Ethidiumbromide was added to the melted gel (4 μ l Ethidiumbromide-solution (10 μ g/ml) in 100 ml) and the gels were analysed and pictured on a UV-Transilluminator (GelDoc EQ (Biorad)).

2.2.4 Extraction of PCR fragments from agarose gels (Gelextraction)

The fragment of interest was cut from the gel using a scalpel and transferred into a 1.5 ml eppendorf. The further extraction was done using the Rapid GFX PCR DNA Purification Kit (Amersham Biosciences) according to the manual.

2.2.5 Restriction enzyme digestion of DNA

The total volume of the reaction was 50 μ l. Depending on the following experiment 1-5 μ g of DNA were digested. Furthermore the reaction consisted of 1/10 reaction buffer and 10U of the desired restriction enzyme and was incubated for 1-2h at 37°C. Afterwards the DNA was cleaned doing a gel extraction (2.2.4) or a phenol-chloroform extraction (2.2.6).

2.2.6 Phenol-Chloroform Extraction and Ethanol precipitation

The standard way to remove proteins from nucleic acid solutions is to extract first with phenol: chloroform and then with chloroform. To the DNA protein mixture an equal volume of phenol-chloroform was added and mixed together until an emulsion forms (Vortex, 30 sec). It was then centrifuged at 13000g for 60s, at RT. Using a pipette, the aqueous phase was transferred into a fresh eppendorf tube and the organic phase was discarded. The phenol-chloroform extraction was repeated twice. Subsequently, an equal volume of chloroform was added to the sample, mixed (Vortex, 30 sec) and centrifuged at 13000g for 60s. Afterwards the aqueous phase was transferred to a new eppendorf tube. Subsequently an ethanol precipitation was performed to concentrate the DNA:

1/20 Vol 5M NaCl and 2.5 Vol Ethanol (100%) were added to the solution. The DNA was precipitated for ≥ 10 h at -20°C . This was followed by a centrifugation step at 13000g for 20 min. The pellet was washed using 70 % Ethanol and again centrifuged at 13000g for 5 min. Then the Ethanol was removed and the pellet was allowed to dry for 5 min before it was resuspended in H_2O .

2.2.7 Ligation

20-40ng of the vector were used for the ligation and the amount of the insert-DNA was adjusted to a molar ratio between 1:1 to 3:1 to the vector. Additionally the ligation reaction contained 1/10 ligation buffer (NEB), 1 μl Ligase enzyme (400,000 units/ml concentration) and finally autoclaved water to a final volume of 10 μl . The reaction was incubated overnight at 16°C and was used the next day to transform bacteria cells (2.2.8).

2.2.8 Transformation of bacteria cells

10 μl of the ligation mix or 10ng plasmid-DNA was transformed into 50 μl of competent *DH5 α* (Invitrogen). The competent bacteria were thawed on ice, and the plasmid –DNA or the ligation mix (2.2.7) were added. After 20min of incubation on ice, a heat shock was performed for 90s at 42°C . After 2min incubation on ice, 500 μl LB media was added and the transformed bacteria were incubated for 1h at 37°C and 200 rpm.

Following this, different concentrations of the transformed bacteria were plated on LB plates carrying the appropriate antibiotic resistance (100 $\mu\text{g/ml}$). The LB plate was then incubated over night at 37°C .

2.2.9 Growing of *Escherichia coli*

E. coli DH5 α (Invitrogen) was grown according to existing protocols (Sambrook et al. 2001).

DH5 α genotype:

F-, Φ 80, lacZ Δ M15, Δ (lacZYA-argF) U169, recA1, endA1, hsdR17 (rK-, mK+), phoA, supE44, λ -, thi-1, gyrA96, relA1, λ -

2.2.10 Minipreparation of plasmid DNA

Using sterile tips single clones were picked from the bacteria plate and transformed to 3-5 ml LB-medium containing the required antibiotic in a concentration of 50 μ g/ml. The culture was incubated overnight at 37°C. The next morning the plasmid preparation was performed using the alkaline extraction procedure after Birnboim (Birnboim and Doly 1979). 2ml of the bacterial culture were centrifuged for 1min (14000rpm). The supernatant was removed and the pellet was resuspended in 150 μ l P1 followed by addition of 150 μ l P2. The bacterial lysis and denaturation of genomic DNA was achieved by incubation for 5min at room temperature. 150 μ l P3 were added to neutralize the solution. After centrifugation for 10min at 4°C and 1400rpm, the supernatant was transferred into a new reaction tube. 1ml ice-cold 96%(v/v) ethanol was added, followed by 20min centrifugation at 4°C and 14000rpm. The supernatant was removed and the pellet washed in 1ml 70%(v/v) ethanol with subsequent centrifugation for 15min at 4°C. The supernatant was removed and the pellet was dried at room temperature. The pellet was solved in 30-50 μ l dH₂O or 5mM Tris (pH 8.0).

2.2.11 DNase-free RNase

RNase A was solved in 10mM NaAc(pH 5.2) to a final concentration of 10mg/ml and was incubated for 15min at 100°C. When the solution had cooled down to room temperature 0.1 volumes of 1M Tris-HCl (pH 7.4) were added to neutralize the pH.

2.2.12 Sequencing of DNA

The sequencing of DNA took place according to the dideoxy chain termination method (Sanger et al., 1977). The reaction was performed using the *Abi Prism BigDye Terminator Cycle Sequencing Kit F* with *AmpliTaq* DNA polymerase (Perkin Elmer Applied Biosystems). Sequencing reactions contained 1 μ l DNA (100-200ng), 1 μ l Primer (10 μ M), 1 μ l *BigDye* version 3.0 and 1 μ l *BigDye* sequencing buffer, at a total volume of 10 μ l.

Reaction profile:

Initial denaturation of DNA took place at 96°C for 1 min. At the beginning of a cycle, there were 10 seconds of denaturation at 96°C. The annealing of the sequencing primer took place for 15 seconds at 52°C (The annealing temperature depends on the sequence of the primer used). The extension was accomplished at 60°C for 4 min. The cycle was repeated 25-30 times.

Purification and analyses:

After the reaction the volume was adjusted to 20µl. The further cleaning and the analysis of the reaction were performed in the Sequencing Facility (Institute for Genetics, Cologne) according to their standards. The obtained sequence files were analysed using Vector NTI 10.0 (Infor Max, Inc.)

2.2.13 *In vitro* transcription to produce in situ probes

To produce labeled RNA probes the T3, T7 or SP6 polymerase (Roche) was used, depending on the promotor present on the template DNA. The probes were labeled using the *Digoxigenin-RNA Labeling Mix* from Roche.

The transcription reaction contained 200-500ng DNA, 1µl 10 X Labeling Mix, 1µl RNA Polymerase (20 U/µl), 1µl 10 X Transcription-buffer (contains 60 mM MgCl₂) and 0.5µl RNase Inhibitor (40 U /µl, Roche). The total volume was adjusted to 10µl with H₂O_{DEPC} (DEPC = Diethylpyrocarbonat). The reaction was incubated at 37°C for 2h and subsequently stopped by adding 1µl RNase free 0,2M EDTA. Purification of the transcripts was done by ethanol precipitation according to Roche protocol. The RNA pellet was resolved in a mixture of 20µl H₂O_{DEPC} and 20µl Formamide and was stored at -20°C.

2.2.14 Injection of morpholino oligonucleotides and mRNA into zebrafish embryos

2.2.14.1 Preparation of capped mRNA for zebrafish injections

Capped mRNA for overexpression of *ifnγ1*, *ifnγ2*, or *ifnφ1*, and for the different *crfb-5'UTR-GFP* morpholino control RNA was made using the mMessage mMachine kit (Ambion) according to the manual.

2.2.14.2 Morpholino design

The appropriate sequences for morpholino design were selected from the full length sequences of the gene candidates and sent to the company Gene tools for synthesis.

The sequences of all the morpholinos used in experiments are listed in the Materials section (table 3). Morpholinos were delivered lyophilized and were immediately diluted in H₂O. The concentration of the stock solution was 3 μ M.

2.2.14.3 Injection of zebrafish embryos

Zebrafish embryos were injected in the 1-2 cell stage into the yolk directly under the first cell(s). Embryos were put in a row on a dark agarose plate (1% Agarose in H₂O containing activated carbon), the water was removed and embryos were injected immediately using FemtoJet® and a Micromanipulator from Eppendorf. The used capillaries (Hildenberg) were pulled using a *Sutter P9 Micropipette Puller* (Sutter) (pulling conditions: heat 537, pull 100, velocity 100, time 150). The concentration of the morpholino was between 0.5 and 0.9mM, and additionally 0.1M KCL and 0.2%(v/v) Phenol red were added to the injection solution. mRNA was injected in range of 100-400ng/ μ l in a solution containing 0.1 M KCL and 0.2% Phenol red. After the injection the embryos were transferred into a petridish with embryo medium and incubated to the desired stage.

2.2.14.4 Isolation of genomic DNA

Genomic DNA was extracted either from embryos or from by fin-clipping from adult fish. The embryos or part of the fin were transferred into a 1.5ml eppendorf, the water was removed and 990 μ l DNA-extraction buffer as well as 10 μ l Proteinase K (Roche) were added. The tube was mixed (vortexed, 10 sec) and incubated for 3h at 55°C. Every 45 min the tube was mixed again (vortexed, 10 sec). Afterwards the DNA was precipitated by adding 1Vol of 100% (v/v) ethanol. The tube was inverted several times and the DNA was pulled out using a glass pipette and transferred to a fresh 1.5ml eppendorf containing 70% (v/v) ethanol. Subsequently, the ethanol was removed, the DNA was dried for 5-10 min at RT. Then the DNA was solved in 500 μ l low TE.

2.2.14.5 RNA isolation and first-strand synthesis (RT)

RNA was isolated from up to 100 embryos or adult tissue using the μ Mac3 mRNA isolation kit (Miltenyi Biotec) according to the protocol. The amount of RNA was quantified using a spectrophotometer (2.2.14.6). 300ng RNA were, in general, used as template for the RT-reaction. The *SuperScript III First-Strand Synthesis System for RT-PCR* (Invitrogen) and oligo dT-primer or random hexamers were used for the first strand reaction (set up according to kit protocol).

2.2.14.6 Quantification of DNA or RNA by spectrophotometric determination

To quantify the amount of DNA or RNA a Biophotometer (Eppendorf) was used. Reading was taken at a wavelength of 260/280 nm according to the manual.

2.2.14.7 Bacterial strains used for infections

E. coli (DH5 α) and *Y. ruckeri* (strain 4015726Q) and *V. anguillarum* carrying the dsRED-expressing pGEMDs3 plasmid (van der Sar et al. 2003) were grown in standard LB medium containing ampicillin (50 μ g/ml). *M. marinum* (ATCC 927) carrying the dsRED-expressing pGEMDs3 plasmid (van der Sar et al. 2003) were grown on Middlebrook-Cohn-7H10 agar (Becton Dickinson) which was enriched with ADC.

ADC-supplement:

2g glucose

5g BSA Fraction V

0.85g NaCl

in 100ml H₂O

E. coli were grown at 37°C, *Y. ruckeri*, *V. anguillarum*, and *M. marinum* at 30.5°C.

For infection with *E. coli*, *Y. ruckeri*, or *V. anguillarum* a 3 ml overnight culture was used. For co-incubation with *M. marinum*, colonies from plates were suspended in PBT.

Bacterial cultures or suspension were centrifuged for 3min at 4000 g, the supernatant was removed, and the pellet washed with PBS. Washing was repeated three times to remove traces of LB, Middlebrook-Cohn-7H10, and metabolites. After washing, the pellet was resuspended in 1ml PBS. Optical density was determined using Ultrospec 10 (GE Healthcare).

For injection of bacteria, the final injection solution contained the washed *E. coli* or *Y. ruckeri* diluted in PBS containing 1/10 Phenol Red.

2.3 Phylogenetic analysis

Standard web-based programs were used for sequence comparisons, alignments, and phylogenies (2.1.5). The phylogenetic trees in the figures were generated using the MEGA software package (Kumar et al. 2004). In all phylogenetic trees presented in this study complete sequences were used rather than only the conserved domains.

The alignments for generating the phylogenetic trees were performed with ClustalW using the Blosum matrix with standard parameters (Thompson et al. 1994). For the

phylogenetic reconstruction the neighbor-joining method (Saitou and Nei 1987) was used with a bootstrap test of 1,000 replicates. Gaps and missing data were treated as pair-wise deletions. The HMMs were generated using the software HMMER (Eddy 1998) and were visualized using the LogoMat-M method (Schuster-Bockler et al. 2004).

3 Results

The zebrafish has become a powerful model to study the immune system of vertebrates (Trede et al. 2004). The ontogeny of the myeloid and lymphoid cell types has been studied in great detail in the zebrafish (reviewed in {Trede, 2001 #155; Traver, 2003 #44}; see section 1.2). These findings have demonstrated that zebrafish possess the full set of immune cells which mediate the innate and acquired immune response in mammals. Furthermore, these and other studies have shown that the zebrafish is exceptionally well suited for the analysis of the innate immune system in vertebrates, especially since an acquired immune response is first detectable at 4-6 weeks of development (Lam et al. 2002).

Several proteins and genes with a function in innate immune defense mechanisms have been identified in the zebrafish. Large gene and protein families have been analyzed, the TLRs and the NITRs (Jault et al. 2004; Meijer et al. 2004; Yoder et al. 2001), both of which showed that immune-related protein families or members thereof have diverged and expanded in fish.

However, it was not clear whether the innate immune mechanisms operating in zebrafish are comparable to those employed by mammals or whether the complexity of these mechanisms is similar. In order to use the zebrafish as a model to study the innate immune system it was therefore of interest to determine whether the components that are known from mammals to be involved in innate immune processes are also present in the zebrafish.

Thus, an analysis was conducted to identify genes that encode homologs of mammalian innate immune components in the zebrafish genome. The results of this search are described in the first section.

Next, genes identified during the genome-wide search were analyzed for their potential function and their involvement in an innate immune response. In order to examine the innate immune response in the zebrafish embryo, infection assays were tested. Those results are presented in the second part.

3.1 *In silico* analysis of innate immune genes in the zebrafish

The advances in genomic resources for the zebrafish have made it both pertinent and feasible to determine which of the genes that encode components of the mammalian innate immune system are also present in fish. In addition to the zebrafish genome, the genomes of two pufferfish, *Takifugu rubripes* and *Tetraodon nigroviridis*, were

searched for homologs of mammalian innate immune components to assess the degree of conservation among different fish species.

At first, sequences of mammalian proteins involved in the TNF, IFN, TLR, and NLR signaling pathways were assembled. Putative homologs of genes encoding these proteins were identified using public databases like Ensembl (Hubbard et al. 2009), ZFIN (Sprague et al. 2006), or RefSeq (Pruitt et al. 2007). In cases when putative homologs could not be found in these databases, TBLASTN (Altschul et al. 1990) searches were performed to screen unfinished clones from the genome sequencing project and to trace sequences from the whole genome shotgun (WGS) project. Identified candidate sequences were analyzed in detail in their genomic context. Manual annotations to generate gene predictions were performed in collaboration with Gavin Laird and Mario Caccamo from The Wellcome Trust Sanger Institute, Cambridge, United Kingdom. For some predicted proteins, the identified sequences were not complete and could not be completed because the available DNA sequences were not sufficiently reliable. Nevertheless, the entire predicted protein sequences were compared rather than just conserved domains, for the divergence not only between the species but also between protein family members would otherwise not be appropriately reflected.

The MEGA software (Kumar et al. 2004) was used to compare the encoded fish proteins with their mammalian counterparts. The retrieved sequences were aligned with the ClustalW program using the Blosum matrix with standard parameters (Thompson et al. 1994). In some case these alignments were manually refined. For the phylogenetic reconstruction the neighbor-joining method (Saitou and Nei 1987) was used and a bootstrap test of 1,000 replicates was applied (Efron 1982; Felsenstein 1985). Since not all sequences are complete and validated, the phylogenetic trees presented in this study aim not to show precise evolutionary distances, but present relationships within protein families and between species.

The following protein groups and protein families were analyzed: adaptors, kinases, IRFs, STATs, TRAFs, class II cytokines and their receptors, and the NLR proteins. The results are presented in order.

3.1.1 Conserved protein families in mammals and fish

3.1.1.1 Adaptor proteins

Previous studies have demonstrated that several adaptor proteins interacting with the TLRs are well conserved in fish (Jault et al. 2004; Meijer et al. 2004; van der Sar et al.

2006). Indeed, as is described in the following, most mammalian adaptors have clear orthologs in the three fish species analyzed (Fig. 3.1).

The adaptors that are involved in innate immune signaling cascades constitute a very heterogeneous group of proteins that do not belong to one common protein family. The phylogenetic tree is therefore not rooted. For a better comparison of the identified proteins, diagrams of their protein structures were drawn (Fig. 3.1). Protein domains were identified by searching Pfam (Finn et al. 2008) or Smart (Letunic et al. 2009) databases. Some domains were not recognized by these programs, although manual inspection indicated clear conservation of the domains in proteins of different species. These domains were included in the diagrams.

Orthologous proteins have been found in each of the three fish species for MyD88, SARM1, TOLLIP, IKK complex associated protein (IKAP), NEMO, TAB1, TAB2, and TAB3, and in the zebrafish and *Takifugu* the gene encoding Tirap (Fig. 3.1).

However, only one homologous gene in each fish was found for the mammalian *TICAM* genes. The fish protein was equally distant to mammalian TICAM1 and TICAM2, indicating a duplication of an ancestral gene in the mammalian lineage and subsequent divergence of the two copies (Fig. 3.1).

The Tetraodon version of the Ikap protein contained two full repeats of the insensitive to killer toxin 3 (IKI3) domain. It has not been clear whether this prediction is due to an error in the genome assembly or whether the gene does indeed contain an internal duplication covering the whole length of the gene found in other species. The two halves of the predicted gene were treated as separate peptides in the phylogenetic tree and the diagram.

3.1.1.2 Kinases

The kinases were the protein family that exhibited the most apparent orthologies between fish and mammals (Fig. 3.2). Orthologs of all the essential kinases involved in PRR-mediated signaling were found in zebrafish and in most cases also in pufferfish. IRAK2, which is thought to serve as an accessory protein in combination with IRAK1, was not found in any of the three fish. This suggests that it has arisen from a duplication event that occurred within the lineages of terrestrial vertebrates, as it could also be found in the chicken and *Xenopus* genome. Alternatively, IRAK2 could have been lost specifically in the teleost lineage (it is also absent in *Medaka* and stickleback). However, this seems less likely because the cartilaginous fish appear to lack an IRAK2 homolog as well, as a search of the ray and shark genomes indicated. Conversely, duplications in the fish lineage were observed for Janus kinase 2 (Jak2)

and NF- κ B essential modulator-like kinase (NIK), whereas duplications for Ikka and Ripk5 were found only in the pufferfish genomes (Fig. 3.2).

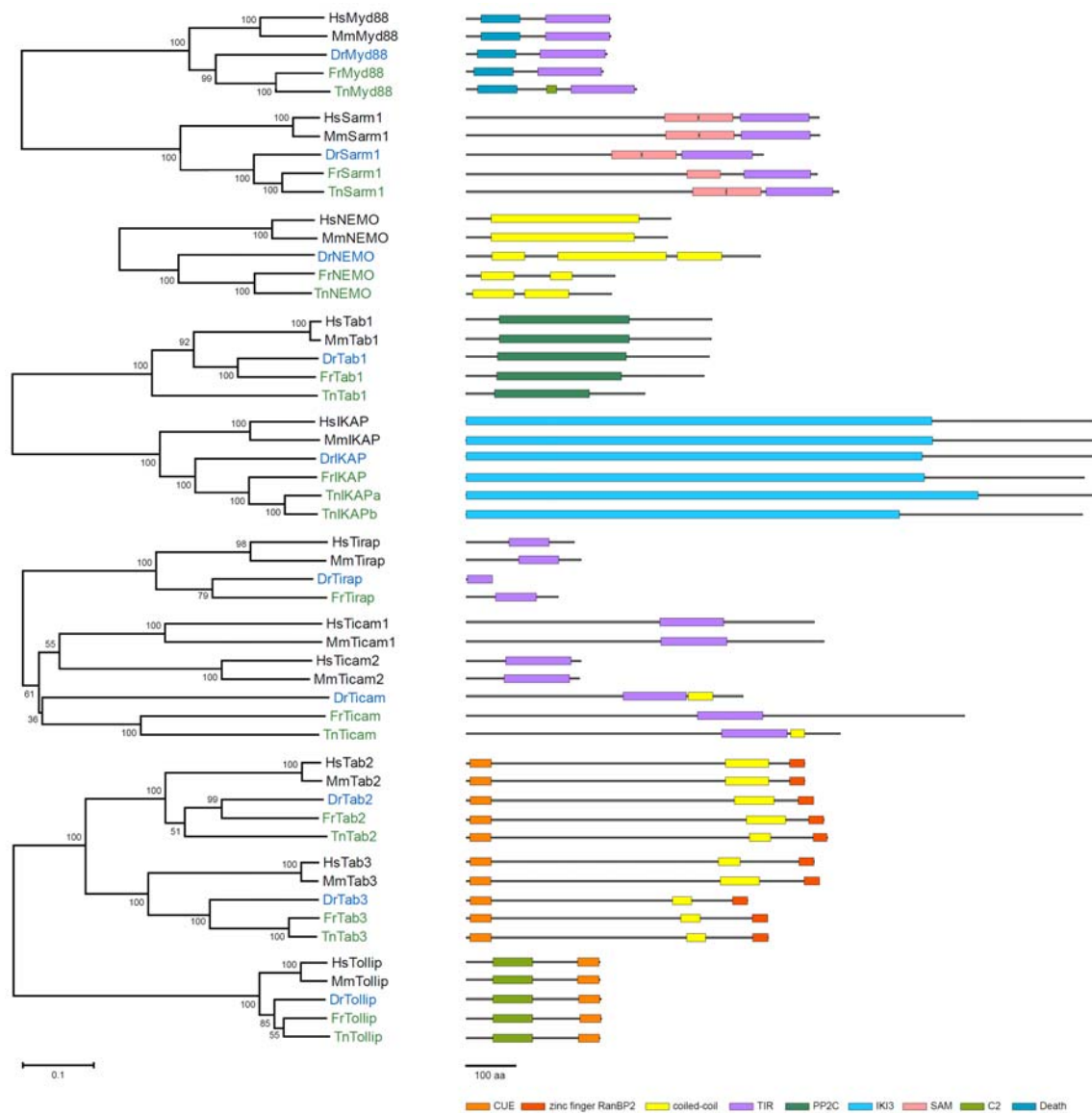


Fig. 3.1: Phylogenetic trees of the innate immune signaling adaptors and diagrams of their protein structures. The fish protein names are highlighted in blue (Dr (*Danio rerio*)) or green (Fr (*Takifugu rubripes*)) and Tn (*Tetraodon nigroviridis*). The branching order was verified by bootstrapping and bootstrap values (in %) are given. Generally, bootstrap values below 85% were regarded as not reliable, those above 95% as highly significant. The number of character changes is represented by branch length. Scale: interval of 0.1 amino acid substitutions. Hs, *Homo sapiens*, Mm, *Mus musculus*. Protein domains are shown as boxes based on identification by Pfam (Finn et al. 2008) or Smart (Letunic et al. 2009). Some domains were not recognized by these programs, although manual inspection indicated clear conservation of the domains in proteins of different species. These domains are also shown as boxes in the diagrams. The identities of the domains are listed at the bottom. Scale bar = 100 amino acids.

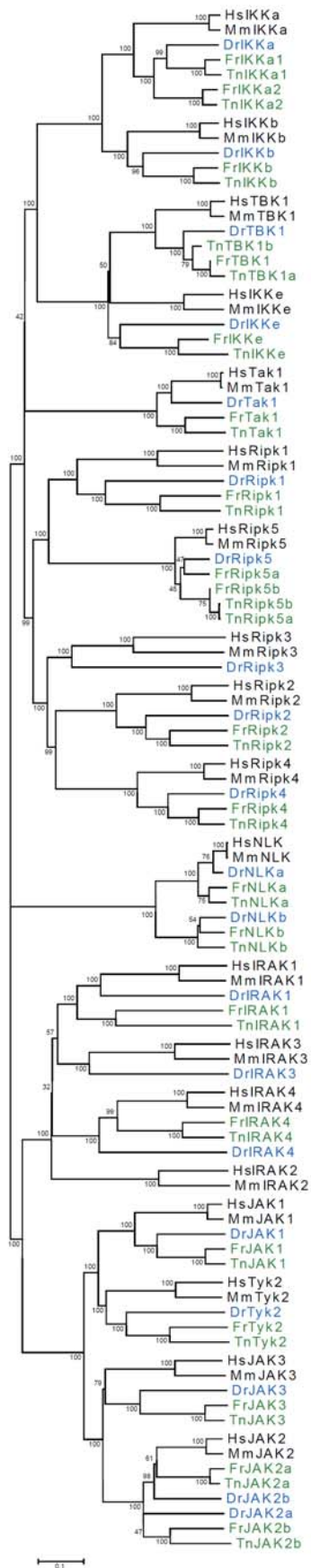


Fig. 3.2: Phylogenetic tree of the kinases.

For details see legend to Fig. 3.1.

3.1.1.3 Interferon regulatory factors (IRFs)

Interferon regulatory factors (IRFs) constitute a family of transcription factors which mediate virus-, bacteria- and IFN-induced signaling pathways and as such play a critical role in antiviral defense, immune response, cell growth regulation, and apoptosis. The IRFs are characterized by an amino- (N-) terminal DNA binding domain with five tryptophan repeats, which forms a helix-turn-helix motif. Besides IRF1 and IRF2, all other IRFs have a carboxy- (C-) terminal IRF association domain that mediates homo- and heteromeric interactions with other family members or transcription factors such as PU.1 or signal transducer and activator of transcription (STAT) (for review see (Mamane et al. 1999; Taniguchi et al. 2001).

For most of the IRFs (IRF1, IRF3, and IRF5 to IRF9), clear orthologous relationships were observed between mammals and fish (Fig. 3.3). In each fish, but not in mammals, an additional IRF was found. According to the nomenclature rule of subsequent numbering, it was named *Irf11*. The fish *Irf11* proteins were equally distant to both IRF1 and IRF2 and also lacked the IRF association domain (Fig. 3.3).

In the zebrafish a duplication of *irf2* was observed (*Irf2a* and *Irf2b*), of which *Irf2a* grouped together with *Irf2* from *Takifugu*, whereas *Irf2b* seems to have diverged. In *Tetraodon* no *Irf2* ortholog was found, but this might be due to the unfinished genome assembly (Fig. 3.3).

For *Irf4* three paralogous genes were found in the zebrafish (*irf4a*, *irf4b*, and *irf4c*). *Irf4a* grouped together with the mammalian IRF4 on one clade of the phylogenetic tree, whereas *Irf4b* and *Irf4c* grouped with the *Irf4s* from the pufferfish, with *Irf4c* appearing to be most divergent (Fig. 3.3). Interestingly, *irf4b* and not *irf4a* was found to map to a genomic region that was syntenic with the region containing IRF4 in mammals and in both pufferfish. This finding indicates that the *irf4b* gene in zebrafish represents the closest relative to the ancestral *irf4* gene, whereas the *irf4a* and *irf4c* gene most likely arose due to species-specific duplication.

In addition to the homologs of the IRFs in mammals and the newly identified *Irf11*, a further *Irf* was found in each of the fish. These predicted proteins were named *Irf10* since they showed a clear orthology to *Irf10* from chicken (Fig. 3.3). This gene seems to have been lost in mammals.

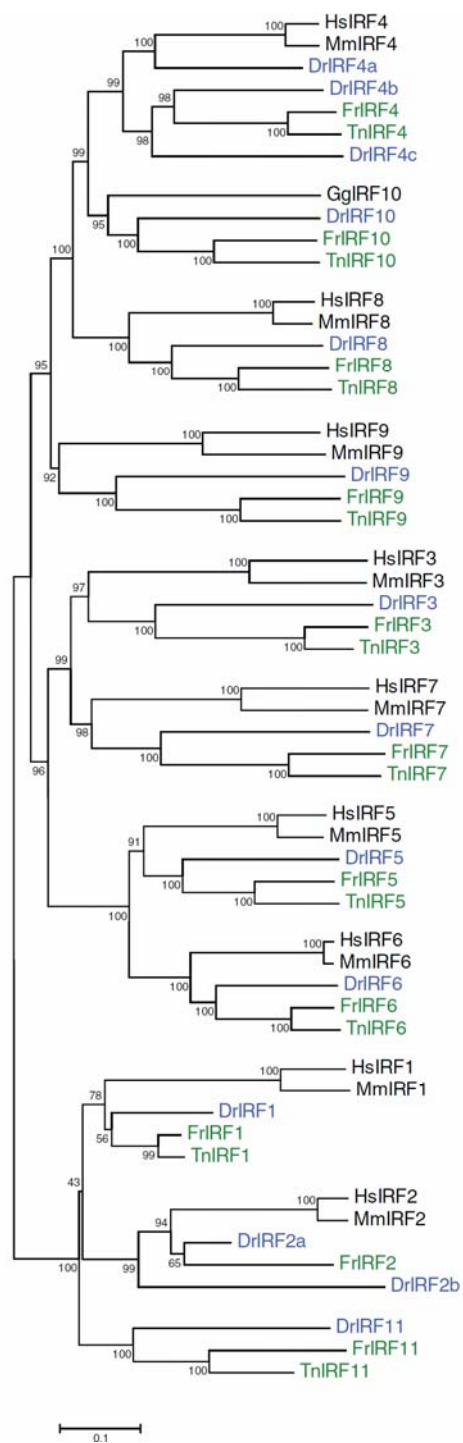


Fig. 3.3: Phylogenetic tree of the IRFs.

Details of the tree are as in Figure 3.1.

3.1.1.4 Signal transducers and activators of transcription (STATs)

STAT proteins comprise a family of transcription factors that are activated by a variety of cytokines, hormones, and growth factors (reviewed in (Darnell 1997; Subramaniam et al. 2001b)). STATs are activated through tyrosine phosphorylation, which is in most cases performed by JAKs. The phosphorylation induces conformational changes that promote dimerization and subsequent nuclear translocation of STAT proteins resulting in regulation of target gene expression. Although initially identified in mammals, JAK/STAT signaling components are highly evolutionary conserved as shown by their presence in invertebrate model organisms such as *Caenorhabditis elegans* and *Drosophila melanogaster* (reviewed in (Arbouzova and Zeidler 2006; Hou et al. 2002)). The mammalian STATs share sequence and domain structure, but the individual STATs have evolved distinct regulatory mechanisms of their intracellular trafficking and employ different transporters.

Clear orthologs of mammalian STAT2, STAT3, STAT4, and STAT6 were found in all three fish species (Fig. 3.4).

For mammalian STAT1 clear orthologs were observed in both pufferfish. In the zebrafish, however, two surprisingly divergent Stat1 proteins were found, but these still resembled STAT1 more than the other STATs. Analysis of the genomic loci revealed shared syntenic relationships between the duplicated zebrafish genes and human *STAT1* (Fig. 3.5). The entire region containing the *MFSD6/NAB1/GLS/STAT1/STAT4* genes on human chromosome 2 shares synteny with a region on zebrafish chromosome 9. On zebrafish chromosome 22 this arrangement of genes was also found to be syntenic, besides for *STAT4*, which has not duplicated in the zebrafish. The positions of flanking genes in the human and zebrafish genome showed indications of a number of rearrangements.

STAT5 has been independently duplicated in mammals and in zebrafish, as reported by Lewis and colleagues (Lewis and Ward 2004).

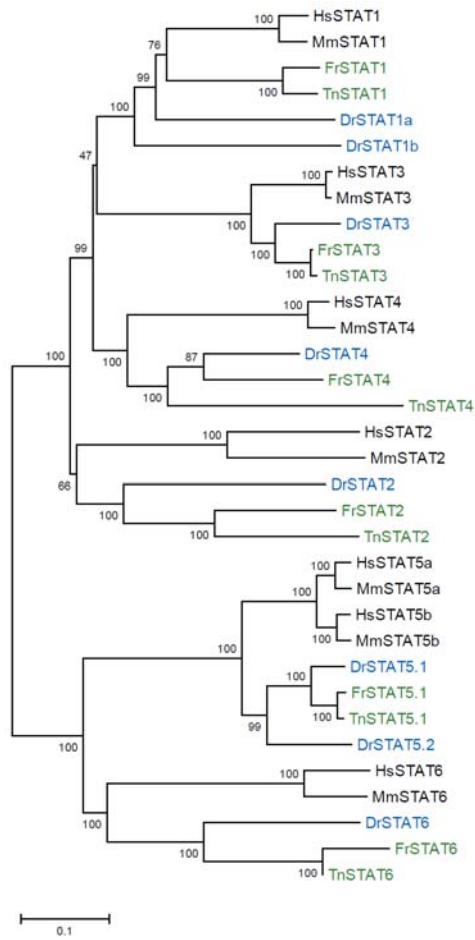


Fig. 3.4: Phylogenetic tree of the STATs.
 Details of the tree are as in Fig. 3.1.

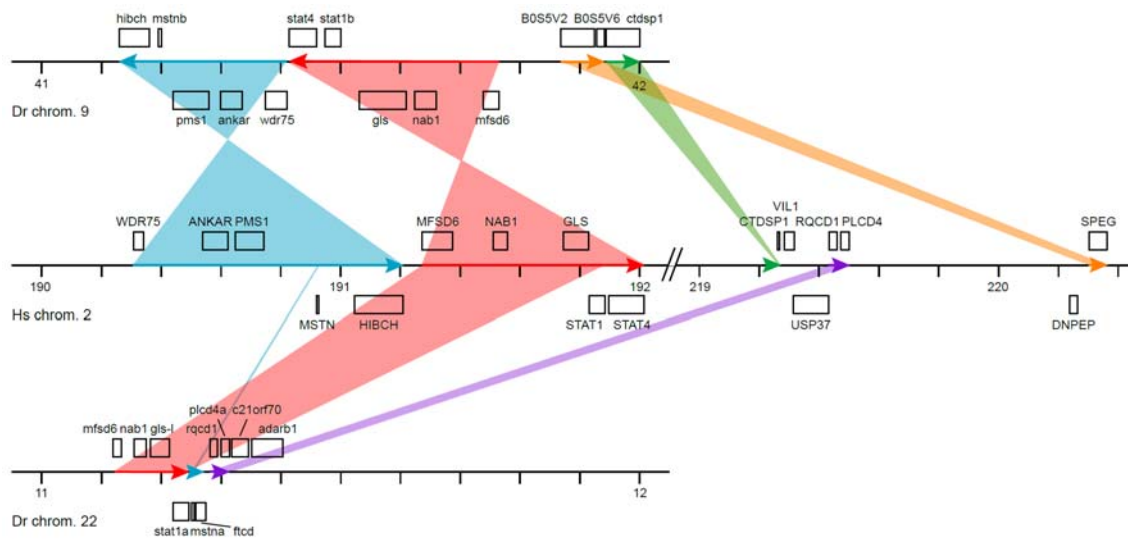


Fig. 3.5: (see legend on next page)

Fig. 3.5: (see previous page) Synteny between regions containing *STAT1* and *STAT4* in the human and zebrafish genome.

The region encompassing *STAT1* and *STAT4* genes on human chromosome 2 shares synteny with a region found on zebrafish chromosome 9. On chromosome 22 in the zebrafish genome a further syntenic region was identified, containing *mfsd6*, *nab1*, *gls-like*, and *stat1* genes, but lacking the *stat4* gene.

Genes transcribed on the top or bottom strands are shown above and below the lines representing the chromosomes. Homologous regions are shown by colored arrows and the syntenic regions, inversions and rearrangements are shaded in the corresponding colors. Numbers represent nucleotide positions in the genome in megabases based on the Ensembl zebrafish Zv8 assembly and the human GRCh37 (Genome Reference Consortium) assembly, both version 56. Gene names are Swissprot (Boeckmann et al. 2003), ZFIN (Sprague et al. 2006), or Ensembl (Hubbard et al. 2009) identifiers. The zebrafish *vil1* and *usp37* genes are located on chromosome 9 at position 47,633219-47,670916 and 1,570732-1,601113, respectively. The human ADARB1, C21orf70, and FTCD genes are located on chromosome 21 between megabases 46,5 and 47,5.

3.1.1.5 TNF-receptor associated factors (TRAFs)

The tumor necrosis factor (TNF) receptor-associated factors (TRAFs) are zinc-finger adaptor proteins, which participate in the regulation of a variety of different biological processes such as immunity, stress response, embryonic development, and bone metabolism (for review see (Chung et al. 2002). The protein family is evolutionary conserved, with family members in various multicellular organisms such as *Drosophila melanogaster* (Grech et al. 2000; Liu et al. 1999; Zapata et al. 2000), *Caenorhabditis elegans* (Wajant et al. 1998), and *Dictyostelium discoideum* (Regnier et al. 1995). Most of the seven mammalian TRAFs are linked to a receptor of the TNFR and the interleukin-1 receptor/Toll-like receptor (IL-1R/TLR) superfamily and participate in a signaling cascade leading to the activation of the NF- κ B and the JNK pathway (Arch and Thompson 1998).

The TRAF proteins (except for TRAF1) are characterized by an N-terminal cysteine- and histidine-rich region containing a RING finger of the C3HC4 type, which has E3-ligase activity and mediates protein-protein interactions, as well as further 1-3 TRAF-specific zinc finger motifs. These are in the majority of TRAF proteins followed by a coiled-coil (leucine zipper) motif. TRAF1 to 6 contain a meprin and TRAF homology (MATH) domain at their C-termini, which is involved in self-assembly and receptor interaction. TRAF7 harbors seven WD40 repeats at its C-terminus instead. These WD40 repeats have been shown to be responsible for interaction with mitogen-activated protein kinase kinase kinase 3 (MEKK3) and to be essential for TRAF7 potentiation of both MEKK3-induced AP1 and C/EBP-homologous protein (CHOP) activation (Xu et al. 2004).

All TRAF protein family members are represented in fish (Fig. 3.6). For TRAF3, TRAF6, and TRAF7 one orthologous protein was found in each of the three fish species, in all cases with the same domain structure and a high degree of similarity. Traf1 and Traf5 were present in zebrafish, but no predictions existed for genes encoding these proteins in the pufferfish genomes. In contrast to zebrafish Traf1, mammalian TRAF1 is lacking the RING finger and zinc finger domains (Fig. 3.6). These domains are present in all other family members of both lineages indicating that they were lost in mammalian TRAF1 after the split of teleosts and tetrapods. Traf4 is duplicated only in zebrafish, as has been observed by Kedinger and colleagues (Kedinger et al. 2005). Several duplication events in the fish lineage were observed for Traf2.

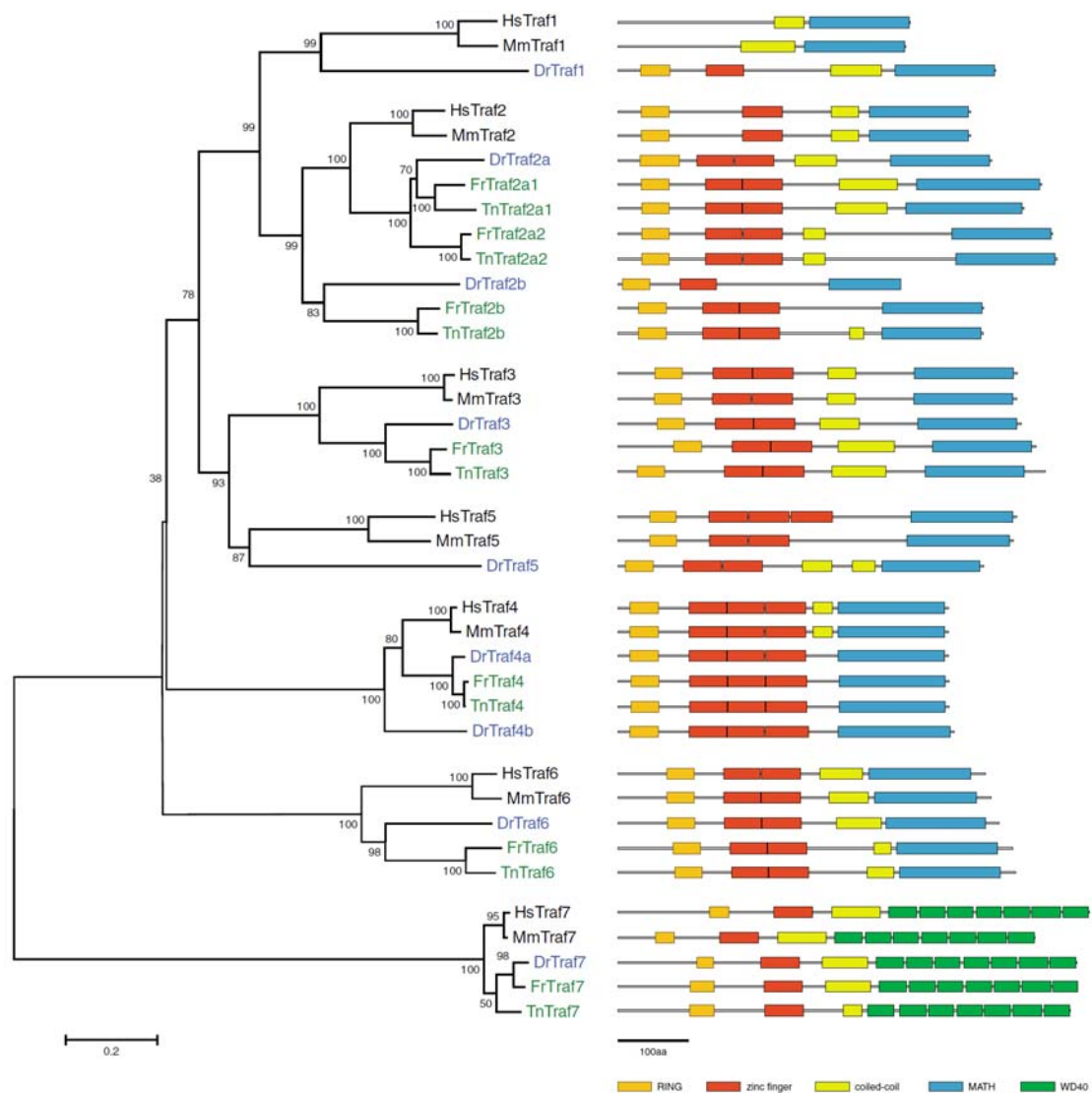


Fig. 3.6: Phylogenetic tree of the TRAFs and diagrams of their protein structures.

Details are as in Fig. 3.1, except that the scale shows 0.2 amino acid substitutions.

3.1.2 Divergent protein families: the class II cytokines

Class II cytokines orchestrate a variety of biological functions such as response against infection, inflammatory processes and antitumor activities (reviewed in (Pestka et al. 2004a; Pestka et al. 2004b; Renauld 2003). Although their homology on the primary sequence level is rather limited, all class II cytokines display a common four α -helical structure. Their genomic organization and structural characteristics indicate that they are derived from a common ancestor. Furthermore, these helical cytokines all bind to the extracellular binding domains of their cognate receptors, the class II cytokine receptors, which are defined by the presence of the extracellular binding domain (D200, see section 3.1.3) and can be clearly distinguished from class I cytokine receptors or hematopoietic receptors.

The class II cytokines can be subdivided into type I-III interferons and interleukin (IL) 10 and its relatives.

In humans, the large group of type I interferons comprises 13 IFN α proteins as well as IFN β , IFN ϵ , IFN κ , and IFN ω . All of these proteins are encoded by intronless genes. The type II interferon is represented by IFN γ , whose encoding gene has three phase 0 introns. The three human IFN λ genes forming the group of type III interferons contain four phase 0 introns. The same genomic organization was found for the genes encoding IL10 and its family members IL-19, -20, -22, -24, -26.

It has been speculated that during evolution after the split of teleosts and tetrapods a retroposition event occurred, through which the intronless type I IFN gene was generated in the tetrapod lineage (Lutfalla et al. 2003). The different type I interferon subtypes and especially the IFN α multigene family would then have diverged by asymmetric crossover, gene duplication and/or gene conversion after the radiation of the major mammalian orders (Diaz et al. 1994; Hughes 1995; Woelk et al. 2007).

Individual Ifns have been reported in several fish species with an ambiguous nomenclature (Altmann et al. 2003; Chen et al. 2005; Chen et al. 2009; Furnes et al. 2009; Grayfer and Belosevic 2009; Igawa et al. 2006; Long et al. 2006; Long et al. 2004; Lutfalla et al. 2003; Martin et al. 2007; Milev-Milovanovic et al. 2006; Robertsen et al. 2003; Savan et al. 2009; Zou et al. 2005; Zou et al. 2004). However, these studies examined only individual fish class II cytokines or limited sets of genes. In the course of this work, ten class II cytokine genes were found in the zebrafish, and five in each pufferfish (Fig. 3.7). The large group of mammalian type I IFNs was clustered on one branch of the phylogenetic tree that did not include any fish class II cytokines. This finding supports the hypothesis that the type I IFNs emerged after the split of teleosts and tetrapods.

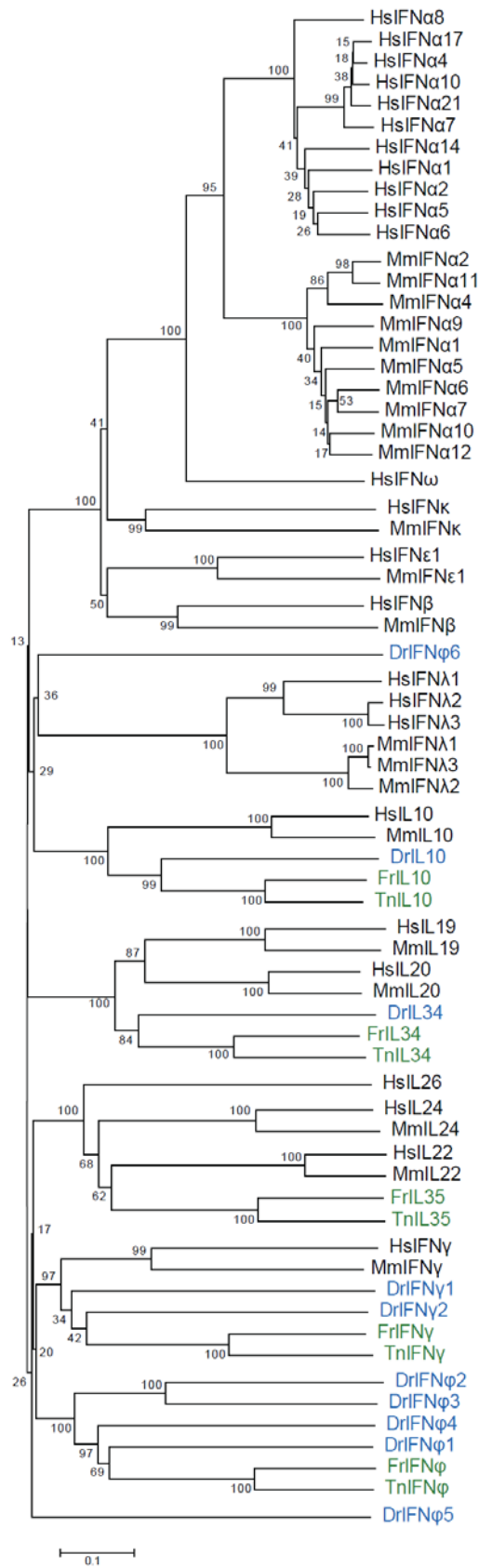


Fig. 3.7: Phylogenetic tree of the class II cytokines.
 Details of the tree are as in Fig. 3.1.

Clear orthologous relationships were observed between the IFN γ genes in all species analyzed. The pufferfish each have one *ifny* gene, whereas the zebrafish has two, *ifny1* and *ifny2* (Igawa et al. 2006), which lie in tandem in a position in the genome that has retained its synteny between mammals and teleosts (Fig. 3.8). Furthermore, all fish *ifny* genes share the intron/exon structure with mammals, namely three phase 0 introns. In the current Ensembl *Takifugu* and *Tetraodon* assemblies (Fugu 4.0 and Tetraodon 8.0, Ensembl release 56, (Hubbard et al. 2009) the *ifny* genes are incorrectly annotated, yielding an additional fifth exon due to the automated genebuild annotation, although the correct sequence is given as reference (Zou et al. 2004).

Apart from the clear fish orthologs of the mammalian type II IFNs, the remaining fish class II cytokines were more similar to the mammalian interleukins and type III IFNs. Like these, they are mostly encoded by genes containing four phase 0 introns, supporting the view that this constitutes the gene structure of the ancestral class II cytokine gene.

Among these class II cytokines, IL10 exhibited an apparent orthology with high bootstrap values between fish and mammals (Fig. 3.7) (Zhang et al. 2005; Zou et al. 2003). This is also supported by the finding that the *IL10* genes are situated adjacent to and on the opposite strand of the *MAPKAP2* genes in all five species (Fig. 3.8).

The genes that had been annotated as *il20* in the zebrafish (Refseq: NP_001076424.1) and *Tetraodon* (Uniprot: Q7SX60), and initially as *il19* and then changed to *il24* in *Takifugu* (Ensembl: SINFRUG00000154816) were found to be equally related to the mammalian *IL19* and *IL20* genes. The previous automated naming of the fish genes was therefore amended in this study. In concordance with the nomenclature rules for vertebrate gene families, this gene has been given the next available number in the interleukin series (*il34*) (Fig. 3.7). The fish *il34* genes and the mammalian *IL19*, *IL20*, and *IL24* genes are located in the vicinity of the *IL10* genes, but duplications and inversions have broken up the syntenic relationships downstream of *IL10* (Fig. 3.8). The phylogenetic analysis showed that it is likely that these genes derive from a common precursor, which has duplicated in mammals to yield *IL19* and *IL20* (Fig. 3.7). The data in the current release of the zebrafish genome assembly (Zv8, version 56) suggest that both the *il10* and the *il34* genes are duplicated. They are placed on subsequent contigs on chromosome 11 in opposite orientations, so that the first *il10* and *il34* genes are on the reverse strand (as in Fig. 3.8), whereas the second *il10* and *il34* genes are placed on the forward strand of the following contig. Since not only the coding sequence, but also the genomic sequence is absolutely identical for both supposedly duplicated genes, this duplication is most likely an artifact in the database, due to an incorrect assembly of subsequent contigs. In regard to the synteny observed

for this region between mammals and fish, the initially identified positions for the *il10* and *il34* gene have been retained in Fig. 3.8.

Whether the mammalian *IL24* gene is the product of a second local duplication or of an older duplication of a larger segment of the genome could not be determined, but it showed a higher degree of primary sequence similarity to the *IL22* and *IL26* gene found in a complex on a different chromosome (Fig. 3.8).

The second group of class II cytokines exhibiting sequence similarity and thus forming a clade in the phylogram, were mammalian *IL22*, *IL24* and *IL26*, and two pufferfish interleukins annotated as '*il24*' in *Tetraodon* (Uniprot: Q7SX82) and 'homologous to *il24*' in *Takifugu* (Ensembl: SINFRUG00000156387). The phylogram showed that this name was problematic, because these proteins were more similar to *IL22*. The encoding pufferfish genes exhibited the same syntenic relation to the flanking *mdm1* gene as the *IL22* genes in mammals (Fig. 3.8). However, the zebrafish gene in the same position (RefSeq: NP_001018628), annotated as *il22* (Igawa et al. 2006), was highly divergent in sequence. Because frequent gene duplications and loss of genes as well as rapid sequence divergence appear to operate within this family, originally orthologous genes may no longer be recognizable. This is further illustrated by the presence of the flanking *IL26* gene in the human genome. The mouse genome has lost this gene, whereas in other mammals (e.g. in the dog genome) an *IL26* ortholog is present. In the zebrafish a class II cytokine gene described as *il26* (Igawa et al. 2006) is present at this position, but in the phylogenetic tree the zebrafish protein did not cluster with the mammalian *IL22/24/26* group (Fig. 3.7). Although the interleukin genes between *MDM1* and *IFN γ* are in orthologous positions in all five species, there is no indication that the mammalian arrangement *MDM1/IL22/IL26/IFN γ* represents the ancestral cluster. It seems equally likely that these two *IL* genes arose by independent duplications of an ancestral gene in mammals and teleosts.

Because the names given to the fish cytokines of this group were extremely confusing and suggested relationships for which there has been no evidence, a new nomenclature was proposed, as shown in Fig. 3.7 and Fig. 3.8 (*ifn ϕ 6* for zebrafish *il22*, *ifn ϕ 5* for zebrafish *il26*, and *il35* for the pufferfish *il24*).

Finally, a group of teleost class II cytokines clustered on a clade without mammalian cytokines (Fig. 3.7). The bootstrap values for this branch and its internal nodes were comparable or even higher than those found for the other groups of orthologous proteins, arguing for a common origin. The majority of these fish genes have four phase 0 introns, as observed for the mammalian *IL10* gene, its related genes, and the *IFN λ* genes. However, they are not more closely related to mammalian *IFN λ* or *IL10* than to other class II cytokines. As these genes were only found in fish, they were

termed *ifn ϕ 1* to *ifn ϕ 4* (Fig. 3.7). *Ifn ϕ 1* has previously been described as 'zebrafish IFN (zIFN)', 'IFNab', and 'IFN λ ' (Altmann et al. 2003; Levraud et al. 2007; Lutfalla et al. 2003), and *Ifn ϕ 2* and *Ifn ϕ 3* as 'type I IFN 2' and 'type I IFN 3' (Zou et al. 2007), whereas *Ifn ϕ 4* had not been identified before. In each pufferfish only one *ifn ϕ* gene was found. Both pufferfish *ifn ϕ* genes appeared most closely related to the zebrafish *ifn ϕ 1* gene.

Taken together, of the ten class II cytokines found in the zebrafish, one is clearly an IL10 ortholog and another ortholog is present for its related proteins of the IL19/IL20 group, which seem to have duplicated in the mammalian lineage. In zebrafish, but not in the pufferfish, *Ifn γ* is duplicated. The six remaining zebrafish class II cytokines cannot be linked to mammalian class II cytokines as they are highly divergent. Therefore they were named *Ifn ϕ* . Four of these form a branch of their own in the phylogenetic tree together with one *Ifn ϕ* from each pufferfish. The remaining two zebrafish class II cytokines are highly divergent and rather appear as outgroups in the phylogenetic tree.

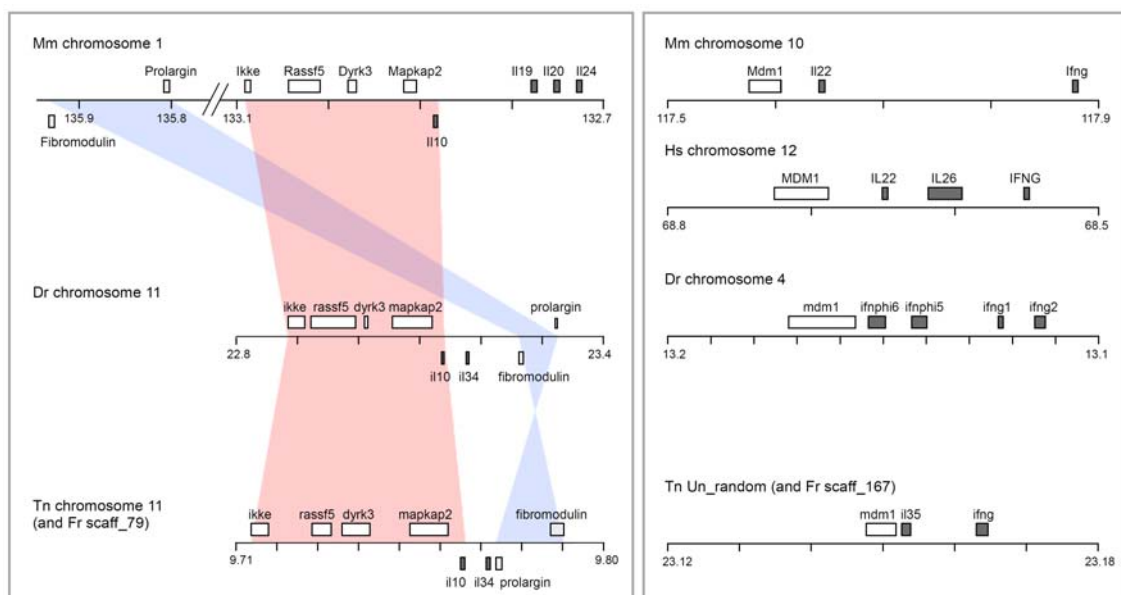


Fig. 3.8: Genomic organization of two class II cytokine gene clusters.

In the left diagram, the syntenic regions surrounding the *IL10* locus are shaded in red and blue. The human *IL10* gene is located on chromosome 1 and the region shows the same arrangement as in the mouse. The two pufferfish genomes exhibit the same arrangement both for the region around *il10* and for the *mdm1* - *il35* - *ifn γ* region, depicted in the right diagram. Chromosomes are shown as lines. Numbers represent nucleotide positions in the genomes in mega bases based on the Ensembl human GRCh37, mouse NCBI m37, zebrafish Zv8, Tetraodon 8.0, and Fugu 4.0 assemblies. Genes transcribed on the top or bottom strands are shown above and below the lines. Class II cytokine encoding genes are shaded in grey.

3.1.3 Divergent protein families: the class II cytokine receptors

The members of the helical class II cytokine receptor family (CRF2) are tripartite single-pass transmembrane proteins defined by structural similarities in their extracellular domain (Bazan 1990; Thoreau et al. 1991). The extracellular domain of 200 amino-acid residues, denoted as D200 domain, is composed of two tandem fibronectin type III (FNIII) domains, a structural motif in the immunoglobulin (Ig) fold superfamily. Conserved residues distinguish the D200 domains of CRF2 members from those of the Ig superfamily and the FNIII family (Bazan 1990; Du Pasquier 2001)

A large group of *CRF2*-like genes has been found in several fish species, but there are no clear orthologies between the receptors in mammals and teleosts (Krause and Pestka 2005; Levraud et al. 2007; Lutfalla et al. 2003). In *Tetraodon rubripes*, 11 genes have been identified and named *cytokine receptor family B (crfb) 1* to *crfb11* (Lutfalla et al. 2003). The authors identified a syntenic relationship between the genomic region encoding IFN α receptor (IFNAR) chain 2, IL10 receptor (IL10R) chain 2, IFNAR1, and IFN γ receptor (IFNGR) chain 2 in mammals and a region containing six class II cytokine receptor genes in *Tetraodon*.

A subsequent study (Krause and Pestka 2005), which included all available sequences throughout the animal kingdom, came to a slightly different conclusion regarding the phylogenetic relationships. In this study the authors subdivided the genes into groups encoding ligand-binding and non-ligand-binding chains before conducting their phylogenetic analysis. However, the justification for the assignment of particular fish genes that have no clear orthologs in mammals to one or the other group was not obvious, especially because no sequence data were given in this study that unambiguously identified the genes analyzed.

Therefore the phylogeny of the class II cytokine receptors in teleosts and mammals was revised in this work.

As had been pointed out previously (Lutfalla et al. 2003), the bioinformatic identification of class II cytokine receptor genes is not trivial, and it was therefore unsurprising that Ensembl contained predictions for only ten such genes in zebrafish.

Three of these did not encode class II cytokine receptors but code for thrombopoietin and titin, which have similar domains. To identify further receptor genes, the zebrafish genome was searched as well as all available zebrafish expressed sequence tags (ESTs) for the subdomains SD100A and SD100B, which constitute the D200 extracellular domain.

In total, 22 candidates were identified, of which seven had incomplete D200 domains or exhibited only limited resemblance to D200 domains. These and the three genes for

thrombopoietin and titin were excluded from further analysis. Gene predictions were available for eight of the remaining 12 putative receptor genes.

Of the four genes that had not been predicted by automated annotation tools, two (*crfb15* and *crfb16*) were found only in the as yet unplaced whole genome shotgun sequences. All 12 genes were re-annotated, using the known gene structure of class II cytokine receptor genes and homology to known class II receptor genes as support. The sequences were used for a phylogenetic analysis, which, in addition to the mouse and human sequences, also included *Takifugu rubripes* and *Tetraodon nigroviridis* Crfb1 to Crfb11 and Il20r2, as well as an additional gene, the product of which was called Crfb13. A set of recently described zebrafish class II cytokine receptor genes included two genes not identified in this study (*crfb2* and *crfb6*), which were added to the analysis (Levraud et al. 2007). Finally, DrCrfb14 was found by Georges Lutfalla, who generously contributed its sequence for inclusion in this analysis.

The phylogram of the class II cytokine receptors (Fig. 3.9) corroborated previous conclusions that this gene family had undergone independent gene duplications and divergence in teleost and mammals. Some of the fish genes could not be matched to likely orthologs in mammals, and vice versa, with four exceptions in which high bootstrap values justified the interpretation of the genes sharing direct common ancestors. The gene encoding tissue factor (TF) (recently renamed to coagulation factor III (F3)) in mammals, clustered with two genes from each fish. The phylogeny indicated independent duplication events in the pufferfish and zebrafish lineage. The pufferfish genes were identified by Georges Lutfalla, who had named them Tf1 and Tf2 (Lutfalla et al. 2003). To reflect the independent duplications in zebrafish and pufferfish, the zebrafish genes were termed Tfa (F3a) and Tfb (F3b).

The other set of genes that reliably grouped together were those encoding IL20R1, IL20R2, and IL22 binding protein (IL22BP), with one representative in each of the mammals and fish. The corresponding orthologs in fish are: Crfb8 (IL20R1); DrCrfb16, Fr/Tn Il20r2 (IL20R2); Crfb9 (IL20BP). For the other relationships between mammalian and fish proteins the low bootstrap values showed that the relationships discussed below must be considered with caution. Generally, bootstrap values higher than 85% were regarded as acceptable, those above 95% as significant. Several mammalian genes had no plausible orthologs in the three fish genomes analyzed, and others had more than one.

Therefore further evidence for evolutionary relationships was sought by analyzing the genomic context of the genes. A summary is shown in Fig. 3.10.

Two sets of genes were linked both in mammals and in the two pufferfish. The first has been the *IFNAR2*, *IL10R2*, *IFNAR1*, and *IFNGR2* complex and its syntenic complex

described by Lutfalla and colleagues for *Tetraodon* (Lutfalla et al. 2003). This synteny has also been maintained in *Takifugu* and in all three cases continued outside the class II cytokine receptor complex, in that the gene neighboring *IFNGR2* is *TM50B* in all cases, followed by *NNP1*. However, the corresponding genes in the zebrafish were found to be no longer linked. The synteny was roughly reflected in the sequence similarities, that *IFNAR2* was most similar to *Crfb1* and *Crfb2* and that the *IL10R2/IFNAR1/IFNGR2* group clustered with the *Crfb3* (only in the pufferfish) /4/5/6/15 group. In particular, the *IL10R2/IFNAR1/IFNGR2* and *crfb3/4/5/6/15* genes encoded receptors with short cytoplasmic domains, whereas *IFNAR2* and *Crfb1* and *Crfb2* had long cytoplasmic tails. However, orthologies were not clear within the group. Therefore it was not possible to conclude whether the ancestral complex that existed before the split of the teleosts and tetrapods contained two genes (a precursor for *IFNAR2* and a precursor of the *IL10R2/IFNAR1/IFNGR2* group) with subsequent independent duplications in teleosts and mammals, or four genes, with fast divergence in the *IL10R2/IFNAR1/IFNGR2* and the *crfb3/4/5/6/15* groups obscuring their common origin.

The second region, in which a syntenic arrangement of genes was observed to have been retained, is the one containing *IFNGR1*, *IL20R1*, and *IL22BP* in mammals, and *crfb9* and the previously undetected *crfb13* in *Tetraodon* and *Takifugu*. Again, the closest relatives of these genes (*crfb9* and *crfb13*, respectively) were not syntenic in zebrafish. Notably, fish *Crfb9* proteins shared the absence of a transmembrane domain with the mammalian *IL22BPs*. In view of this and the syntenic arrangement, the most reasonable interpretation is a homology of *IFNGR1/Crfb13* and *IL22BP/Crfb9*. In summary, teleost fish have approximately the same number of class II cytokine receptors as mammals, but the genes have evolved rapidly and independently since the separation of the species.

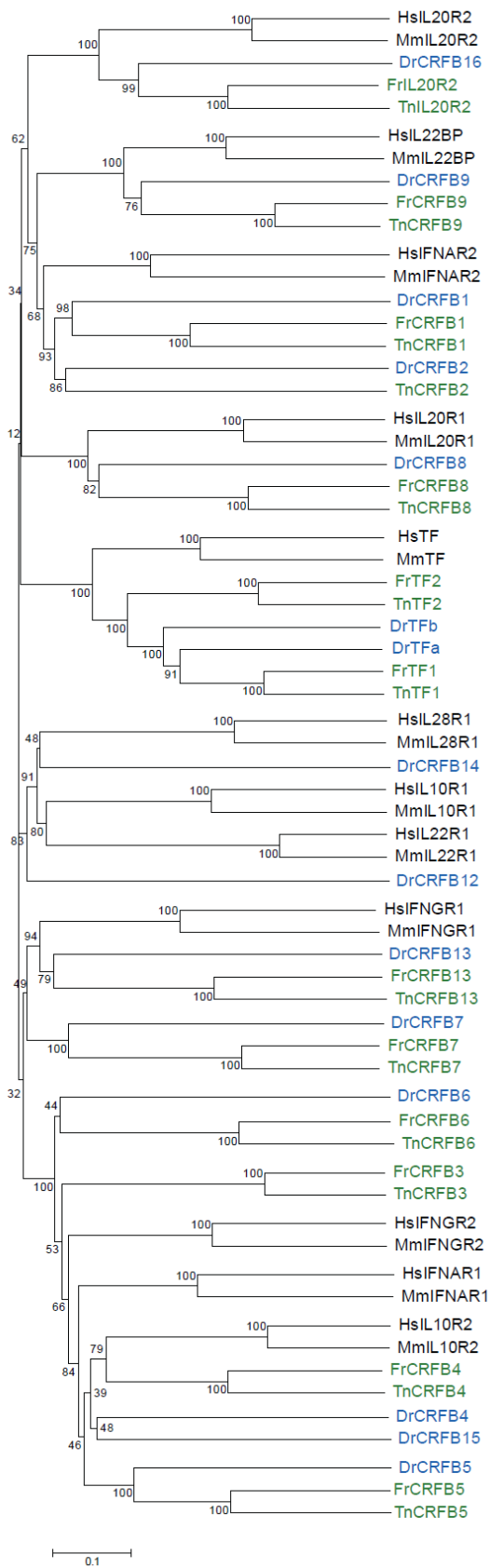


Fig. 3.9: Phylogenetic tree of the class II cytokine receptors.
 Details of the tree are as in Fig. 3.1.

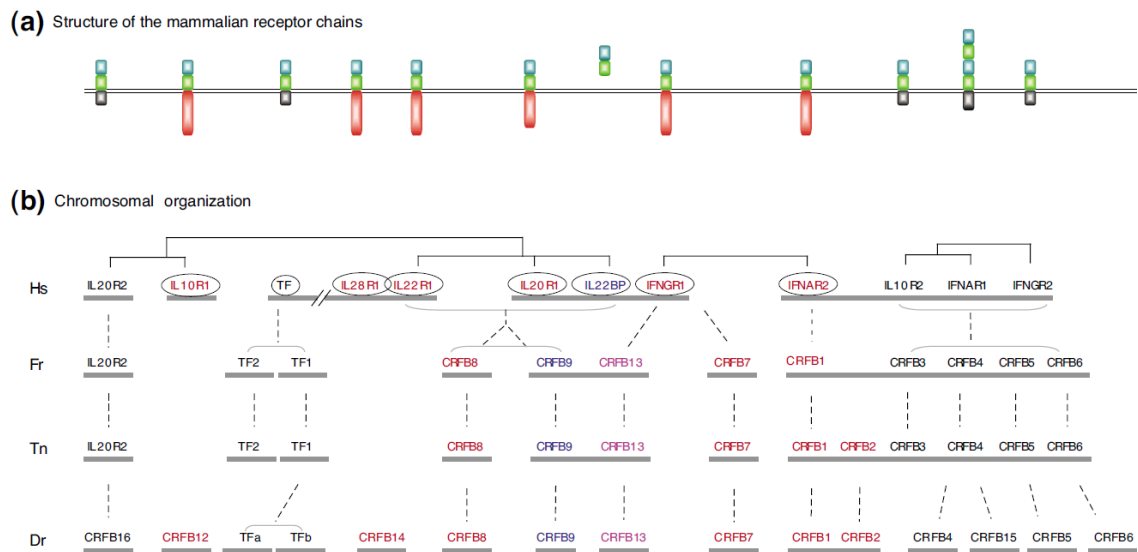


Fig. 3.10: Syntenic organization of class II cytokine receptor genes.

(a) Diagram of the structures of the mammalian receptor chains, with the blue and green rectangles representing the S100A and S100B domains, the red rectangle the intracellular domain of the ligand binding chains, and the grey rectangle the intracellular domain of the non-ligand binding chains and TF (after (Renauld 2003).

(b) Synteny between regions containing class II cytokine receptor genes in mammals and fish.

Fat horizontal lines indicate chromosomes in the four species. The brackets above the human genes show evolutionary relationships between the paralogs. Vertical broken lines indicate suggested evolutionary relationships between the genes in the different species, based on the tree in Fig. 3.9. Color coding of names: red: long intracellular domain; black: short intracellular domain; blue: no intracellular domain; pink: intermediate length intracellular domain. Circled names: ligand binding chains.

3.1.4 Divergent protein families: the NLR proteins

A large family of cytoplasmic proteins, characterized by the presence of a nucleotide-binding domain, the NACHT domain (Damiano et al. 2004; Koonin and Aravind 2000) or the closely related NB-ARC domain (van der Biezen and Jones 1998a), has been implicated in inflammation and innate immune signaling in animals and plants (see section 1.4.3). Some of these have been shown to recognize intracellular pathogen associated molecular patterns (PAMPs) through their C-terminal Leucine-rich repeats (LRRs). They differ in their N-terminal effector domains, e.g. CARD or pyrin domains, which mediate signal transduction to downstream targets ultimately leading to the expression of proinflammatory cytokines or the activation of the apoptotic pathway (see section 1.4.3).

An initial search in the fish genomes for homologs of the known mammalian NLR proteins of the NOD subfamily yielded orthologs for NOD1 and NOD2 in zebrafish and *Takifugu*, and for NOD3 (recently renamed as NLRC3) and NOD9 (recently renamed as NLRX1) in all three fish species. Two proteins in zebrafish and *Takifugu* and one in *Tetraodon* were annotated as ‘NALPs’ but did not group with the mammalian NALPs on the phylogenetic tree. No clear orthologs were found for any of the mammalian NALPs in fish (Fig. 3.11).

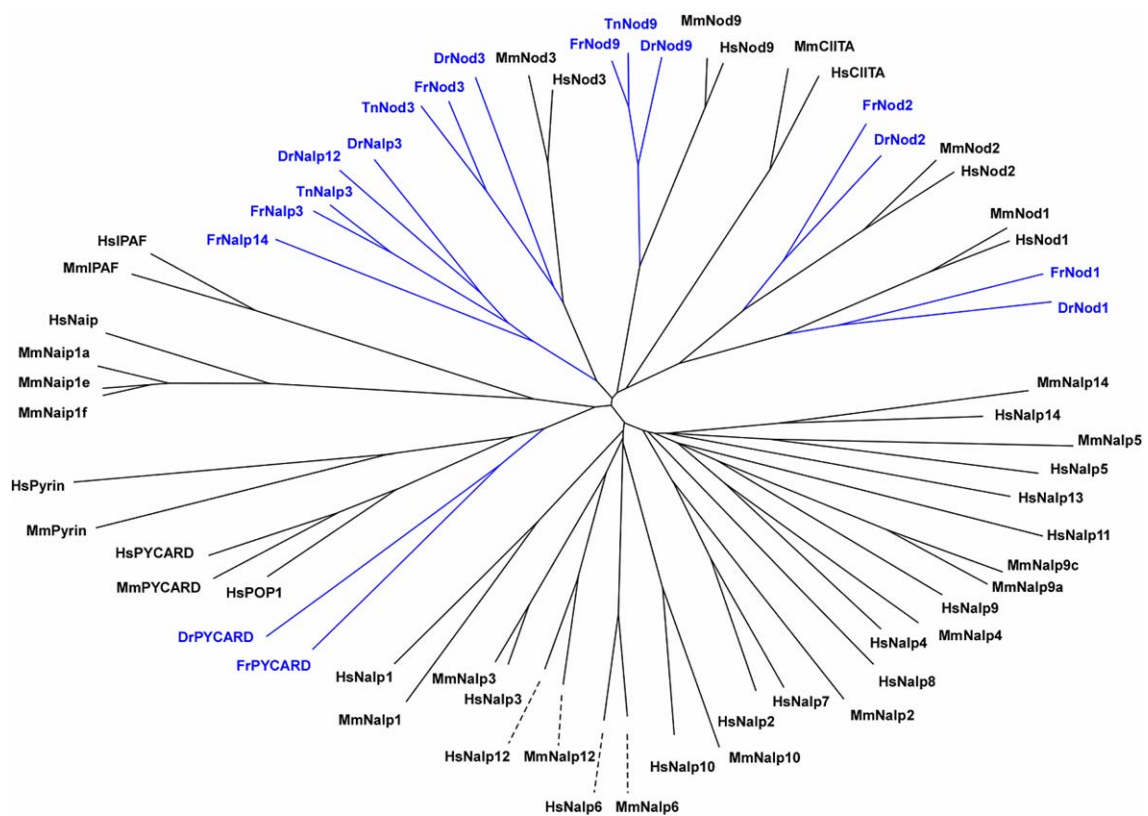


Fig. 3.11: Unrooted phylogenetic tree of the initially predicted set of NLRs and their adaptors in fish and mammals.

Orthologs of mammalian NOD (NLRC family and NLRX1) proteins were found in fish. Predicted piscine ‘Nalps’ did not group with mammalian NALPs (NLRPs). There were no orthologs in fish for mammalian CIITA, IPAF (NLRC) or NAIP proteins.

This unrooted tree illustrates the relatedness of the predicted protein sequences without making assumptions about common ancestry. Therefore the presence of additionally analyzed NLR adaptor proteins (PYRIN, PYCARD (also called ASC), and POP1), did not interfere with the construction of this tree. The number of character changes is represented by branch length. Mammalian NALP6 and NALP12 showed a much longer branch length compared to the other NLRs. To represent this, a dashed line is used.

The sequences used for generating this tree had been retrieved before a new nomenclature system for human and mouse NLR genes had been agreed upon (Ting et al. 2008). Mammalian proteins are depicted in black, fish proteins in blue.

With the subsequent release of the zebrafish genome assembly those annotated NALP-encoding genes were retired.

When the whole zebrafish genome assembly was then screened for sequences encoding the NACHT-domain, a large number of highly similar sequences were found, but none of these were located within annotated or even *ab initio* predicted genes by GeneScan, the automated gene prediction algorithm. It turned out that these sequences were omitted from annotation, exactly because their number and the similarity between them was so high, so that they were regarded as repetitive elements within the zebrafish genome.

These genes were therefore manually annotated using ESTs as guides. A large set of novel NACHT-domain containing genes was identified. After completion of the initial annotations, automated predictions for 205 NACHT-domain encoding genes were deposited at RefSeq (Pruitt et al. 2007). These showed only a partial overlap with the sequences generated by manual annotation and many of the RefSeq predictions were incomplete or contained two NACHT domains, indicating incorrect annotations. Thus, the zebrafish genome was re-screened and re-annotated. Finally, more than 200 genes of this class were found. These were numbered sequentially by chromosome number and by their order on the chromosome. It was not possible to produce perfect gene models for all of them, because, as described below, they encoded novel N-terminal sequences. In the absence of sufficient EST evidence, reliable conclusions for the 5' ends of the genes could not be drawn in all cases. Similarly, the C-terminal regions encoding the LRRs were difficult to predict reliably.

The two pufferfish genomes were also searched for members of this gene family to find out whether the group found in zebrafish was specific to this species, or whether the massive gene duplication had occurred early in the fish lineage. 70 members of this family were found among the annotated genes in the genome of *Takifugu rubripes*. A large number of matches found in the *Tetraodon* genome were not part of predicted or annotated genes, as had been the case in the zebrafish. Again, these sequences had been masked as repeats. A set of sequences was then manually assembled using homology to the zebrafish and *Takifugu* sequences as guides. The majority of the members of this gene family, 40 out of 49, were located within incompletely assembled contigs/scaffolds that had not been assigned to chromosomes (the 'Un_random' set). Initially, the searches for NACHT-domain encoding genes in the *Tetraodon* genome resulted in a number of predictions that spanned separate contigs, but which had additional fragments of genes of this family interspersed within their predicted introns. This suggested that these predictions were not correct, but were due to accidental occurrence of apparently spliceable gene fragments in neighboring contigs of this

assembly that were in fact not located next to each other in the genome. This view was supported by the finding that three sequences, which were very closely related to consecutive parts of the other fish *nod2* genes, were positioned on widely separated contigs in the Un_random assembly. These three fragments were combined into one sequence, which was called TnNod2.

3.1.4.1 NLR protein families in mammals and fish

A phylogenetic tree of all 277 NLR-like proteins from human, mouse, and the three fish species revealed the following relationships (Fig. 3.12). The 'canonical' NOD proteins NOD1, NOD2, NOD3 (NLRC3), NOD9 (NLRX1), as well as APAF1 and CIITA, were present in all five species, and showed clear orthologous relationships (Fig. 3.13). Although not a member of the NLR family, APAF1 was included in the analysis, because of its relation to the family due to the presence of the NB-ARC domain (see section 1.4.3).

The NALP/NLRP proteins formed a separate branch, representing a mammalian expansion of NLR proteins. For most of the proteins on this branch, there were closely related pairs of mouse and human proteins, but several cases of mouse- or human-specific duplications could also be found, notably the mouse *Nalp4* (*Nlrp4*) genes. Two zebrafish sequences that clustered with this group, 2.03 and 2.05, consisted only of a NACHT domain with a divergent P-loop and should therefore not be considered NALP-(NLRP-) like proteins.

Similarly, mammalian IPAF (NLRC4) and NAIP proteins had no orthologs in fish. Although IPAF and NAIP contain different N-terminal effector domains (CARD and BIR repeats, respectively), they clustered on one clade in the phylogenetic tree (Fig. 3.13). The high bootstrap values suggested that they share a common ancestry, and arose most likely during the mammalian radiation. This is supported by the observation that NAIP-like proteins could not be identified in other terrestrial vertebrates, or are, at least currently, not annotated in the genomes of birds (chicken and zebrafinch), amphibians (*Xenopus*) or reptiles (Anole lizard). A putative IPAF (NLRC4) ortholog was found to be predicted for the Anole Lizard (*Anolis carolinensis*), but it remains to be determined whether a clear orthology can be established or whether this predicted protein represents a divergent homolog of other NOD (NLRC) proteins.

Most striking was the observation that the large groups of newly identified fish sequences lay on mostly species-specific branches (Fig. 3.12). The majority of the zebrafish proteins formed a branch of their own, which included no proteins from either of the two pufferfish.

Consistent with the closer relationship between the two pufferfish, the proteins from these two species were less clearly separated. Whereas one branch contained exclusively a subset of proteins from *Takifugu*, the branch that comprised the majority of *Tetraodon* proteins also included several *Takifugu* proteins. There were two branches with several cases of apparent orthologies between *Takifugu* and *Tetraodon*, i.e. proteins from the two species that were more similar to each other than to any other predicted protein in their own species, indicating the existence of the encoding genes before the split of the two species and suggesting conservation of their function. Again, it is of note that the *Tetraodon* protein predictions were less reliable and often incomplete, leading to spurious homology-assignments. The relationship of these sequences to the other fish sequences therefore represents an approximate picture that must be interpreted with caution.

Whereas most of the novel fish NLR proteins were more related to each other than to mammalian NLR proteins, there were exceptions (beside the canonical proteins mentioned above).

One group of new fish proteins was identified, which was named NACHT-P1/ Nwd1 and clustered in phylogenetic trees with APAF1. To determine if this was a fish-specific NLR protein the mouse and human genomes were searched for similar sequences. One clear ortholog was found in each case, neither of which had been characterized previously. Their N-terminal parts contained no motifs known from other proteins. Like the APAF1 proteins these sequences contained WD40 repeats instead of LRRs (Fig. 3.13).

FrNACHT-P2 and TnNACHT-P2 had an unusual N-terminal addition, a filament-domain. No other sequence in any organism was found that encoded a protein composed of a filament-domain in conjunction with a NACHT-domain.

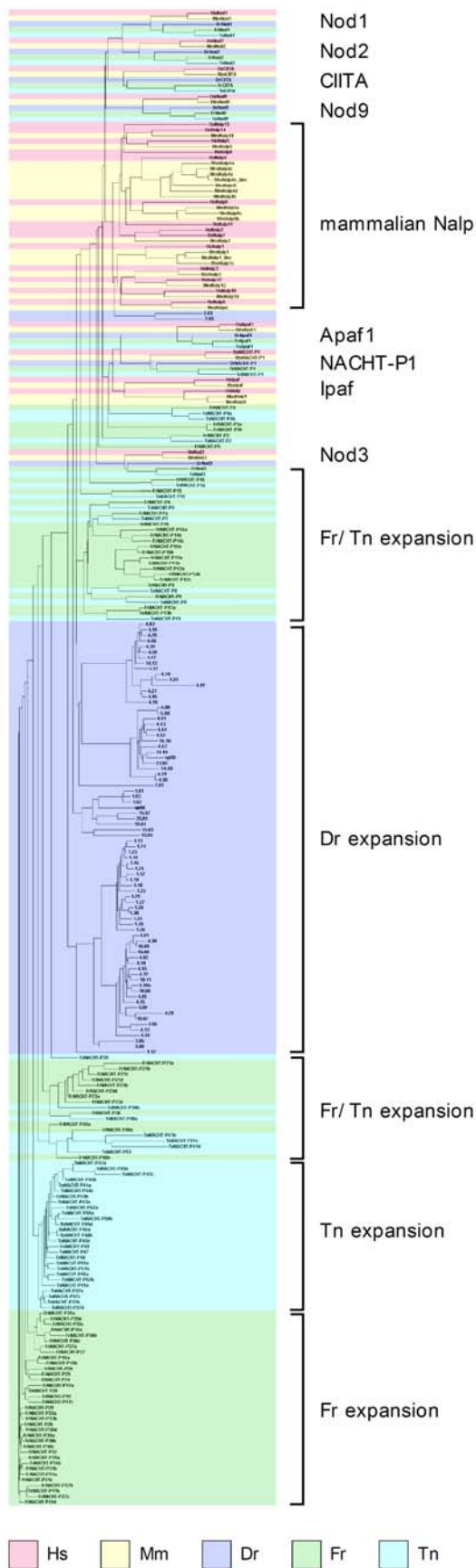


Fig. 3.12: (see legend on next page)

Fig. 3.12: (see previous page) Phylogenetic tree of 277 NLR proteins.

Each sequence has been assigned a background color to illustrate species relationships: pink =human, yellow = mouse, blue = zebrafish, green = *Takifugu*, and turquoise= *Tetraodon*. The 'canonical' proteins NOD1, NOD2, NOD3 (NLRC3), NOD9 (NLRX1), CIITA, and APAF1, which show clear homologous relationships between the five species, cluster at the top (rainbow colors). The mammalian NALP (NLRP) proteins cluster together (pink/yellow region). Each fish has a large group of species-specific proteins (blue, green, and turquoise regions). In addition, *Takifugu* and *Tetraodon* share several apparently orthologous gene pairs (green and turquoise region).

The phylogenetic tree was generated using ClustalW phylogenetic calculations based on the neighbor-joining method of Saitou and Nei (Saitou and Nei 1987).

3.1.4.2 Fish-specific NLR proteins

The large groups of novel, fish-specific Nlr proteins were highly conserved in each species, indicating recent species-specific expansions (Fig. 3.12). Like other NLR proteins, they contained C-terminal LRRs. However, the majority of the fish NLRs did not contain any of the N-terminal effector domains that had been found in conjunction with NACHT-domains in mammals or plants (such as CARD, PYD, or TIR domains).

Not only the NACHT-domain, but also the region immediately upstream of the NACHT domain was found to be highly conserved in all of the fish proteins (Fig. 3.14). To find out whether this region corresponded to other known peptide motifs, a statistical model was generated, using multiple sequence alignments of this conserved region. These profile Hidden Markov Models (HMMs) (Eddy 1998) specify position-specific letter emission distributions and also position-specific insertion and deletion probabilities to describe the conserved region upstream of the NACHT-domain. To visualize the generated HMMs the LogoMat-M method (Schuster-Bockler et al. 2004) was used (Fig. 3.15).

The profile Hidden Markov Model (HMM) built from the zebrafish sequences was used for a BLAST search (TBLASTN) of the mammalian genomes. No good matches were found. When the three fish genomes were searched, only those genes were found in the zebrafish and in *Takifugu* that were already identified via their NACHT domains. In the *Tetraodon* genome many, but not all of the matches found were upstream of NACHT domains or were part of the previous *nlr* gene predictions. As the remaining ones were again located mainly in the Un-random set, no attempt was made to link them to the predictions for the NACHT domains, for the reasons discussed above. As in the other two fish genomes, none of the matches were within gene predictions for other (i.e. non-NACHT-domain) genes.

These findings indicated that this domain, which was called the fish-specific NACHT associated (Fisna) domain, had been recruited specifically by a common ancestor of the novel Nlr proteins in the fish lineage. Confirming this view, a cursory search of other fish genomes showed highly similar sequences in catfish and Medaka, also associated with NACHT-domain encoding genes.

Although, as mentioned above, there was no evidence for the presence of this domain other than in fish, two short peptide motifs within the Fisna domain could be identified in mammalian NLRC proteins: LK/E/NQ/K/RYTE/D in mammalian NOD2 (LEDYTE), and LYIIEGESEGVNEEHEVLQ just downstream of the first motif, in mammalian NOD3 (NLRC3) (LLLVD/EGLSDLQQK/REHDLM/V/TQ) (Fig. 3.15). The region containing these sequences in NOD2 and NOD3 (NLRC3) was neither part of the NACHT nor of the CARD domain and had not been assigned a cell biological function. Their conservation in the new *nlr* gene families might indicate a shared origin and possibly shared functions.

A similar expansion of Nlr encoding genes was recently found in the sea urchin (Hibino et al. 2006; Rast et al. 2006). Jonathan Rast generously shared the sequence data, so that the predicted sea urchin protein sequences could be compared to the newly found fish Nlrs. In addition to sharing high similarity with the fish proteins in the NACHT domain and the LRRs, the sea urchin proteins also had a region upstream of the NACHT domain that was highly conserved among the sea urchin set of proteins and included sequence motifs similar to those in the fish proteins and in mammalian NOD2 (Fig. 3.15).

Further study of the amino-terminal regions of the new zebrafish NLR proteins showed that many of them contained considerable stretches of predicted peptide sequences upstream of the Fisna domain, in some cases with multiple related sequence repeats. Manual editing of the automated alignment created by ClustalW (Thompson et al. 1994) revealed the following structure of the amino-terminal regions of this protein family (Fig. 3.16).

Based on sequence similarity in the NACHT-domain and in the Fisna domain, the protein family was subdivided into four groups (Fig. 3.14). In each of these groups further group-specific motifs were identified upstream of the Fisna domain (Fig. 3.16).

The amino-terminal sequences in group 1 were highly conserved and not found in any of the other groups (darker green shading in Fig. 3.16). A comparison with mammalian proteins showed that the conserved sequence motif in group 1 exhibited similarities to the PYD found in mammalian NALP (NLRP) proteins and in associated adaptor molecules.

The analysis of the N-terminal sequences in group 2 identified a shared motif of 101 residues, immediately upstream of the Fisna domain (lighter green shading in Fig. 3.16). This motif showed a distant resemblance to the PYD-like motif found in group 1. The most amino-terminal sequences in group 2 contained motifs shared with members from groups 3 and 4.

A motif shared by members from these three groups was a repeat occurring in one, two, or three copies per protein, or in one case, in ten copies (different hues of blue shading in Fig. 3.16, indicating different versions of the repeat). Group 2 members had a version of this repeat with a four-amino-acid insertion, which was also found in some members of group 3. These repeats were usually combined with a specific amino-terminal peptide of 14 amino acid residues (pink shading in Fig. 3.16). Other conserved amino-terminal peptides (yellow or orange shading in Fig. 3.16) are associated with a particular type of repeat.

Group 4 is the least homogeneous, showing divergence both within the group and in comparison with the other groups, in the repeats as well as in the Fisna and NACHT domains.

No significant homologies to the repeat sequence were found in mammals.

In summary, the Fisna domain is found in all of the novel fish NLR proteins and is located immediately upstream of the NACHT domain. It is specific for the fish NLRs, as it could not be identified in combination with other domains than the NACHT and was also not found in other species than fish. Similarities found in the NACHT and Fisna domain led to subdivision of the zebrafish NLRs into four groups. The group-specific similarities were also observed in the amino-terminal parts of the novel NLR proteins. These contain up to three different motifs, two of which are found only in fish. Groups 1 and 2 contain a PYD-related domain upstream of the Fisna domain. Members of groups 2 to 4 can in addition contain one or more copies of a motif that is also specific for the novel fish NLR proteins. Members of groups 3 and 4 contain multiple variants of this motif but no PYD-like sequences.

The genes encoding the novel proteins were found to be distributed throughout the zebrafish genome. Some chromosomes harbored single genes, or a few, widely spaced genes, but many of the genes occur in large tandem clusters (Fig. 3.17). The group distribution was also observed to be variable. Some chromosomes contain only members of one or two groups e.g. on chromosome 1 the majority of *nlr* genes were found to encode group 3 and group 4 proteins. Other chromosomes, e.g. chromosome 4, harbor *nlr* genes coding for all four groups. Within the large gene clusters several groups were often found, with tandem duplicated genes from one group interspersed with genes from other groups.

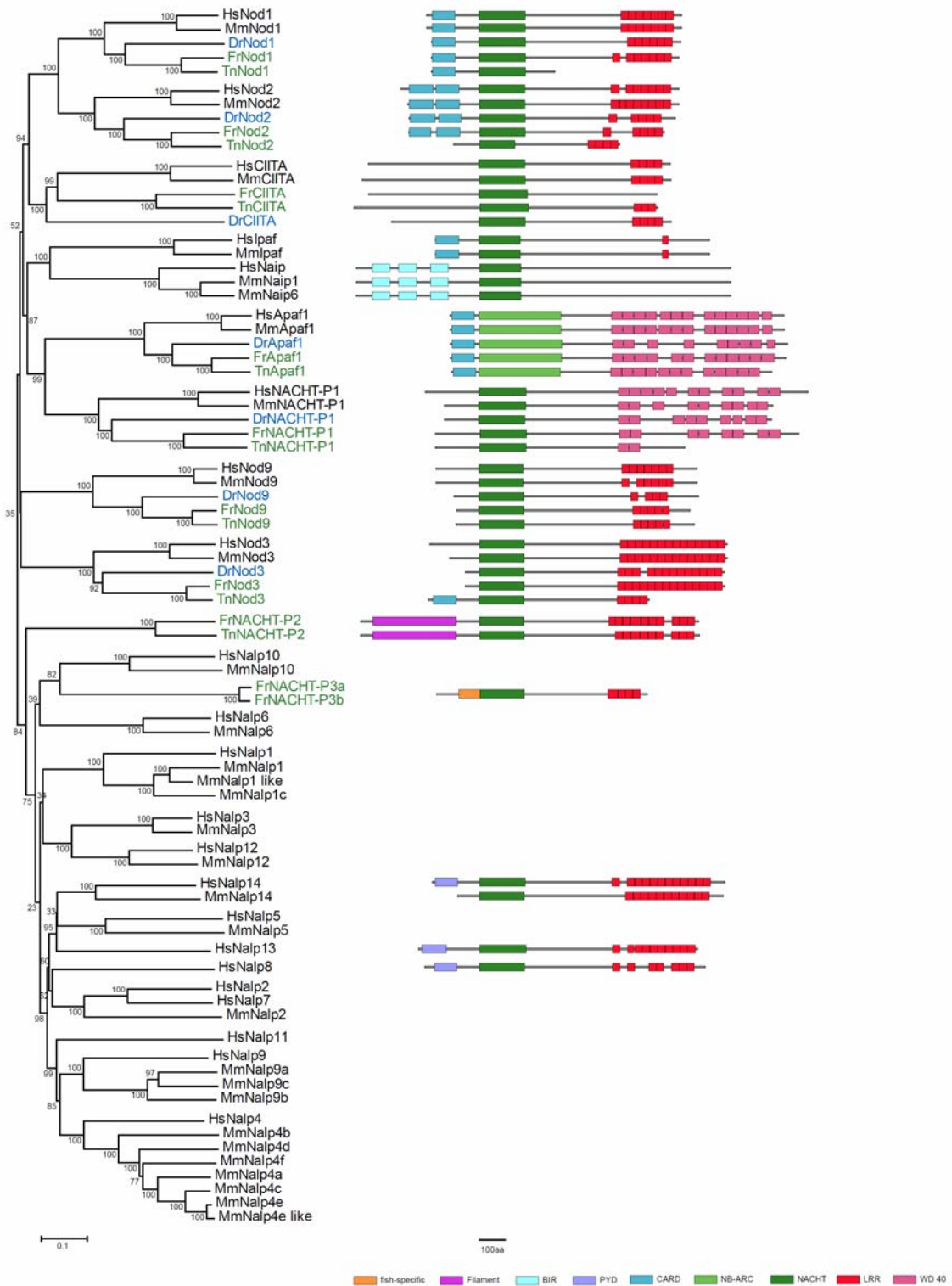


Fig. 3.13: Phylogenetic tree of NLRs shared by mammals and fish and diagram of their protein structures.

In addition to the NOD1, NOD2, NOD3 (NLRC3), Nod9 (NLRX1), CIITA, and APAF1, a novel NLR protein is shared by all five species, which was named NACHT-P1 (NWD1). The protein domain structure diagram shown next to NACHT-P3 is representative of the majority of the novel fish-specific NLR proteins. Further details of the tree are as in Fig. 3.1.

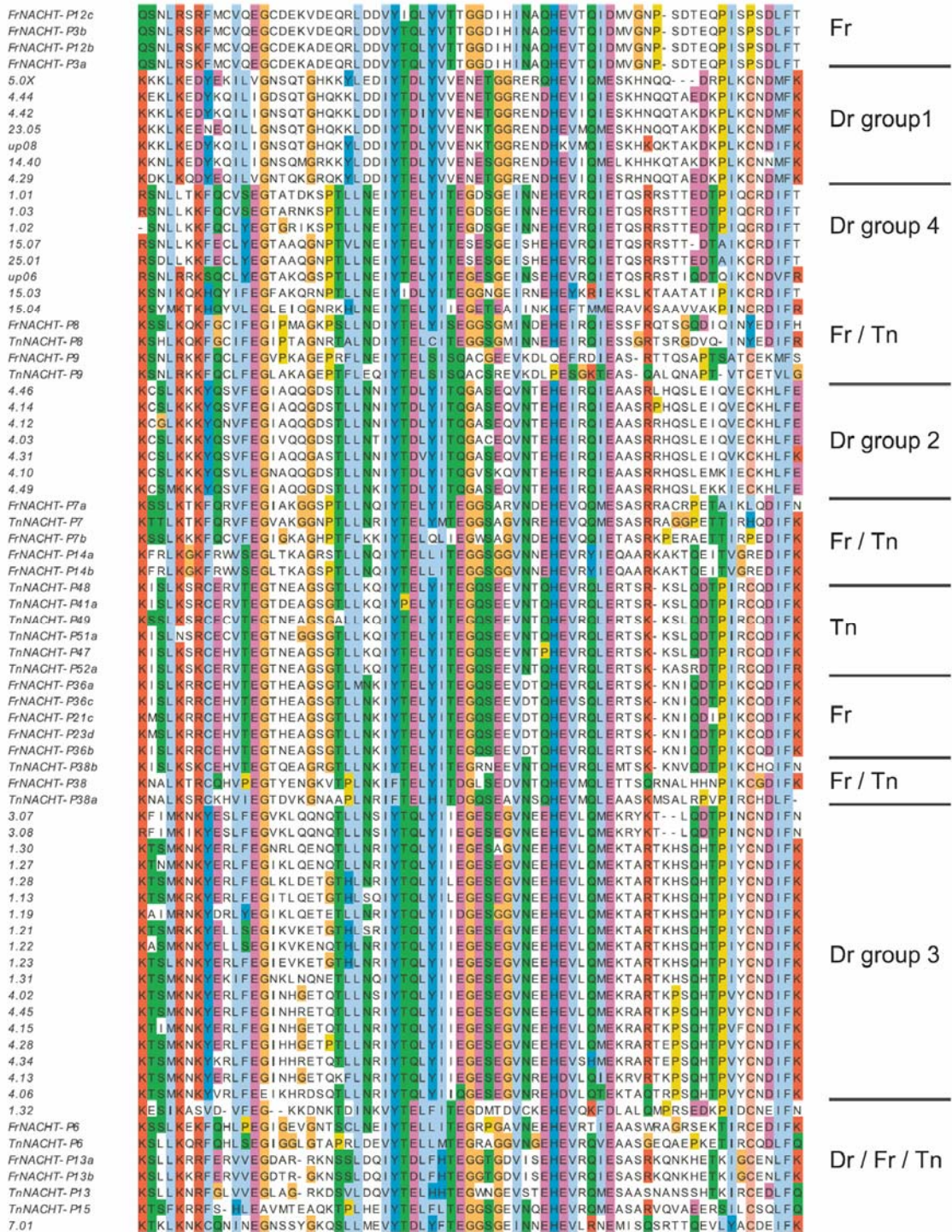


Fig. 3.14: The fish-specific domain upstream of the NACHT domain.

Alignment of the fish-specific NACHT associated (Fisna) domain in a representative subset of 75 fish NLRs. The group names on the right refer to the subdivision of the *Danio rerio* groups according to similarities in the NACHT and the Fisna domain or indicate which species form the group.

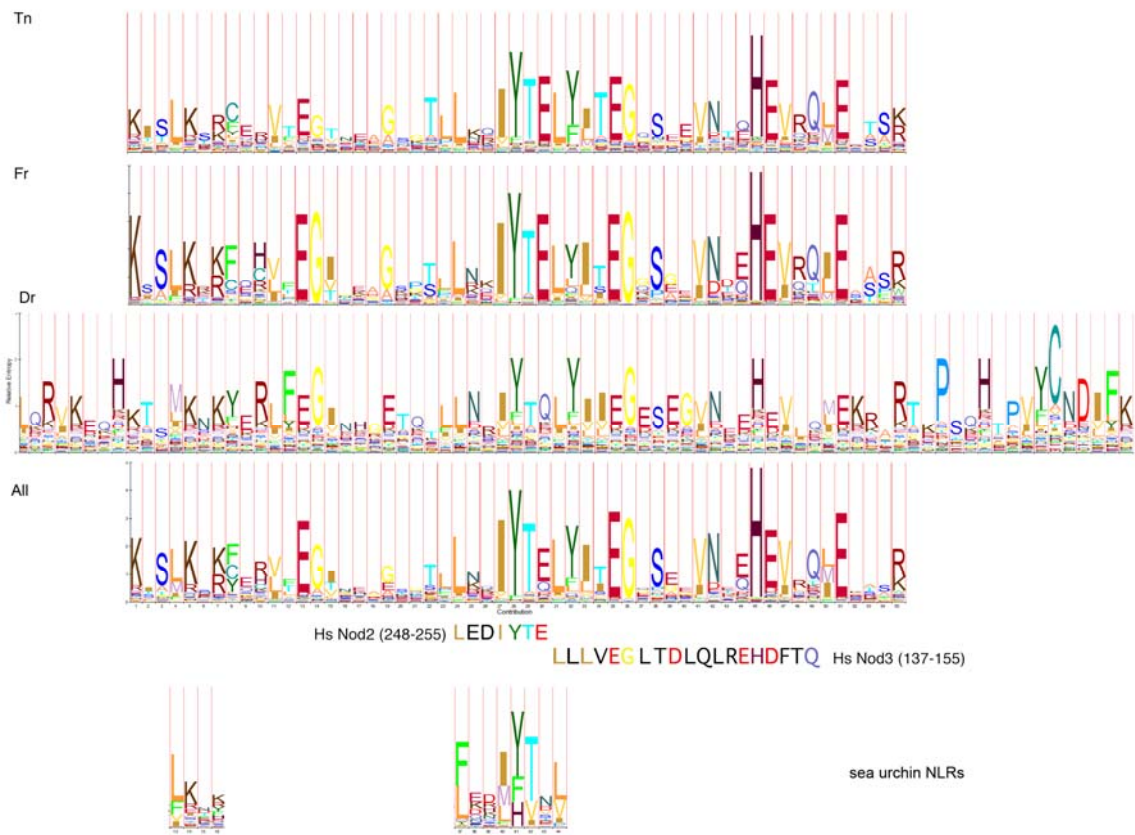


Fig. 3.15: Hidden Markov Model (HMM) logos of the Fisna domain.

The fish-specific domain upstream of the NACHT domain found exclusively in fish (Fisna) is highly conserved in all novel fish NLRs. HMM logos representing the consensus sequence of the Fisna domain in each fish species as well as the consensus of all fish Fisna domains are shown. For the HMM logo depicting the zebrafish Fisna consensus, extended sequences were used in comparison to the pufferfish sequences, for those found in zebrafish exhibited high conservation outside the 'core' consensus.

Peptide sequences from human NOD2 and NOD3 (NLRC3) with similarity to short stretches of the Fisna consensus, color coded to highlight conserved residues, are listed underneath as are stretches of HMM logos from the regions upstream of the NACHT domain present in 140 sea urchin NLR proteins.

Profile HMMs present a probabilistic model. The relative size of a letter expresses its emission probability from a state distribution. Letters are sorted in descending order depending on their probability. The HMMs were generated using the software HMMER (Eddy 1998) and were visualized using the LogoMat-M method (Schuster-Bockler et al. 2004).



Fig. 3.16: Structure of the amino-termini of the novel zebrafish NLR proteins.

The ClustalW multiple alignment of a set of 46 representative zebrafish NLRs was truncated after the start residue of the Fisna domain, and the alignment of the remaining amino-terminal sequences was edited manually using Jalview (Clamp et al. 2004).

(A) Overview of the alignment with characteristic sequence motifs shaded in color: green = pyrin-like domain (PYD) in group 1 and 2; blue = repeated motif (different shades of blue mark different versions of the repeat); yellow/orange = conserved amino-terminal amino acid residues; and pink = specific amino terminal peptide of 14 residues.

(B) Details of the alignment in panel A in which amino acid similarities and identities are highlighted in ClustalW colors. A set of mammalian PYD domains are aligned above the zebrafish group 1 and group 2 PYD-like domains to illustrate the similarity.

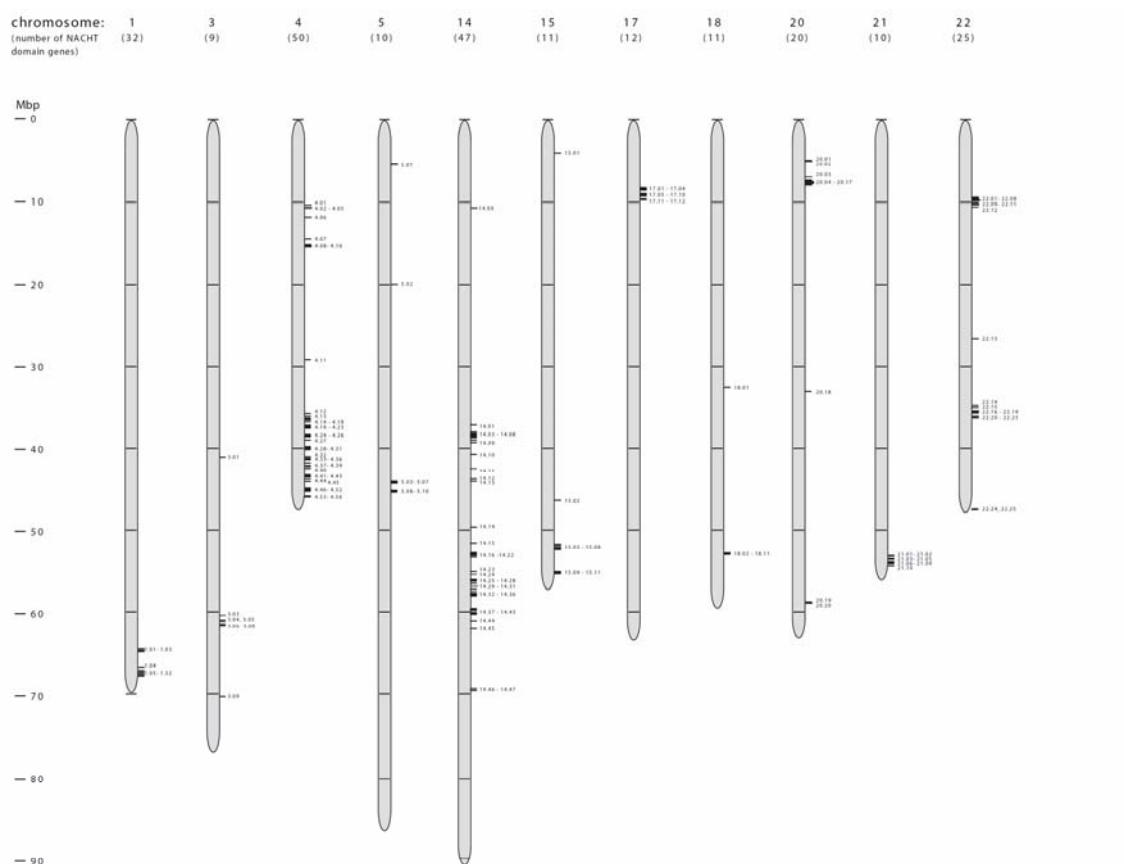


Fig. 3.17: Chromosomal locations of the novel zebrafish NLR proteins.

The 11 chromosomes containing the main clusters of *nlr* genes are shown. The number of *nlr* genes on each chromosome is listed below the chromosome number. Further 42 genes are distributed on 11 other chromosomes, and 20 genes are on as yet unplaced contigs. This list includes a compilation of all predictions (automated as well as manually annotated) and locations of hits from a TBLASTN search for NACHT domains. Future improvements of the genome assembly and further manual annotations will most likely result in minor changes of this map. Genes are denoted by lines on the right of the chromosome irrespective of orientation.

3.2 *In vivo* analysis of innate immune genes in the zebrafish

The aim of the following part of this work was to analyze the *in vivo* function of genes putatively involved in innate immunity. For these functional studies, suitable infection assays had to be established. Mammalian IFN γ is a key mediator in innate and acquired immune response mechanisms. The role of *lfn* during an innate immune response in the zebrafish embryo had not been analyzed. Supporting the functional characterization of the *ifn γ* genes by Dirk Sieger, putative *lfn* target genes were evaluated and infection studies were performed. *crfb* genes were analyzed for their potential to transduce the *lfn γ* signal.

The developmental expression of the canonical *nlr* genes was investigated and the *nwd1* (*nacht-p1*) gene was selected for further analysis.

3.2.1 Infection of zebrafish embryos

The zebrafish as a model organism offers the opportunity for large-scale screens. Such assays could provide a means to identify components of the innate immune system that render the embryo susceptible or resistant to an infection. As a method of choice the co-incubation method was tested, which would allow the simultaneous assessment of large quantities of embryos under different pathological situations. Alternatively, microinjection of pathogenic bacteria into zebrafish embryos was conducted, as this method should assure higher infection rates although it would allow to study only limited numbers of individuals.

Three different fish-specific pathogens were tested: *Mycobacterium marinum*, *Vibrio anguillarum* and *Yersinia ruckeri*. These bacterial strains expressing DsRed were provided by Astrid van der Sar and Wilbert Bitter, VU University Medical Center, Amsterdam, The Netherlands.

Whereas *M. marinum* had been used for infection studies in embryonic, larval and adult stages of zebrafish (Davis et al. 2002; Swaim et al. 2006; van der Sar et al. 2004) and *V. anguillarum* for analysis of its virulence in zebrafish larvae (O'Toole et al. 2004), studies using *Y. ruckeri* had previously not been performed in the zebrafish

3.2.1.1 Infection of zebrafish embryos by co-incubation

Co-incubation of zebrafish embryos with the different bacteria was performed at various time points. The earliest time point was at 28 hpf, a time of development when macrophages are present to mount a response and the embryo is well vascularized (see section 1.21). Further subsets of embryos, each with a sample size of 20 embryos, were incubated starting at 2 dpf, when granulocytes can be discerned

(Lieschke et al. 2001). Additional subsets were incubated starting at 3, 4, and 5 days of development (Fig. 3.18 and 3.19). A summary of the different bacterial concentrations used in the co-incubation experiments and the different sets of experiments performed is shown in Fig 3.20.

The survival rate of the embryos was measured from 1 day post infection (dpi) up to 6 dpi. Control embryos were grown in embryo media. In Fig 3.18 representative results of these co-incubation experiments are shown (yellow, orange, olive, and brown colored columns). The co-incubation with either of the bacterial strains did not lead to a significant decrease in the survival rate of the embryos, as only up to 10% of the embryos died during the co-incubation, compared to 5% of the control embryos.

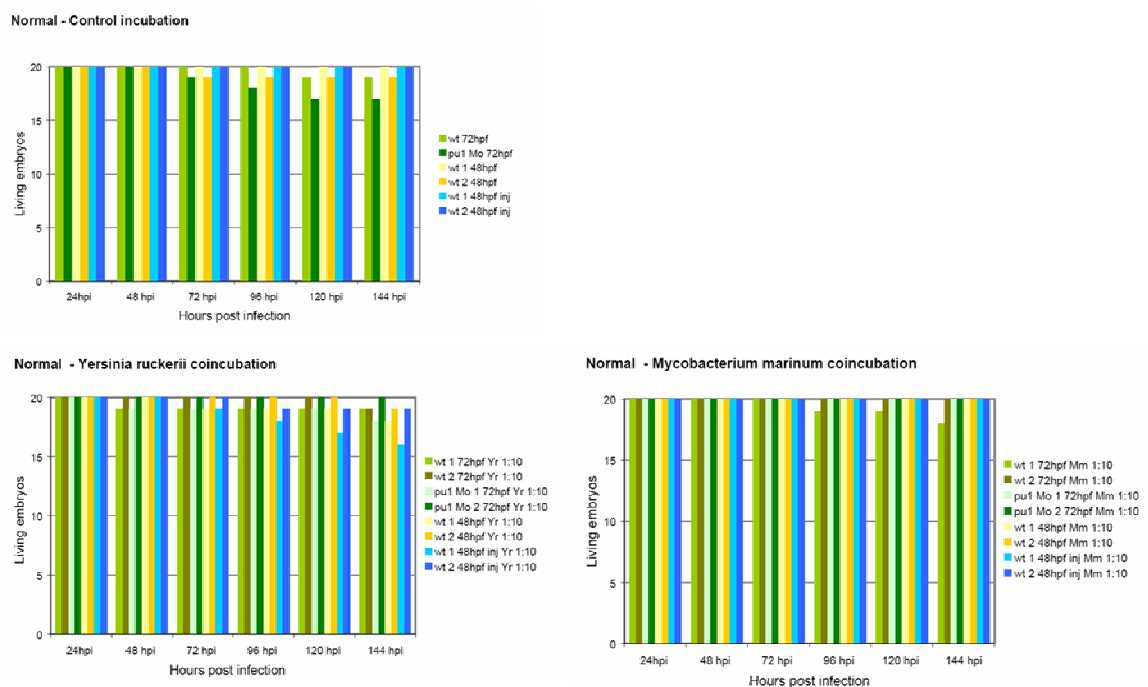


Fig. 3.18: Co-incubation of embryos with *Yersinia ruckerii* or *Mycobacterium marinum*

Diagrams showing control incubation or incubation with either of the two pathogens. The bacterial suspension was for both bacteria a 1:10 dilution of an OD1 suspension, the embryos were therefore incubated with 4×10^6 colony forming units (cfu) *Yersinia ruckerii* or 2×10^7 cfu *Mycobacterium marinum*. Embryos ($n = 20$) were incubated at 48 hpf or 72 hpf and monitored for survival. Numbers of living embryos were determined from 1 day post infection (dpi) until 6 dpi. *pu.1* morphants or non-injected sibling embryos were incubated at 3 dpi (control: dark green and olive columns, respectively; bacterial co-incubation: light and dark green columns for the *pu.1* morphants, olive and brown columns for the sibling embryos). Embryos injured at the tail fin (blue columns) and their non-injured siblings (yellow/orange columns) were incubated at 48 hpf. Similar results were obtained in at least two independent experiments.

To facilitate the infection process, embryos were also incubated on a rocking platform, assuming that this would keep the bacteria more motile and bring the pathogens into closer contact with their presumptive hosts. Although the induced infections were more pronounced as estimated from the fluorescence of the DsRed labeled bacteria, they still did not lead to lethality in the infected embryos (Fig 3.19, yellow, orange, and olive colored columns). The incubation on the rocking platform lowered the survival rate of the control embryos (survival > 70%) and the co-incubation with either *Y. ruckeri* (survival >70%) or *M. marinum* (survival >75%) led to comparable survival rates.

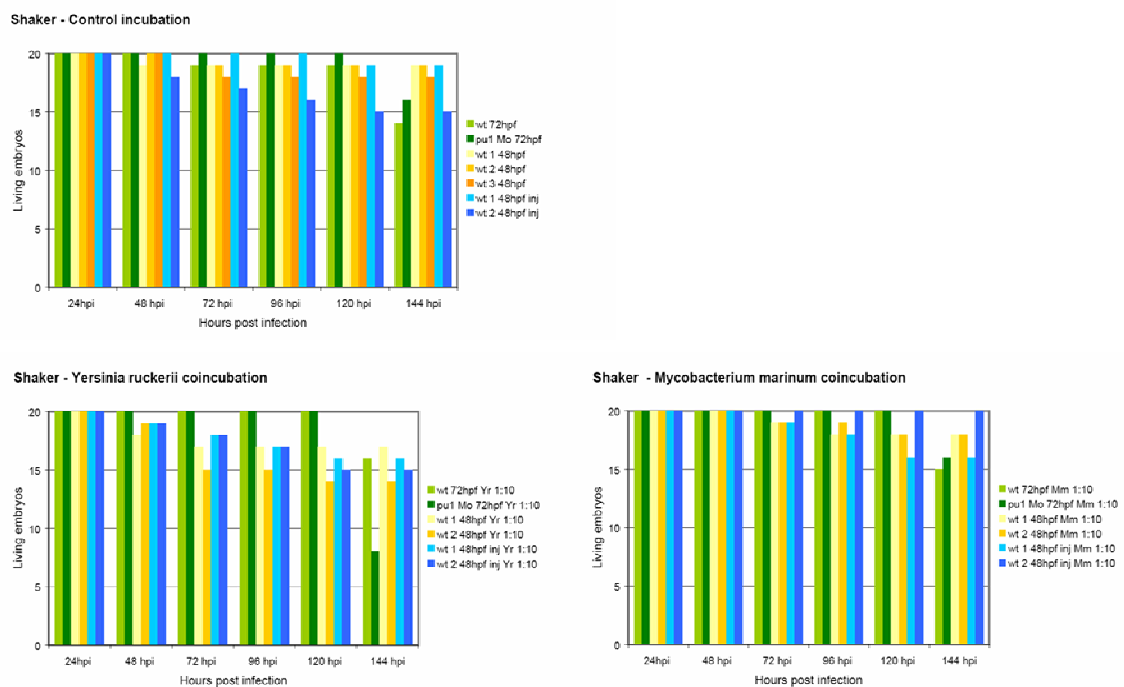


Fig. 3.19: Co-incubation of embryos with *Yersinia ruckeri* or *Mycobacterium marinum* on a rocking platform. Details of the diagram are as in Fig. 3.18, besides for *pu.1* morphant and non-injected sibling incubations which was performed for only one set of embryos.

In both assays the embryos were infected, but by and large the infection was restricted to the gastrointestinal tract, as shown by fluorescence microscopy (Fig. 3.21). The infection induced by co-incubation with *Vibrio anguillarum* was similar to that observed with the other bacteria in terms of survival rate of the infected embryos (>85% during normal co-incubation; >70% during shaker co-infection), but since the fluorescence signal in the bacteria was very weak, this pathogen was not used in further experiments.

In another approach, the embryos were locally wounded at the tail fin, in order to generate an entry site for the infectious bacteria. Accumulation of bacteria at the side of wounding was initially observed, but the embryos were able to clear the infection within 24 hours post infection (hpi) and the local wounding did not seem to alter the embryo's capacity to limit the infection to the intestine (Fig. 3.18 and Fig. 3.19, blue columns; not injured sibling embryos, yellow and orange columns).

It was also examined how embryos lacking macrophages and granulocytes react to the co-incubation. At the one-cell stage, embryos were injected with an antisense morpholino oligonucleotide (Mo) directed against the 5' untranslated region of the Pu.1 transcription factor (kindly provided by Vera Binder), which has been shown to be required for myeloid cell differentiation (Rhodes et al. 2005). The previous experiments indicated that only the natural entry route for the bacteria, i.e. uptake and digestion, led to an infection. The co-incubation was therefore started at 72 hpf, when the intestine becomes motile. Although movements of the jaw start slightly later, this time point was chosen, because at even later stages the knockdown effect would be greatly diminished and eventually lost by 5-6 dpf. The *pu.1* morphants showed a stronger inflammation in the gastrointestinal tract (Fig. 3.21), but also the morphants were able to cope with the infection (Fig. 3.18, light and dark green columns; Fig. 3.19, dark green columns). This suggests that the depletion of myeloid derivatives did not lead to higher susceptibility to the bacterial infection upon co-incubation.

Co-incubation with *Y. ruckeri* led to accumulation of the bacteria in the entire pleuroperitoneal cavity, whereas co-incubation with *M. marinum* resulted in confined areas of fluorescent bacteria within this cavity. These rod-like structures, which might represent granuloma, were also observed in brightfield microscopy (Fig. 3.21)

Taken together, these results indicate that a transient infection of zebrafish embryos and larvae could be achieved by the co-incubation, and that the infection was more pronounced when the co-incubation was performed on a rocking platform. The age of the embryos or larvae at the start of the co-incubation had no impact on the outcome of the infection. Local wounding at the tail fin or morpholino-mediated knock-down of macrophage precursors did not render the embryos or larvae significantly more susceptible to the infection. Due to the restriction of the infection to the gastrointestinal tract, this co-incubation method was found to be not suitable to induce systemic infections.

	Yersinia ruckerii					
conc. used (cfu)	4 x 10 ⁴	4 x 10 ⁵	8 x 10 ⁵	4 x 10 ⁶	8 x 10 ⁶	4 x 10 ⁷
age of embryos at start of incubation						
wt 28hpf	x	x	x	x	x	x
wt 48hpf	x	x	x	x	x	x
wt 72hpf	x	x	x	x	x	x
wt 96hpf	x	x	x	x	x	x
wt 120hpf	x	x	x	x	x	x
wt 48hpf injured				x		
pu1 Mo 72hpf				x		

	Vibrio anguillarum					
conc. used (cfu)	3 x 10 ⁵	3 x 10 ⁶	6 x 10 ⁶	3 x 10 ⁷	6 x 10 ⁷	3 x 10 ⁸
age of embryos at start of incubation						
wt 28hpf	x	x	x	x	x	x
wt 48hpf	x	x	x	x	x	x
wt 72hpf	x	x	x	x	x	x
wt 96hpf	x	x	x	x	x	x
wt 120hpf	x	x	x	x	x	x
wt 48hpf injured						
pu1 Mo 72hpf						

	Mycobacterium marinum					
conc. used (cfu)	2 x 10 ⁵	2 x 10 ⁶	4 x 10 ⁶	2 x 10 ⁷	4 x 10 ⁷	2 x 10 ⁸
age of embryos at start of incubation						
wt 28hpf	x	x	x	x	x	x
wt 48hpf	x	x	x	x	x	x
wt 72hpf	x	x	x	x	x	x
wt 96hpf	x	x	x	x	x	x
wt 120hpf	x	x	x	x	x	x
wt 48hpf injured				x		
pu1 Mo 72hpf				x		

Fig. 3.20: Overview of the different bacterial concentrations used in the co-incubation assay.

Different dilutions of OD1 bacterial suspensions were used in the co-incubation experiments. *Y. ruckerii* OD1: 4×10^7 colony forming units (cfu); *V. anguillarum* OD1: 3×10^8 cfu; *M. marinum* OD1: 2×10^8 cfu. Each indicated combination (x) was tested in at least three independent experiments.

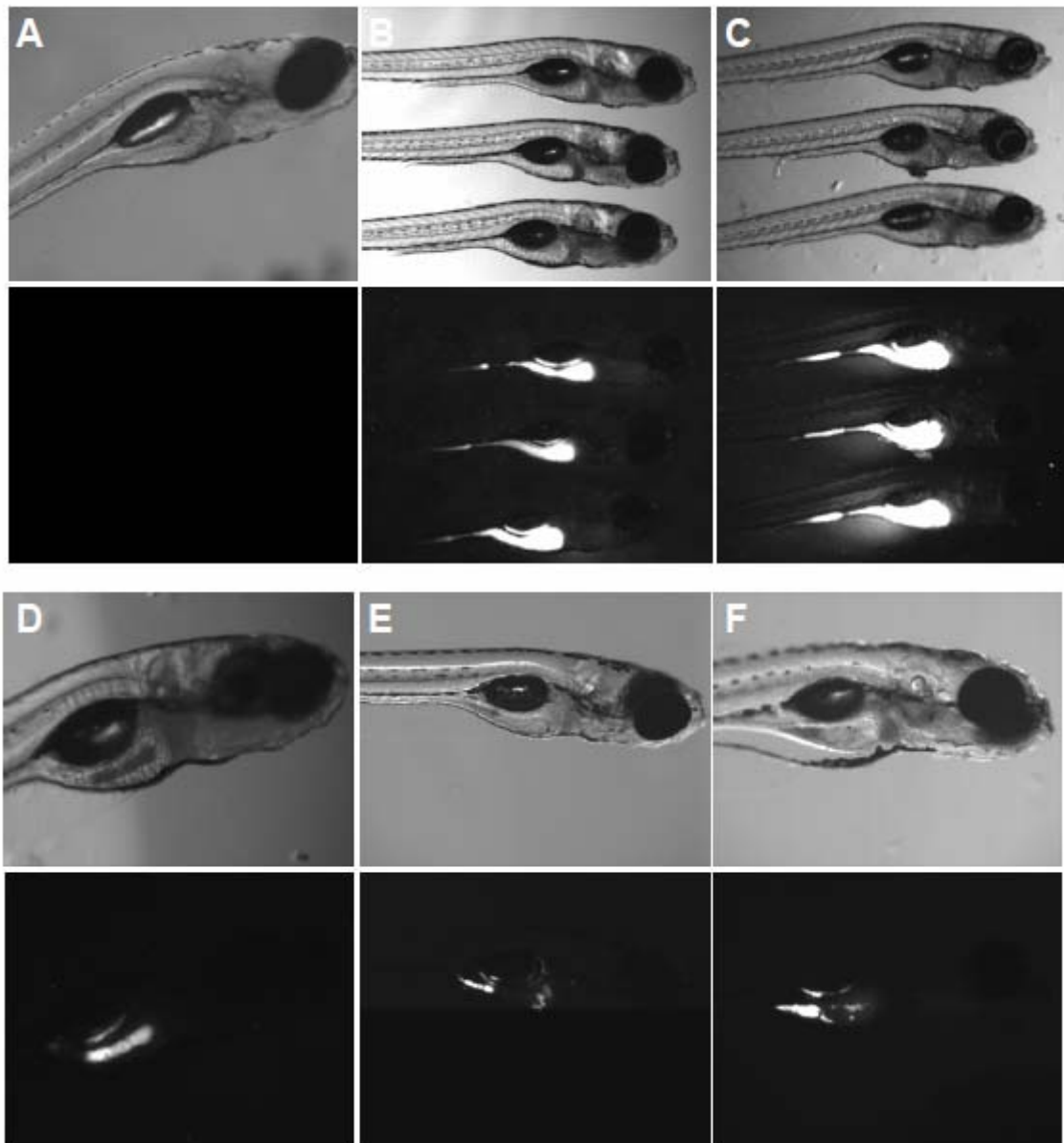


Fig. 3.21: Co-incubation of larvae and pathogenic bacteria

Bright field and DsRed fluorescence images of larvae at 8 or 9 dpf. (A) *pu.1* morphant exhibiting normal development, incubated in embryo media, 8dpf. (B) embryos incubated at 72 hpf in *Y. ruckeri* suspension (4×10^6 cfu), 5dpi, 8 dpf. (C) sibling *pu.1* morphants of embryos shown in B, incubated at 72 hpf in *Y. ruckeri* suspension (4×10^6 cfu), 5dpi, 8 dpf. (D) embryo incubated at 72 hpf in *M. marinum* suspension (2×10^7 cfu), 5dpi, 8 dpf. (E) embryo incubated at 72 hpf in *M. marinum* suspension (2×10^7 cfu), 6dpi, 9 dpf. (F) sibling *pu.1* morphant of embryo shown in E, incubated at 72 hpf in *M. marinum* suspension (2×10^7 cfu), 6dpi, 9 dpf. (A)-(F) lateral view, anterior to the right.

3.2.1.2 Infection of zebrafish embryos by microinjection

As the co-incubation method was not suitable to induce a systemic inflammation in the embryo or larva, the zebrafish embryos were manually injected with pathogenic bacteria. This was performed by microinjection into the PBI or the caudal posterior vein of the embryos at 28 hpf and 32 hpf. Although the sample size is reduced in comparison to the co-incubation method, the injection of bacteria was found to induce a systemic inflammation to which, depending on the concentration and the type of bacteria, the embryos will succumb. Representative infection assays with DsRed expressing *E.coli* or with DsRed labeled *Y.ruckeri* are shown in Fig 3.22. Embryos survived the injection of doses of up to ~3000 colony-forming units (cfu) of *E. coli* (DH5 α), and were able to clear the infection within 2-3 days. By contrast, injection of as few as 30 cfu *Y. ruckeri* killed the embryos within 3 days. The ability of the embryos to clear the *E.coli* infection is also reflected by the low fluorescence intensity observed at 1 dpi (Fig. 3.27). The injection of *Y. ruckeri* led to distribution of the bacteria throughout the cardiovascular system. (Fig 3.23)

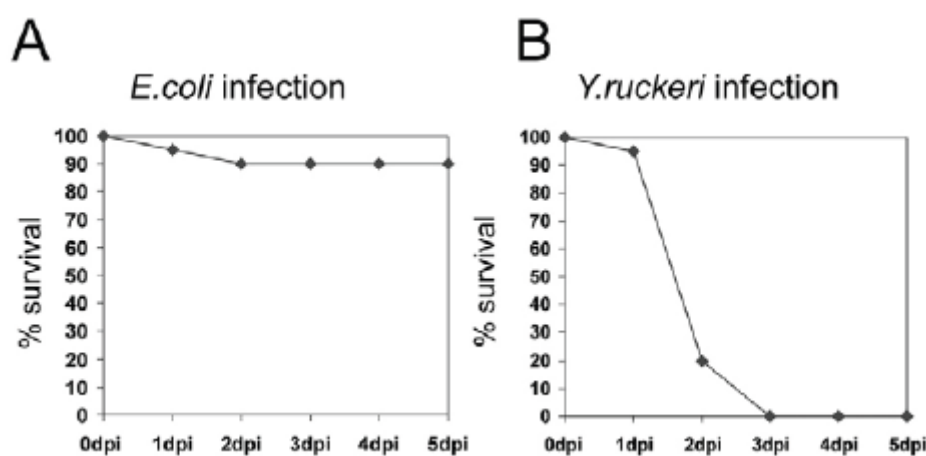


Fig. 3.22: *E. coli* and *Y. ruckeri* infection of zebrafish embryos.

(A) Survival of zebrafish embryos infected with *E. coli*. Embryos were infected with 3000 cfu of *E. coli* at 28-30 hpf and monitored for survival. The percentage of surviving embryos was plotted against days post-infection (dpi). (B) Survival of zebrafish embryos infected with *Y. ruckeri*. Embryos were infected with 30 cfu of *Y. ruckeri* at 28-30 hpf to monitor survival. The percentage of surviving embryos was plotted against dpi. Data in (A) and (B) represent the mean of two independent experiments (n=40, each).

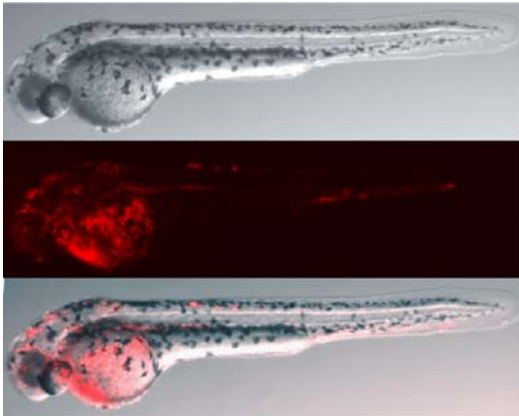


Fig. 3.23: *Yersinia ruckeri* infected embryo.

Bright field, DsRed fluorescence, and overlay image of a 54 hpf old embryo infected with 30 cfu of *Yersinia ruckeri* (24hpi). Injection was performed at 30 hpf. Circulating bacteria are observed by fluorescence throughout the cardiovascular system, most prominently in the pericardial cavity and on top of the yolk sac. Lateral view, anterior to the left.

3.2.2 Functional characterization of *ifn γ* genes and potential target genes

Infection by microinjection of bacteria was employed to determine the function of IFN γ in the embryos' immune response, as this cytokine serves as a potent activator of macrophages and as a key inducer of a proinflammatory response in mammals.

It has been previously shown in the zebrafish that both *ifn γ* genes are inducible by LPS and polyIC in tissue culture cells (Igawa et al., 2006). One of the genes, *ifn γ 2*, was found to induce *mxb* and *mxc* in ZF4 cells and to mediate resistance against viral infections in these cells (Lopez-Munoz et al., 2009). However, treatment of adult zebrafish with IFN γ 2 failed to mediate resistance against viral and bacterial infections (Lopez-Munoz et al., 2009).

The function of *ifn γ 1* had not been analyzed, so far. In order to determine whether the two predicted zebrafish *ifn γ* genes correspond to mammalian IFN γ in their innate immune functions, the zebrafish embryo was used to test their roles in activating target genes and defending the fish against pathogens.

The basal expression of the two *ifn γ* genes during embryonic and larval development was examined by Dirk Sieger, who showed that *ifn γ 1* mRNA is most likely supplied maternally and present throughout embryonic development, whereas *ifn γ 2* mRNA was only observed at very low levels at later stages of development (6 dpi) (Sieger et al. 2009).

3.2.2.1 *ifn γ* target genes in the zebrafish

The finding that the zebrafish *ifn γ* genes are expressed in the early embryo raised the question if the signaling pathway might be active. In an overexpression approach it was tested whether *ifn γ 1* or *ifn γ 2* were able to activate the transcription of putative target genes. A set of zebrafish homologs of known mammalian IFN-inducible genes was analyzed by comparing the expression levels in untreated embryos to those which overexpressed *ifn γ 1* or *ifn γ 2*. The overexpression was achieved by injection of *in-vitro* transcribed capped *ifn γ 1* or *ifn γ 2* mRNA into 1-2-cell stage embryos. At 28 hpf mRNA was isolated from pooled embryos and reversely transcribed into cDNA. The RT-PCRs were performed by Dirk Sieger (Fig. 3.24).

The putative zebrafish *Ifn γ* targets included *ifn ϕ 1*, which had been analyzed before and shown to be inducible by viral infection (Altmann et al. 2003; Levraud et al. 2007). Further target genes were *nramp*, *adar*, *mx*, *ifi30*, *cathepsin D (cathD)*, *p27*, *cr3*, *gp91*, and *Imp2*.

Additionally, zebrafish genes encoding putative homologs of the mammalian guanylate-binding proteins (GBPs) and the immunity-related GTPase proteins (IRGs) were examined.

An initial characterization of the *irg* homologs in the zebrafish was performed during my diploma thesis (Stein, 2005). GBPs and IRGs belong to the family of IFN-inducible GTPases, together with the myxovirus resistant proteins (Mxs) and the very large inducible GTPase proteins (VLIGs) (Boehm et al. 1998; Haller and Kochs 2002; Klamp et al. 2003). The majority of the genes examined showed a high basal expression, which was not influenced by overexpression of *ifn γ 1* or *ifn γ 2* (Fig. 3.24). *ifn ϕ 1*, *Imp2*, and several of the *irg* genes were inducible by overexpression of either *ifn γ* gene. The *irg* genes *irge3*, *irge4*, *irgf1*, *irgf3*, and *irgf4* were strongly induced by both *ifn γ* s, and three additional genes, *irge2*, *irgg1*, and *irgq1*, were weakly induced (Fig. 3.24).

Further analyses performed by Dirk Sieger showed that the *irgf1* gene is specifically induced by both *ifn γ* proteins and as such a suitable 'read-out' in infection assays.

Whereas *irgf1* gene expression is barely detectable in the untreated embryo, its expression was found to be constitutive in non-immune related tissues of adult zebrafish, like the heart or the testis (Fig. 3.25). Several *irg* genes were found to be expressed in the testis, but *irgf1* showed the highest expression level in all three testes analyzed. This finding was unexpected, as expression in the testis is particular for the *irgc* gene of mice and humans, which is in both species not inducible by IFN γ (Bekpen et al. 2005). However, the members of the zebrafish *Irge* and *Irgf1* protein families are most likely a result of a species-specific expansion (Bekpen et al. 2005).

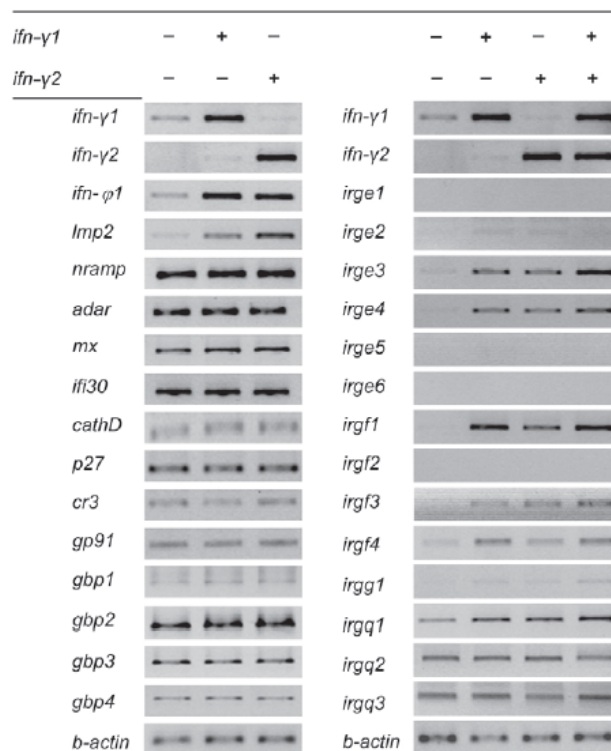


Fig. 3.24: RT-PCR analysis to identify *Ifnγ* targets.

Potential target gene expression was assayed at 28 hpf in control embryos and in embryos injected with *ifnγ1* and *ifnγ2* mRNA, as indicated by the '+' signs at the top of the lanes. mRNA injections were performed in 1-2-cell stage embryos. To verify successful injections, the levels of *ifnγ1* and *ifnγ2* were also tested by RT-PCR. β -actin was used as a control. RT-PCR analysis was performed by Dirk Sieger.

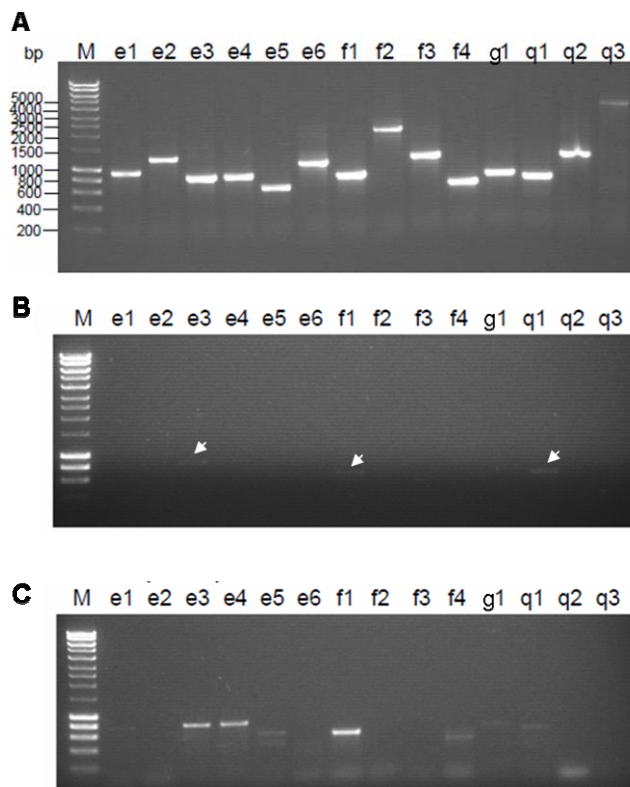


Fig. 3.25: (legend on next page)

Fig. 3.25: (see previous page) *irgf1* is constitutively expressed in the testis.

(A) RT-PCR on genomic DNA verifies that all primer pairs used were able to amplify the predicted *irg* products (also for Fig.3.24). (B) Weak *irg* expression in the adult heart was observed for *irge3*, *irgf1* and *irgq1* by RT-PCR (arrows). (C) *irg* expression in the adult testis was observed for *irge3*, *irge4*, *irge5*, *irgf1*, *irgf4*, *irgg1*, and *irgq1* by RT-PCR.

3.2.2.2 Effects of altered *ifny* expression during bacterial infection

To test whether Ifn signaling has a role in protecting the embryo against pathogens, the levels of interferons were raised or lowered in combination with bacterial infections. *ifny1* and *ifny2* were either overexpressed or downregulated using morpholinos (Mo) against the 5' untranslated region (UTR) of *ifny1* and *ifny2* and compared to the effect on infections with that of untreated sibling embryos. To block a potential influence of Ifn ϕ 1 signaling, a morpholino directed against the Ifn ϕ 1 receptor chain *Crfb1* was used (Levraud et al. 2007). To test the efficacy of the morpholinos, GFP constructs were generated that contained the morpholino target sequences upstream of eGFP. Dirk Sieger generated *ifny1-eGFP* and *ifny2-eGFP* in vitro transcribed fusion RNAs. The generation of *crfb1-eGFP* in vitro transcribed fusion RNA is described in section 3.2.3.2. The different RNAs were injected into one-cell stage embryos with or without the corresponding morpholinos. Injection of the fusion eGFP-RNAs led to strong fluorescence in the injected embryos, which was effectively shut down by the corresponding morpholinos (Fig. 3.29 *crfb1* Mo; (Sieger et al. 2009) *ifny* Mo). Thus, all three morpholinos blocked translation efficiently.

The survival rates were assayed of embryos that were injected with *crfb1*, *ifny1* and *ifny2* morpholinos and infected with ~3000 cfu of *E. coli*. Embryos in which any of the signaling pathways had been blocked were able to clear the bacteria and showed survival rates that were comparable to untreated embryos (Fig. 3.26), indicating that knockdown of a single interferon signaling pathway does not abolish resistance to *E. coli*.

However, only 24% of embryos injected simultaneously with *ifny1* and *ifny2* morpholinos survived the *E. coli* infection (Fig. 3.26). This was reflected in the extent of bacterial clearance determined by a time-course analysis of the infection in the surviving embryos (Fig. 3.27). At 3 hours post infection (hpi) the amount of fluorescent bacteria was comparable in untreated embryos and *ifny1* + *ifny2* Mo-injected sibling embryos. At 15 hpi the infection in the *ifny1* + *ifny2* Mo-injected embryos appeared slightly more pronounced. While the majority of untreated embryos had almost cleared the infection at 24hpi, the *ifny1* + *ifny2* Mo-injected embryos showed a strong and

eventually lethal infection. Knockdown of both *ifny1* and *ifny2* also increased the mortality caused by infection with *Y. ruckeri* (Fig 3.35).

In contrast to infection by *Y. ruckeri*, which appeared to be confined to the blood vessels, infection by *E.coli* led to extravasation into the surrounding tissue (Fig. 3.27). The *ifny1* + *ifny2* Mo-injected embryos developed completely normal and did not show any signs of retardation before infection (Fig. 3.27). This is also reflected by the high survival rate of their non-infected siblings (Fig. 3.26).

These experiments showed that *Ifny1* and *Ifny2* can protect the early zebrafish embryo against bacterial infections. The finding that either of the gamma interferons is sufficient to protect the embryo against *E. coli* suggests that they have largely or completely overlapping functions, which is consistent with their effects on target gene activation.

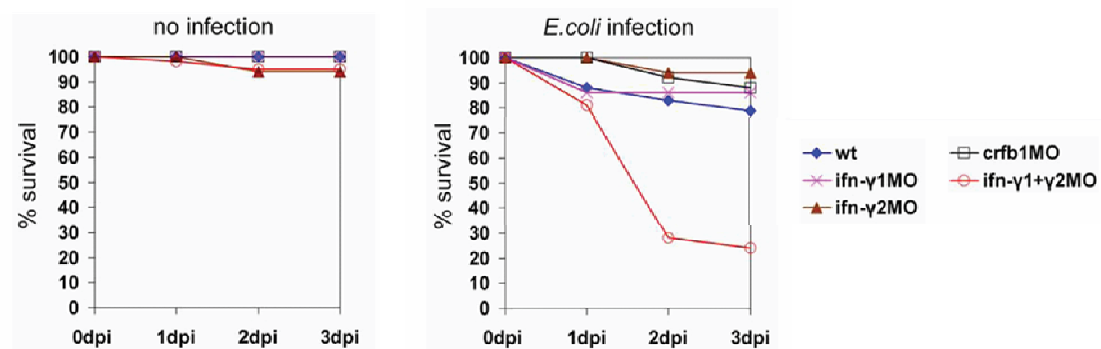


Fig. 3.26: Survival of *ifn-γ* knockdown embryos infected with *E. coli*.

Embryos were left untreated (control) or injected with morpholinos specific for *ifny1*, *ifny2*, or *crfb1* (each 0.6mM) alone, or in combination, as indicated (data represent the mean of two independent experiments; n=40 for each treatment). X-axis: percentage of surviving embryos; y-axis: dpi. The left panel shows the survival rates for embryos that were not infected. The right panel shows the survival rates for the embryos that were infected with *E. coli* (3000 cfu.) at 28-30 hpf.

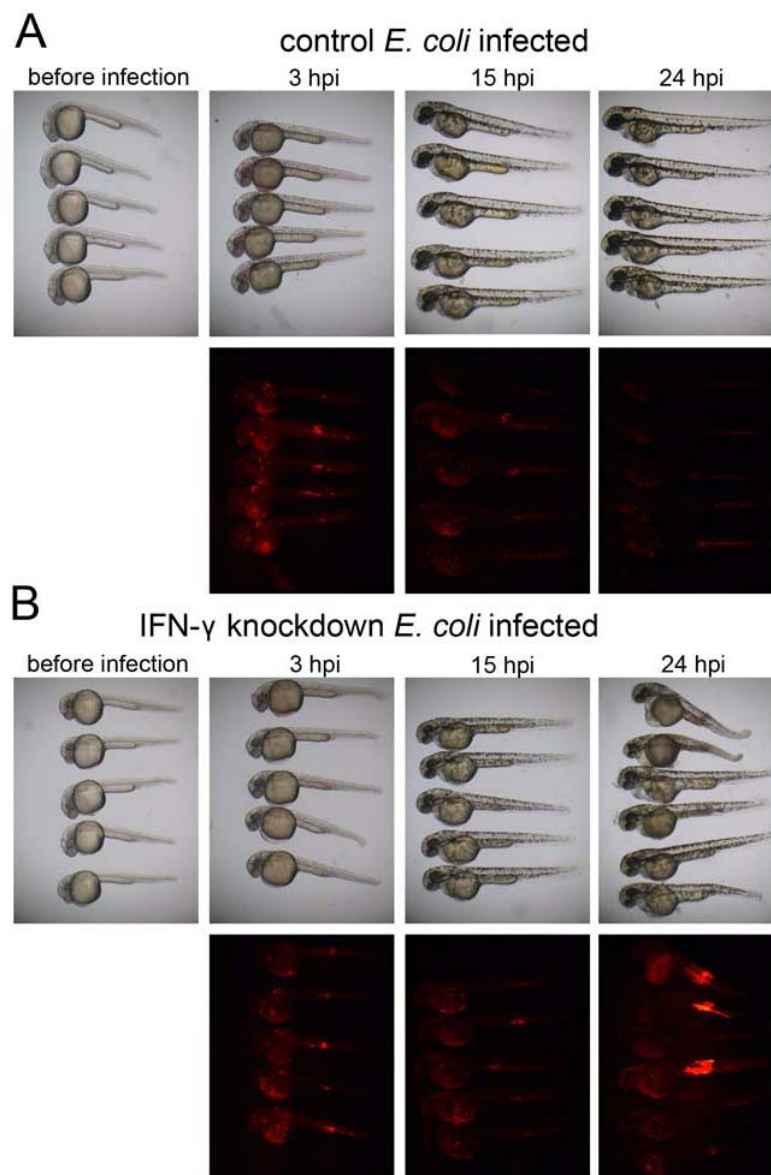


Fig. 3.27: Time-course analysis of *E.coli* infection.

Bacterial infection in untreated embryos (A) and *ifn1* + *ifn2* Mo-injected embryos (B). Bright field and DsRed fluorescence images. *ifn1* + *ifn2* Mo (0.6mM each) were injected at the 1-cell stage. The untreated or morpholino-injected embryos (n = 20 for each set) were infected with *E. coli* (2600 cfu) at 30-31 hpf. Before infection, and at 3, 15 and 24 hpi, five randomly selected embryos were photographed. The *ifn1* + *ifn2* morphants did not show any signs of toxicity induced by the Mo, or developmental defects. Before the infection, at 3 hpi, and at 15 hpi the *ifn1* + *ifn2* morphants appeared morphologically like their untreated siblings. The first dying embryo in the morpholino-treated set was seen at 18.5 hpf. There were no dead or dying embryos in the untreated set at 24 hpi.

3.2.3 Analysis of genes encoding putative IFN γ receptor chains

3.2.3.1 Sequence analysis of putative IFN γ receptor chains

In the phylogenetic analysis 16 genes were predicted to code for members of the class II cytokine receptor family in the zebrafish (see section 3.1.3). An additional gene, encoding a predicted receptor chain with an intracellular domain of intermediate length, *crfb17*, was identified by Georges Lutfalla, Laboratoire de Dynamique des Interactions Membranaires Normales et Pathologique, Montpellier, France.

The sequence similarity between mammalian and fish class II cytokine receptor chains is extremely low and mostly confined to the extracellular D200 domain. By manual alignment three predicted proteins could be identified in the zebrafish, which contained peptide motifs with close homology to essential motifs found in the mammalian IFNGR chains (Fig 3.28).

In mammals the IFNGR1 is involved in mediating ligand binding, ligand trafficking through the cell, and signal transduction. The IFNGR2 plays only a minor role in ligand binding but is required for signaling. Both mammalian IFNGR chains have no intrinsic kinase/phosphatase activity and associate with JAK1 and JAK2.

The IFNGR1 harbors three critical intracellular motifs: a JAK1-binding site, a ligand binding and degradation motif, and a STAT1-binding site. The membrane proximal Leu-Pro-Lys-Ser (LPKS) sequence was found to function as the constitutive binding site for JAK1 (Farrar et al. 1991; Greenlund et al. 1994). The proline residue in this motif has been shown to be dominantly involved in the JAK1 recruitment (Greenlund et al. 1995; Kaplan et al. 1996). The zebrafish *Crfb13* and *Crfb17* contain the essential proline residue but differ in composition of the surrounding sequence (Fig. 3.28). Adjacent to the JAK1 binding motif is a Leu-Ile dipeptide in the human IFNGR1 which has been shown to be important for receptor-mediated ligand internalization and degradation (Farrar et al. 1992; Farrar et al. 1991). The leucine residue is conserved in mammals and was also found in *Crfb13* and *Crfb17*. The STAT1-binding motif of mammalian IFNGR1 is located near the C-terminus and contains the residues Tyr-Asp-Lys-Pro-His (YDKPH). It forms the docking site for latent STAT1 when the tyrosine residue is phosphorylated. Mutational analysis demonstrated that the tyrosine, aspartate, and histidine residues were important for the STAT1-binding (Farrar et al. 1991; Greenlund et al. 1994; Greenlund et al. 1995). In *Crfb17* all three residues are conserved, whereas *Crfb13* displays a lysine instead of the histidine (Fig. 3.28).

The IFNGR2 contains a JAK2-binding motif (PPSIPLQIEEYL) which is located in immediate vicinity to the transmembrane domain (Bach et al. 1996). A highly similar sequence was found in *Crfb6* (Fig. 3.28).

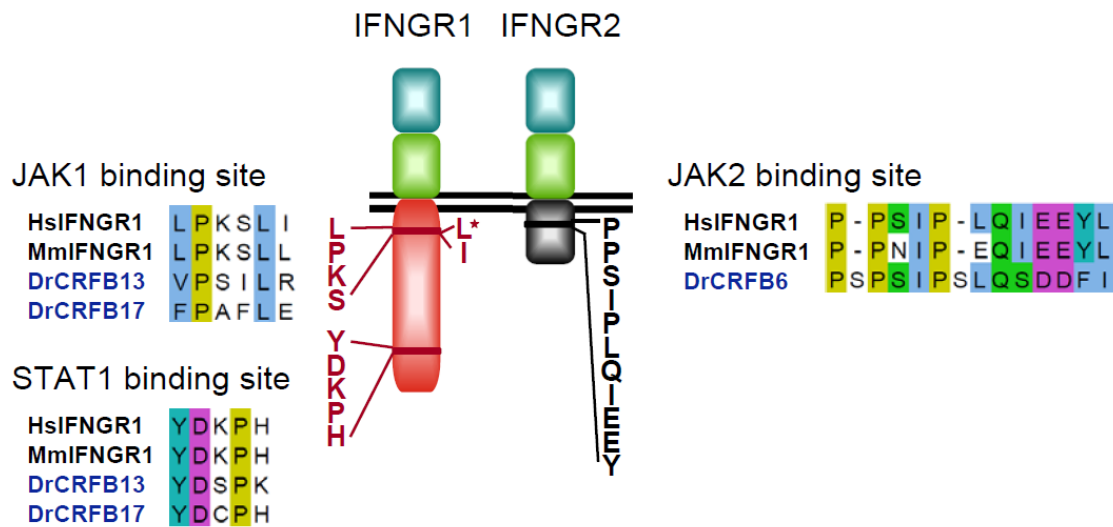


Fig. 3.28: Essential motifs of the mammalian IFNGR1 and IFNGR2 are conserved in zebrafish Crfbs. Schematic drawing representing single mammalian IFNGR1 and IFNGR2 chains. The cell membrane is denoted by two horizontal black lines. Green and blue boxes depict the extracellular S100 subdomains. Red and black rectangles show the intracellular domains. Within the intracellular domains, positions of the JAK1-binding site followed by the ligand internalization and degradation motif (denoted by an asterisk) as well as the STAT1 binding site and the JAK2 binding site are drawn to scale. The human sequence of these motifs is shown to the left and right of each chain in vertical writing. Sequence alignments of human, mouse and zebrafish interferon- γ receptor chains displaying the above mentioned motifs are shown to the left and right of the drawing.

3.2.3.2 Morpholino mediated knockdown of putative IFN γ receptor chains

To test which of the zebrafish Crfbs are involved in IFN γ signal reception, morpholino oligonucleotides were designed to knock them down. The *crfb6* and *crfb13* genes were analyzed as well as two additional candidates, the *crfb7* and *crfb15* genes.

The *crfb7* gene codes for a receptor chain with a long intracellular domain, whereas the *crfb15* gene encodes a class II cytokine receptor with a short intracellular domain (Fig 3.10). Conserved intracellular motifs were not found in the predicted protein sequences of these genes. An antisense morpholino for the *crfb17* gene was designed and validated by Georges Lutfalla.

For the *crfb6* and *crfb7* gene AUG-morpholinos were designed, which target the start AUG of the open reading frame (ORF). For the *crfb13* and *crfb15* genes splice-morpholinos were chosen.

To test the efficiency of the AUG-morpholinos, *crfb6-GFP* fusion RNA and *crfb7-GFP* fusion RNA were generated. The fusion RNA consists of the *crfb* 5'UTR and the first nucleotides of the ORF fused in frame to the coding sequence of *GFP*, so that the morpholino target site is present to perform the knockdown of this fusion RNA. Another

5'UTR-*GFP* fusion RNA was generated to test the morpholino designed against *crfb1*. *Crfb1* had been shown to be a functional receptor chain for *lfn* ϕ 1 (Levraud et al. 2007), and was used in this work as a negative control, since it did not transduce the *lfn* γ signal (Sieger et al. 2009).

Injection of the *crfb6-5'UTR-GFP* RNA in the 1-cell stage resulted in a bright fluorescence in the embryos (Fig.3.29 A, A'). Co-injection of *crfb6-5'UTR-GFP* RNA and the *crfb6* morpholino led to a full knockdown of the transcript since no fluorescence could be detected in the injected embryos (Fig.3.29 B, B'). Co-injection of *crfb6-5'UTR-GFP* RNA and *crfb1* morpholino did not affect *GFP* expression, showing that the *crfb6* morpholino effect was specific (Fig. 3.29 C, C'). In the untreated siblings no fluorescence was detectable (Fig. 3.29 D, D').

These results could not be observed when injecting *crfb7-5'UTR-GFP* RNA together with the *crfb7* morpholino. The injection of the *crfb7-5'UTR-GFP* RNA in the 1-cell stage resulted in a strong fluorescence (Fig 3.29 E, E'), but in combination with the *crfb7* morpholino, only a decrease in fluorescence could be detected (Fig 3.29 F, F'). The co-injection of *crfb7-5'UTR-GFP* RNA and the unrelated *crfb1* morpholino led to a strong fluorescence (Fig 3.29 G, G'). This shows that the *crfb7* morpholino led only to a partial knockdown of *crfb7*.

The injection of the *crfb1-5'UTR-GFP* RNA in the first cell stage also resulted in a bright fluorescence in the injected embryos (Fig. 3.29 I, I'), which was abrogated when the *crfb1* morpholino was co-injected (Fig. 3.29 J, J'). The observed effect was specific for the *crfb1* morpholino, since coinjection of the *crfb1-5'UTR-GFP* RNA with the *crfb6* morpholino showed no decrease in fluorescence in the injected embryos (Fig. 3.29 K, K').

Taken together the control experiments showed that the *crfb6* morpholino and the *crfb1* morpholino caused an efficient knockdown of the target transcript. With the *crfb7* morpholino, on the other hand, only incomplete knockdown could be achieved.

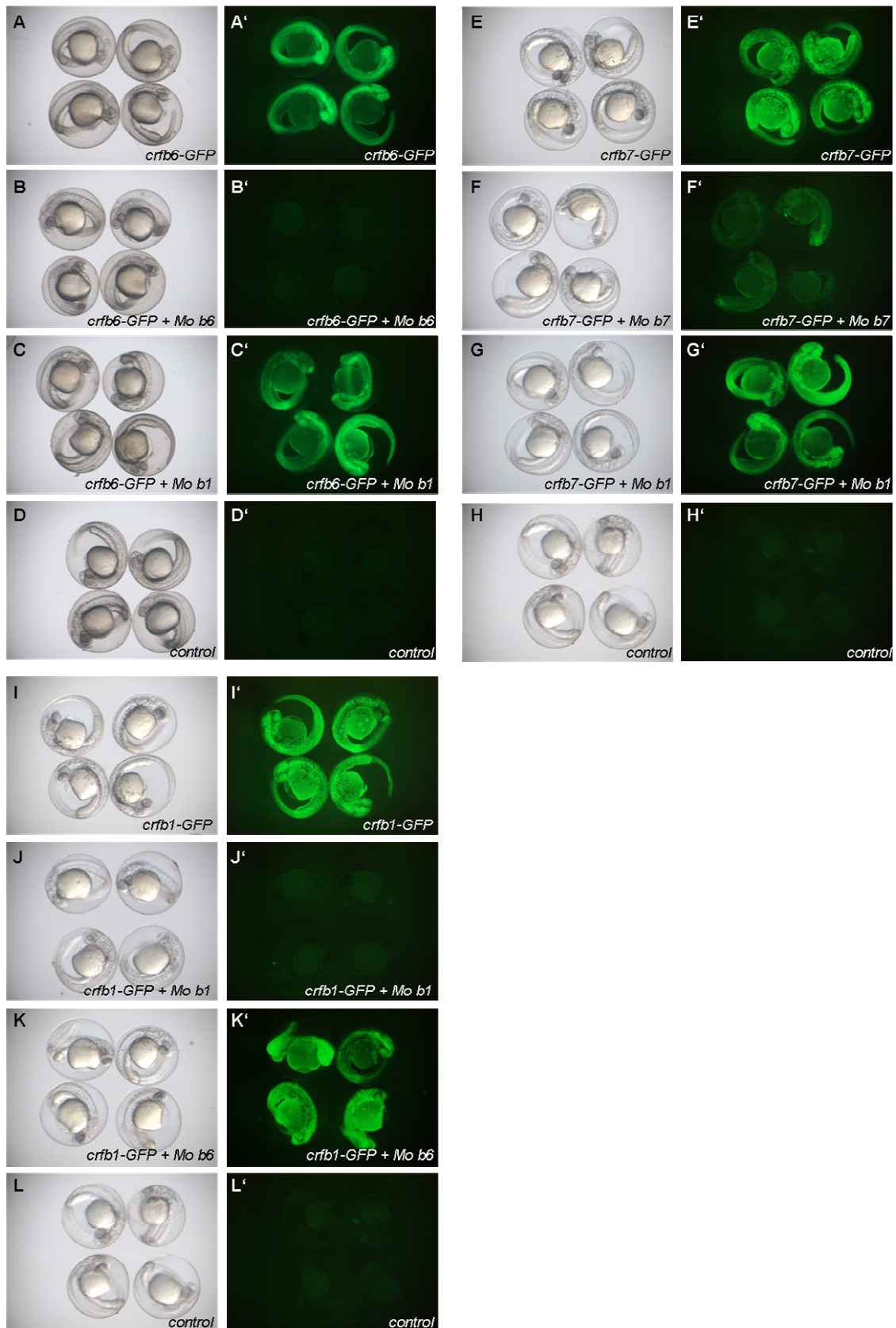


Fig. 3.29: UTR-GFP control RNA injections to validate the AUG morpholinos.

Brightfield and fluorescence images. (A)- (D') *crfb6* and untreated control, (E)- (H') *crfb7* and untreated control, (I)- (L') *crfb1* and untreated control; (A), (A') *crfb6*-5'UTR-GFP RNA injected embryos (100ng/ μ l), (B), (B') *crfb6*-5'UTR-GFP RNA (100ng/ μ l) + *crfb6* Mo (0.6mM) injected embryos; (C), (C') *crfb6*-5'UTR-

GFP RNA (100ng/μl) + *crfb1* Mo (0.6mM) injected embryos, (D), (D') untreated sibling embryos; (E), (E') *crfb7-5'UTR-GFP* RNA injected embryos (100ng/μl), (F), (F') *crfb7-5'UTR-GFP* RNA (100ng/μl) + *crfb7* Mo (0.9mM) injected embryos; (G), (G') *crfb7-5'UTR-GFP* RNA (100ng/μl) + *crfb1* Mo (0.6mM) injected embryos, (H), (H') untreated sibling embryos; (I), (I') *crfb1-5'UTR-GFP* RNA injected embryos (100ng/μl), (J), (J') *crfb1-5'UTR-GFP* RNA (100ng/μl) + *crfb1* Mo (0.6mM) injected embryos; (K), (K') *crfb1-5'UTR-GFP* RNA (100ng/μl) + *crfb6* Mo (0.6mM) injected embryos, (L), (L') untreated sibling embryos; Injections were repeated at least two times with similar results. 91-97% of the *crfb-5'UTR-GFP* RNA injected embryos showed fluorescence. The embryos injected with *crfb6-5'UTR-GFP* RNA + *crfb6* Mo and those injected with *crfb1-5'UTR-GFP* RNA + *crfb1* Mo did not show fluorescence; 78% of the embryos injected with *crfb7-5'UTR-GFP* RNA + *crfb7* Mo showed decreased fluorescence, the remaining 22% showed fluorescence. (A)-(L') whole mount embryos (28hpf).

In order to determine whether *Crfb6* participates in the signaling of *Ifny1* or *Ifny2*, one-cell stage embryos were injected with *in vitro* transcribed *ifny1* or *ifny2* mRNA alone or in combination with the *crfb6* morpholino. The mRNA of the embryos was isolated at 28-30 hpf and the generated cDNA used for RT-PCR analysis of *irgf1* expression levels (Fig. 3.30). The activation of *irgf1* expression by *Ifny* was not altered by the *crfb6* morpholino, although this morpholino induced an efficient knockdown of the *crfb6-5'UTR-GFP* RNA transcript. Notably, also a higher morpholino concentration than that used for the knockdown of the *crfb6-5'UTR-GFP* RNA transcript did not lead to a down-regulation of *Ifny*-induced *irgf1* expression.

However, in some of the experiments with the *crfb6* morpholino, a weak reduction of the *Ifny2*-induced *irgf1* expression was detected. Quantitative- (Q-) RT-PCR analyses after knockdown with a *crfb6* splice-morpholino using *irgf1* expression levels as a read-out show that knockdown of *crfb6* leads to a decrease of *IFN*2-induced *irgf1* expression. These analyses were conducted by Georges Lutfalla and Dina Aggad. This finding suggests that *Crfb6* might be involved in a receptor complex, which transduces only the *IFN*2 signal.

A potential role for *Crfb7* in *IFN* signaling could not be determined. Further attempts to design a *crfb7* splice-morpholino were unsuccessful, as no product could be amplified from genomic DNA. Several primer pairs were tested to amplify potential intron/exon boundaries, yet no products were generated. This might have been caused by an incorrect assembly of the genomic sequences at these loci, as RT-PCR products from mRNA could be generated (data not shown).

An additional AUG-Mo, which targeted the first 25 nucleotides of the *crfb7* ORF, was designed by Georges Lutfalla. However, also this morpholino was found to be non-functional.

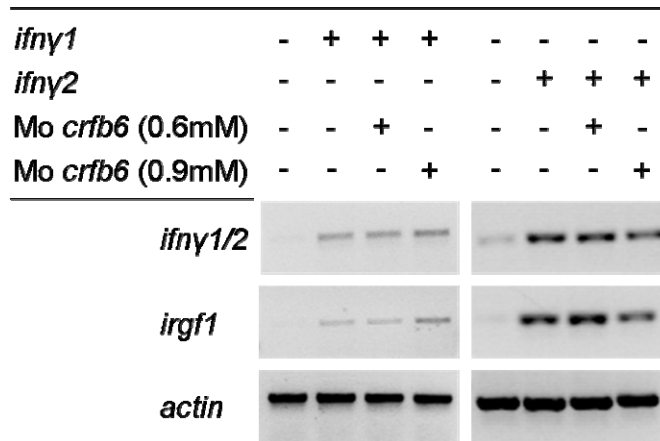


Fig. 3.30: RT-PCR analysis to determine the effect of *crfb6* Mo on *irgf1* expression.

Embryos were injected at the 1-cell stage with *ifny1* or *ifny2* mRNA (100ng/ μ l each) and in combination with the *crfb6* Mo, as indicated by the '+' signs at the top of the lanes. *ifny1*, *ifny2*, and *irgf1* gene expression was assayed at 28 hpf. To verify successful injections, the levels of *ifny1* and *ifny2* were also tested by RT-PCR. β -actin was used as a control. This result was verified in at least three independent experiments.

The efficiency of the *crfb13* and *crfb15* splice-morpholino was determined by RT-PCR. A morpholino designed against an intron/exon boundary modifies pre-mRNA splicing, which should result either in an insertion of an intron or in the deletion of an exon.

Two *crfb15* splice-morpholinos were designed. The first one was found to be non-functional, whereas the second splice-morpholinos induced the integration of an intron into the pre-mRNA. However, knockdown of *crfb15* in combination with overexpression of either *ifny* gene did not result in down-regulation of *irgf1* expression. This suggested that *crfb15* does not participate in the receptor complex involved in transducing the IFN γ 1 or IFN γ 2 signal (data not shown).

The *crfb13* gene was found to be expressed throughout development (Fig.3.31A). To test the efficiency of the *crfb13* splice-morpholino, the morpholino was injected at different concentrations into 1-cell stage embryos. The mRNA of the embryos was isolated at 28-30 hpf and the generated cDNA used for RT-PCR analysis of *crfb13* expression levels. The product size indicated that the splice-morpholino induced mis-splicing of the pre-mRNA (Fig.3.31A). Sequencing of the PCR-product identified that an alternative internal splice site was used in the *crfb13* morphants, which led to a deletion of 140 nucleotides in the transcript sequence (Fig.3.31B). This deletion induced a frameshift in the ORF, which would result in an abrogated protein that lacks the

transmembrane and intracellular domains (Fig.3.31C). Based on these findings it was concluded that the *crfb13* splice-morpholino could be used to induce a knockdown of *crfb13*.

To examine whether Crfb13 participates in the signaling of Ifn γ 1 or Ifn γ 2, 1-cell stage embryos were injected with *in vitro* transcribed *ifny1* or *ifny2* mRNA alone or in combination with the *crfb13* splice-morpholino. The mRNA of the embryos was isolated at 28-30 hpf and the generated cDNA used for RT-PCR analysis of *irgf1* expression levels. The effect of the knockdown of *crfb13* on *irgf1* expression levels were initially observed as shown in Fig.3.31, which will be discussed below. However, in several experiments the *irgf1* expression levels were not significantly altered and also the knockdown of *crfb13* seemed not complete, as two products were generated in the RT-PCR. The product band corresponding to the morpholino-induced deletion showed only a low signal intensity, whereas a product band slightly smaller in size than the *crfb13* product without deletion showed a strong intensity (data not shown). Sequencing of this PCR-product showed that the zebrafish embryos were polymorphic for the splice-site that the morpholino targeted (Fig.3.2).

Adult male and female fish were genotyped and the offspring of those that were not polymorphic for the morpholino target site were used in all further experiments.

In these experiments the effect of knockdown of *crfb13* on *irgf1* expression levels was again determined. Concomitant knockdown of *crfb13* and overexpression of *ifny2* resulted in a substantial decrease in *irgf1* expression levels (Fig. 3.33). In contrast, knockdown of *crfb13* in combination with overexpression of *ifny1* only partially reduced *irgf1* expression. These results indicate that Crfb13 is involved in transducing the Ifn γ 2 signal, whereas Ifn γ 1 signaling appears not to depend on Crfb13, or only partially.

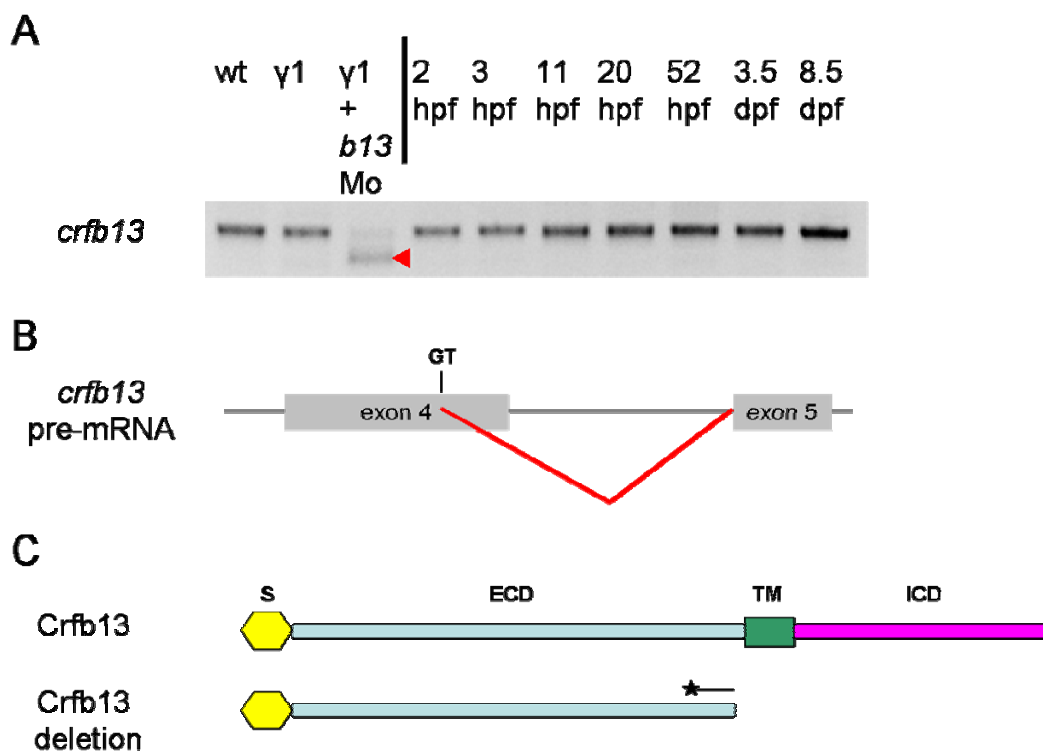


Fig. 3.31: Analysis of the *crfb13* splice-Mo effect on *crfb13*.

(A) RT-PCR analysis shows that *crfb13* is robustly expressed during embryonic and larval development (right side). Expression is also observed in untreated (wt) and *ifn γ 1* overexpressing embryos. Injection of *crfb13* splice-Mo (0.9 mM) at the 1-cell stage results in a different PCR-product size for *crfb13* (red arrowhead). The mRNA was isolated at the indicated stages and at 30 hpf (for wt, *ifn γ 1*, and *ifn γ 1*+ *crfb13*-Mo). (B) Sequencing of the PCR-product marked in A with a red arrowhead showed that the morpholino induced the usage of an internal splice site (labeled with GT) in exon 4, which leads to a deletion of 140 nucleotides in exon 4 and results in a frameshift within the ORF. (C) Schematic drawing of the predicted protein structures for Crfb13 and for the Crfb13 fragment with the deletion in exon 4. The Mo-induced splice event in the transcript sequence is denoted by a star. Due to the induced frameshift in the ORF the amino acid sequence downstream of the frameshift is scrambled (denoted by a black horizontal line). A stop codon terminates the ORF, so that a potentially produced protein lacks the transmembrane (TM) and the intracellular domain (ICD) and is therefore non-functional.

S = signal peptide, ECD = extracellular domain.

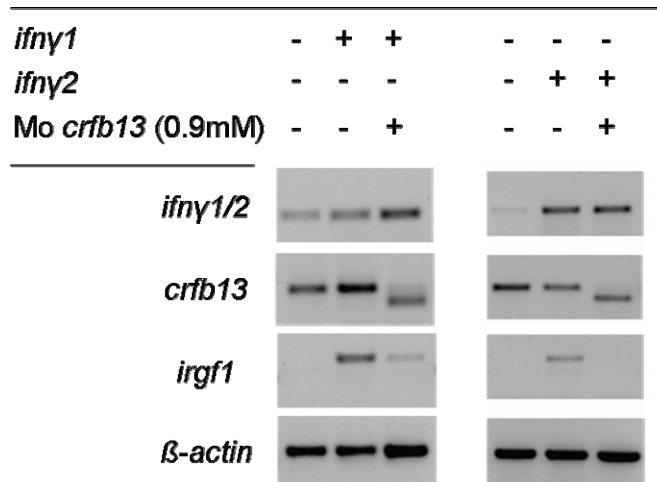


Fig. 3.33: RT-PCR analysis to determine the effect of *crfb13*-Mo on *irgf1* expression levels.

Embryos were injected at the 1-cell stage with *ifny1* or *ifny2* mRNA (100ng/ μ l each) and in combination with the *crfb13* Mo, as indicated by the '+' signs at the top of the lanes. *ifny1*, *ifny2*, *crfb13* and *irgf1* gene expression was assayed at 30 hpf. To verify successful injections, the levels of *ifny1*, *ifny2*, and *crfb13* were also tested by RT-PCR. β -actin was used as a control. This result was verified in at least three independent experiments.

3.2.3.3 *crfb13* knockdown during bacterial infection

It could be demonstrated that knockdown of *crfb13* interferes with the expression of the IFN γ -inducible gene *irgf1*, when *irgf1* expression is stimulated by *ifny2*. To find out whether the knockdown of *crfb13* also affected the innate immune response in the embryo, the potential role of *crfb13* was tested in response to infection with bacteria.

Embryos were injected at the 1-cell stage with the *crfb13* morpholino and were infected at 28-32 hpf with *Y. ruckeri* and monitored for survival. A different subset of embryos was only infected with the bacteria and served as a control, whereas in another subset both *ifny* genes were knocked down.

The infection of the embryos was conducted using different bacterial concentrations. When the embryos were infected with a relatively low dose of *Y. ruckeri* (approximately 5-10 cfu), the observed infection in the *crfb13* morphants was mild and did not lead to a decrease of survival of these embryos. The observed survival rates were similar to those observed for the infected, but otherwise untreated control. Embryos in which both *ifny* genes were down-regulated showed only at 42 hpi onwards a decrease in survival rate, so that after 48 hpi 60% of the infected embryos were alive in comparison to approximately 80% in the *crfb13* knockdown and in the infected control embryos (Fig. 3.34). Without the challenge of infection the development of untreated control embryos, *crfb13* morphants and *ifny1* + *ifny2* morphants was unaffected (Fig. 3.34).

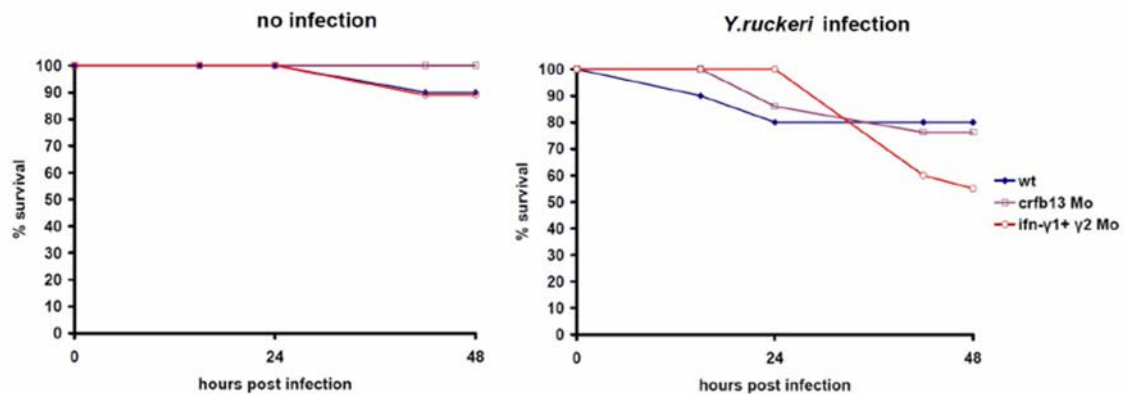


Fig. 3.34: Survival of *crfb13* knockdown embryos infected with 5cfu *Yersinia ruckeri*.

Embryos were left untreated (control) or injected with *crfb13* Mo (0.9mM) or *ifnγ1* + *ifnγ2* Mo (0.6mM each) ($n = 25$ for each treatment). The left panel shows the survival rates of embryos that were not infected, in the right panel the embryos were infected with *Yersinia ruckerii* (5-10 cfu) at 32 hpf. (Experiments were repeated two times with similar results. Data from one experiment are shown.) X-axis: hours post infection (hpi), y-axis: percentage of surviving embryos.

When the embryos were infected with a higher concentration of the pathogenic bacteria (30 cfu), a dramatic decrease in survival rate was observed for the *ifnγ1* + *ifnγ2* morphants. Less than 40% of the infected embryos survived the first 24 hpi and after 48 hpi all of these morphants had succumbed to the infection. Contrary to this, the *crfb13* morphants were not affected by the infection with *Y. ruckerii* and showed again survival rates comparable to those of the infected control embryos. Since the bacteria were labeled with DsRed, the infection was monitored using fluorescence microscopy. Fluorescence images of infected embryos showed circulating bacteria in the blood system and suggest a slightly higher bacterial load in the *ifnγ1* + *ifnγ2* morphants (Fig. 3.36). It is of note that at the time point of imaging more than 60% of the *ifnγ1* + *ifnγ2* morphants had already died because of the infection and that therefore their bacterial load could not be determined by fluorescent imaging. The morpholino-injected embryos displayed a normal development, which is supported by the finding that the observed survival rates are similar in all non-infected embryos (Fig. 3.35).

Taken together, these results indicate that the lack of *crfb13* alone had no influence on the survival rate after infection with *Y. ruckerii*.

It was therefore tested next, whether knockdown of *crfb13* in combination with a simultaneous knockdown of either *ifnγ1* or *ifnγ2* would influence the outcome of the infection. Indeed, less than 50% of the embryos injected simultaneously with *crfb13* and *ifnγ1* morpholinos survived the first 24 hours after infection, compared to 85% of infected control embryos (Fig. 3.37). Concomitant knockdown of both *ifnγ1* and *ifnγ2*

led to a similar decrease in survival. On the other hand, simultaneous knockdown of *crfb13* and *ifny2* did not result in a higher susceptibility to infection than that observed for the infected controls. Also the double-morpholino-injected embryos showed normal development and did not exhibit any signs of retardation before infection, as also reflected by the survival rate of their non-infected siblings.

These results suggest that Crfb13 has a functional role in transducing the *Ifny2* signal, whereas signaling induced by *Ifny1* is independent from Crfb13. The functional characterization of the zebrafish *ifny1* and *ifny2* gene showed that these genes act partially in a redundant manner. The receptor usage however, appears to be specific for each of the *Ifny* proteins.

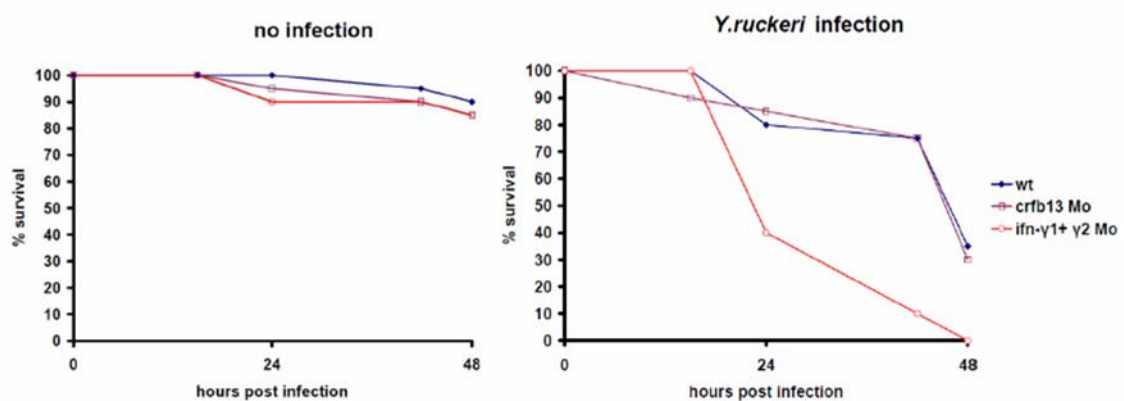


Fig. 3.35: Survival of *crfb13* knockdown embryos infected with 30cfu *Yersinia ruckeri*.

Embryos were left untreated (control) or injected with *crfb13* Mo (0.9mM) or *ifny1* + *ifny2* Mo (0.6mM each) at the 1-cell stage (n = 25 for each treatment). The left panel shows the survival rates for embryos that were not infected, in the right panel the embryos were infected with 30cfu *Yersinia ruckeri* at 32 hpf. (Experiments were repeated two times with similar results. Data from one experiment are shown.)

X-axis: hours post infection, y-axis: percentage of surviving embryos.



Fig. 3.36: Embryos infected with 30 cfu of DsRed-expressing *Yersinia ruckeri*.

Bright field and DsRed fluorescence images of embryos at 24 hpi (56 hpf). A. Embryo infected with bacteria, but otherwise untreated (control). B. Embryo injected with *crfb13* Mo (0.9mM) at the 1-cell stage and infected with *Y. ruckeri*. C. Embryo injected with *ifn-γ1* + *ifn-γ2* Mo (0.6mM each) at the 1-cell stage and infected with the pathogenic bacteria. The embryos were infected with ~30 cfu of *Y. ruckeri* at 32 hpf.

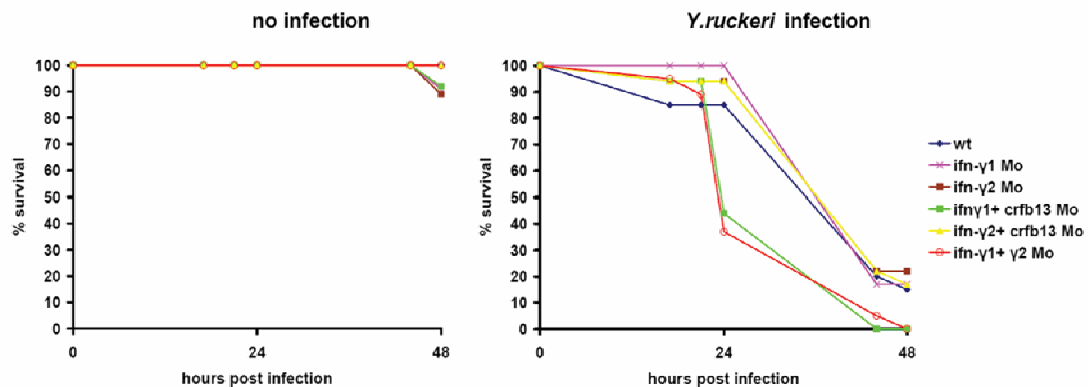


Fig. 3.37: Survival rates of embryos after knock-down of *ifn- γ* and *crfb13* and concomitant infection with *Yersinia ruckeri*

Embryos were left untreated (control) or injected with *crfb13* Mo (0.9mM) or *ifn γ 1* + *ifn γ 2* Mo (0.6mM each) at the 1-cell stage (n = 25 for each treatment). The left panel shows the survival rates for embryos that were not infected, in the right panel the embryos were infected with 30cfu *Yersinia ruckeri* at 32 hpf. X-axis: hours post infection, y-axis: percentage of surviving embryos. (Experiments were repeated three times with similar results. Data from one experiment are shown.)

3.2.4 Conserved NLR proteins in the zebrafish

Although the transcription factor CIITA belongs to the family of NLR proteins, the zebrafish *CIITA* gene was not further analyzed in this study. As a transcriptional activator of MHC class II genes, it seemed not likely to be involved in innate immune signaling.

To assess the expression of the *nod1*, *nod2*, *nod3*, *nod9*, *apaf1*, and *nwd1* genes, their basal expression was determined (Fig 3.38A). mRNA was isolated from pooled wild-type (wt) embryos at different developmental stages. The generated cDNAs were used for RT-PCR analysis. All analyzed genes were expressed during the embryonic and early larval development, albeit at different levels. The *nod1* and *apaf1* genes showed a robust expression throughout development. Early expression of *nwd1* was weak compared to the control (*β -actin*).

To test whether the *nlr* genes respond to bacterial infection or *ifn* overexpression, RT-PCRs were performed. Embryos were either injected at the 1-cell stage with *in vitro* transcribed *ifn γ 1*, *ifn γ 2*, or *ifn λ* RNA or were infected at 24 hpf or 30 hpf with *E. coli* or *Y. ruckeri*, respectively. mRNA was isolated from these embryos at 30 hpf (*ifn*-overexpression and *E. coli* infection) or 54 hpf (*Y. ruckeri* infection). Only *nod2* and *nod3* showed a weak induction upon infection with *Y. ruckeri*, and in the case of *nod2* also upon *ifn γ 1* overexpression. Furthermore, a splice variant of *nod2* was found. *Whole mount in-situ hybridization* was also performed. Besides for *nwd1*, all other *nlr*

genes were ubiquitously expressed, with the strongest staining for *nod1* and *apaf1* in the cranial region (data not shown).

The *nwd1* (*nacht-p1*) gene was selected for further analysis.

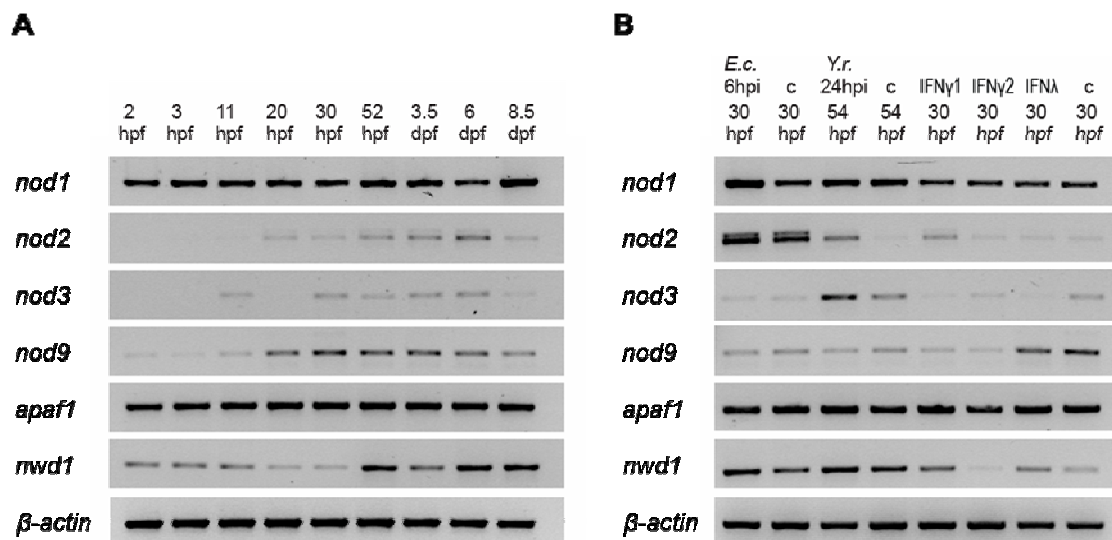


Fig. 3.38: RT-PCR analysis of the basal, infection- and lfn-induced expression of the canonical *nlr* genes and *apaf1*.

(A) For expression analysis during development, mRNA was extracted from embryos or larvae at the indicated time points. (B) Embryos were either injected with *ifn γ 1*, *ifn γ 2*, or *ifn λ* RNA at the 1-cell stage or were infected at 24 hpf or 30 hpf with 3000cfu *E. coli* or 30cfu *Y. ruckeri*, respectively. mRNA was isolated from these embryos at 30 hpf (*ifn*-overexpression and *E. coli* infection) or 54 hpf (*Y. ruckeri* infection).

β -actin was used as control.

3.2.4.1 Characterization of the *nwd1* (*nacht-p1*) gene

The discovery of a novel NLR family member not only in fish but also in mammals was unexpected. With the release of the zebrafish zv6 genome assembly the initial version of the *nwd1* (*nacht-p1*) gene was found during the search for NACHT-domain encoding genes. In contrast to the fish-specific NLRs it was annotated by the Ensembl automatic analysis pipeline. Orthologous predicted proteins were found in both mammals and in *Takifugu*, whereas the sequence for the *Tetraodon* Nwd1 (Nacht-p1) was manually derived. Using these sequences the phylogenetic tree and the estimate of the domain structure (Fig. 3.39) were generated.

When the NWD1 protein sequence was compared to all other NLRs analyzed in this study, NWD1 appeared to be most closely related to APAF1. This is accountable to the presence of the WD40 repeats, which occurred in the analysis of the 277 NLR proteins only in those two proteins. The NACHT domain of the NWD1 proteins shared the overall domain architecture of the NACHT domains of other NLR family members,

whereas the NB-ARC domain of APAF1 shows certain sequence variations that distinguish it from the NLR NACHT domain. The central motif of the NACHT domain, the ATP/GTPase specific P-loop (Walker A motif) has the sequence GPPGx(V/I)GKT and is therefore in line with the consensus sequence for the P-loop of NACHT-domain proteins: GxxGxGKT, where x is variable. However, the P-loop sequence was found to be highly conserved in NWD1 predicted sequences from more than 25 different vertebrate species (data not shown), and was not found in the other 272 NLR genes analyzed in this study.

While the NACHT domain and the WD40 repeats were easily identified, the N-terminal part of the NWD1 sequence did not exhibit any homology to known protein domains. In order to test whether the predicted sequence contained the full-length ORF of this gene, EST sequences were searched. One EST sequence was found upstream of the *nwd1* gene, the sequence of which was in frame with the predicted ORF for the *nwd1* gene. This led to a hypothetical ORF of 4596bp bases, thereby extending the previous ORF by 924 base-pairs (bp). But also this extended 5' end did not code for any known protein domain.

To determine the *nwd1* sequence, splice variants, and polymorphisms, the entire transcript of the gene was sequenced. This was performed with a 'primer walk' along the predicted transcript sequence. Additionally a 5 kb RT-PCR product (Fig. 3.39) of an *nwd1* transcript was generated, sequenced and compared to those sequences derived from the primer walk. The cDNA used for this was generated from mRNA isolated at 52 hpf. The sequence of the 5kb RT-PCR product did not have any overlaps nor did it contain internal stop codons. It seems therefore likely that a 5kb transcript of *nwd1* is expressed in the zebrafish embryo. The obtained sequencing results refined the predicted sequence of *nwd1*. By comparing the generated sequences an internal alternative intron was found. Whereas sequences generated by the 'primer walk' led to the identification of the sequence of exon 17, this exon was disrupted in the 5 kb transcript. Analysis of the missing sequence by comparison to the entire sequence of exon 17 showed that splice sites are present at the beginning and end (AG-GT) of this sequence within exon 17. Furthermore, the open reading frame of the 5 kb transcript was not affected by the absence of parts of the sequence of exon 17, suggesting that an alternative internal intron was spliced out in this transcript. The genomic structure of the *nwd1* gene and a schematic of the mRNA is presented in Fig 3.40. The *nwd1* sequence and additional information regarding the sequencing are listed in section 8 appendix.

As shown in Fig 3.40 the *nwd1* gene harbors 8 potential transcriptional start sites. To assess a putative functional role of Nwd1, a splice-Mo was designed, since it could not

be excluded that an AUG-Mo would lead to usage of an alternative start site. The designed splice-Mo was directed against the exon/intron boundary 3' to exon5, which encodes the NACHT domain. However, morpholino-mediated knockdown of *nwd1* was not achieved with this morpholino. RT-PCR analysis of *nwd1* transcripts derived from morpholino-injected embryos did not show an additional or shifted product band (data not shown). Sequencing of these RT-PCR products revealed no change in the transcript sequence indicating that the splice-morpholino is not functional. Alternative intron/exon boundaries could not be used as targets for other splice morpholinos, for various reasons. The intronic sequences were often not suited for morpholino design due to hairpin structures or repetitive intronic sequences, e.g. 5' to exon 5 (intron4/exon5). A morpholino against intron/exon boundaries of the first four exons could not be chosen, because it was not clear, which of the multiple start codons are used and it could be expected that morpholino knockdown would lead to usage of alternative start sites in neighboring exons. Moreover, it could not be excluded that the majority of *nwd1* transcripts were made from the start sites found in exon 5 and the knockdown would then not interfere with these transcripts. To target an intron/exon boundary of a different exon 3' to the NACHT-domain encoding exon 5 seemed also not promising, since it has been shown that NLR proteins lacking the C-terminus are constitutively active due to the loss of autorepression by the LRRs.

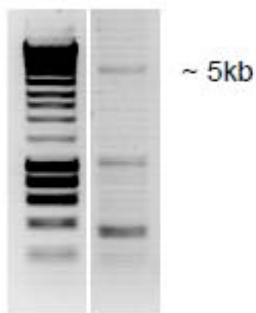
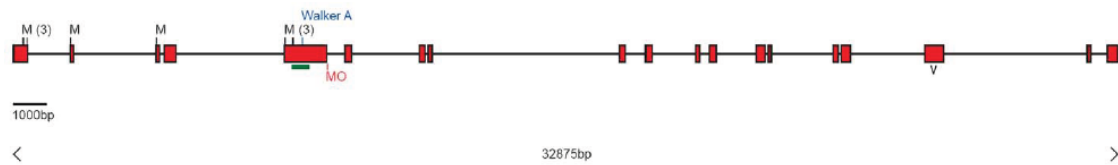


Fig. 3.39: RT-PCR analysis of a 5kb *nwd1* transcript.

Left lane shows the DNA marker (Hyperladder, Invitrogen), right lane shows the PCR products. The 5kb RT-PCR product was cloned into pCRII-Topo. Positive clones showed identical sequences, of one positive clone the entire insert was sequenced. The mRNA was isolated from embryos at 52 hpf. Sequencing of the two other PCR products (~ 350bp and ~ 1050bp in size) identified the amplification of two unrelated gene transcripts.

A Genomic organization



B mRNA

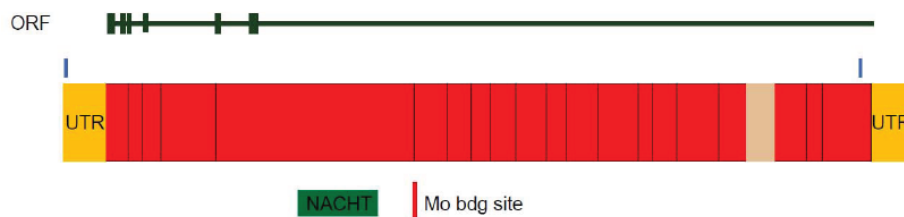


Fig. 3.40: Gene and transcript organization of the *nwd1* gene.

(A) Schematic of the genomic organization of the *nwd1* gene. The black horizontal line denotes the 33kb fragment of chromosome 11 containing the *nwd1* gene. The 19 exons are represented by red boxes. The eight potential start AUGs are depicted by small vertical lines and labeled with M. The NACHT-domain encoding sequence is marked by a green box below exon 5. The Walker A motif encoding sequence within the NACHT-domain is shown by a small blue vertical line. The morpholino-binding site at the exon 5 – intron 5 boundary is indicated in red. The alternative internal intron in exon 17 is indicated. Scale: 1000bp

(B) Schematic drawing of the *nwd1* coding sequence and exon view, based on the cDNAs generated. The putative ORF with eight alternative start sites is depicted as a black horizontal line, positions of the start AUGs are indicated by small vertical lines. The coding exons are labeled in red, the UTRs in orange. The splicable intron of exon 17 is shown in light red. Small blue vertical lines present the start and end of the 5kb *nwd1* transcript. The NACHT-domain encoding sequence is indicated by a green box and the Mo binding site by a vertical red line. The drawing is based on the sequencing results obtained.

To determine the expression pattern of *nwd1*, *whole mount in-situ hybridization* reactions were performed, which revealed that *nwd1* is specifically expressed in the neuromasts and the olfactory placodes (Fig. 3.41) at 55 hpf. Live neuromast staining was performed using the vital dye 4-Di-2-Asp (Sapede et al. 2002). *In-situ hybridization* using younger embryos (24-33 hpf) showed a weaker expression in the olfactory placodes and a ubiquitous expression in the head and the pectoral fin (data not shown). This finding correlates with the basal expression levels during development as detected by RT-PCR (Fig. 3.38), where an increase in expression was observed from 52hpf onward.

The mechanoreceptive neuromast organs respond to water turbulence and form a system of mechanosensory structures across the head and trunk, collectively called the lateral line system. The lateral line system is only present in amphibians and fish. To

test whether the *Nwd1* gene is expressed in the mouse, RT-PCRs were performed on mRNA of various organs of adult mice. The RT-PCR analysis of mouse *Nwd1* showed expression of this gene in the brain, testis, and thymus of adult mice (Fig 3.42). The expression in the testis was very low. However, sequencing of the PCR products verified the expression in all three organs.

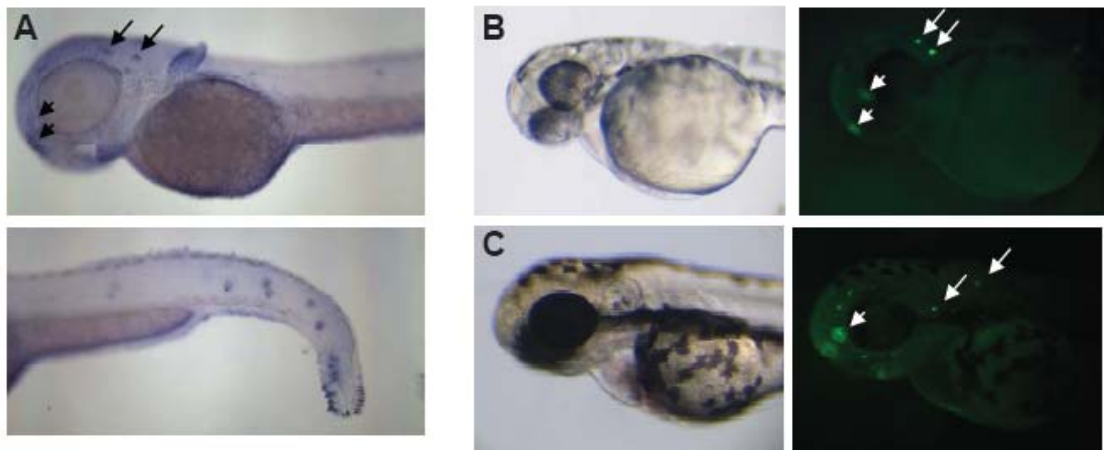


Fig. 3.41: zebrafish *nwd1* is expressed in neuromasts.

(A) WISH on 55hpf old embryos shows expression of *nwd1* in the developing neuromasts in the head (black arrow) and along the trunk. (B) Live staining of neuromasts (white arrow) with 4-di-2-Asp in 48hpf old embryos. (C) Live staining of neuromasts with 4-di-2-Asp in larva at 80hpf.

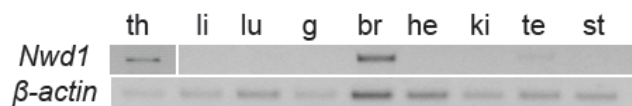


Fig. 3.42: RT-PCR expression analysis of mouse *Nwd1*.

RT-PCR on mRNA derived from adult mouse tissues. β -actin is used as control. th = thymus, li = liver, lu = lung, g = intestine, br = brain, he = heart, ki = kidney, te = testis, st = stomach. PCR-products found in thymus, brain, and testis were verified by sequencing.

4 Discussion

The zebrafish has lately been recognized as a versatile tool to obtain insights into the developing immune system of vertebrates and to study host-pathogen interactions. Various experimental infection models have been employed to study both human and fish pathogens in zebrafish, such as mycobacteria (Davis et al. 2002; Swaim et al. 2006), streptococci (Brenot et al. 2004; Neely et al. 2002), staphylococci (Prajnsar et al. 2008), *Bacillus subtilis* (Herbomel et al. 1999), and *Salmonella typhimurium* (van der Sar et al. 2003).

Compared with mammalian infection models, the zebrafish offers the advantage of forward genetic screens, along with the economy of infecting large numbers of animals. Moreover, the zebrafish embryo is readily accessible for genetic manipulation and allows real-time visualization of host-pathogen interactions.

However, it has not been clear whether the zebrafish innate immune system would employ similar defense strategies to those known from mammals and whether the complexity of the system is comparable to that of higher vertebrates.

4.1 *In silico* analysis of innate immune genes

The findings presented in this work show that the PRR and class II cytokine signaling systems known from mammals are also present in fish. Although the main constituents were found, differences were observed in the degree to which the various protein groups are conserved. These differences pertain not only to the divergence in sequence, but also to the creation of new genes by duplications.

4.1.1. Protein families with largely conserved orthology

The highest degree of conservation was found for those protein families or protein groups which act downstream of the TLRs, NLRs, or IFNs in mammals. These are the adaptor molecules, the kinases, the TRAFs and the transcriptional regulators, the IRFs and STATs.

The members of these groups exhibited by and large high sequence conservation between the different species and retained orthologous relationships, such that there was one copy found for each gene in each species, with these genes being more closely related to each other than to other genes of the group.

However, duplication of genes as well as absence of orthologous genes in mammals or fish were also observed and will be discussed in the following.

For the mammalian TIR-containing adaptor proteins TICAM1 and TICAM2 only one homologous protein was found in each fish species. The phylogenetic analysis showed that these proteins were equally distant to both mammalian TICAM proteins (section 3.2.1.1 and Fig. 3.1). This finding indicates that an ancestral gene was duplicated in the mammalian lineage followed by subsequent divergence of the two copies. Sequence and domain structure analysis of the TICAM proteins in the five species (Fig. 3.1) suggested that the mammalian TICAM1 protein exhibits more resemblance to the presumptive ancestral gene product than TICAM2.

This conclusion stands in contrast to a study by Sullivan and colleagues, who proposed that TICAM2 was lost specifically in the teleost lineage (Sullivan et al. 2007). However, *ticam2* genes seem to be absent from amphibians, birds, and reptiles, as they were not identified in the genomes of *Xenopus*, chicken (Sullivan et al. 2007) and data not shown), and Anole lizard (data not shown). A predicted ortholog in the Anole lizard did not show any resemblance to mammalian *TICAM2* and did also not encode a TIR domain.

Although, as mentioned above, there are indications that *TICAM1* might be similar to an ancestral mammalian *TICAM* gene, the phylogenetic analysis does not support the conclusion of Sullivan and colleagues that the fish *ticam* gene unambiguously corresponds to *TICAM1* in mammals nor that *TICAM2* was lost in fish.

Moreover, it has been recently reported that zebrafish TLR4 does not recognize LPS and negatively regulates NFκB signaling (Sepulcre et al. 2009). In mammals, LPS is an agonist for TLR4 and leads to the expression of NFκB- and IRF3-inducible genes. The TICAM adaptor proteins mediate the TLR4-induced IRF3 activation, in that TICAM2 physically bridges TLR4 and TICAM1 and functionally transmits LPS-TLR4 signaling to TICAM1 resulting in activation of IRF-3. Based on their results, Sepulcre and colleagues suggested that the ability of TLR4 to recognize LPS was acquired after the divergence of fish and tetrapods. This is further supported by their finding that the essential co-receptors of TLR4, MD2 and CD14, are not present in fish.

This strongly argues for the emergence of TLR4-mediated signaling involving TICAM1 and TICAM2 during the mammalian radiation, rather than the specific loss of all these genes, including *ticam2*, specifically in fish.

An apparent contradiction to the findings presented here and the conclusions drawn has been a report of both *Ticam1* and *Ticam2* in *Hydra* (Miller et al. 2007). An examination of the sequences given in their study revealed that cnidarians too have only one *Ticam*. The authors refer to the synonymous TRIF for TICAM1 and TRAM for TICAM2. However, the gene cited as *tram* in this study is in fact not encoding the TRIF-

related adaptor molecule (Tram), but encodes an unrelated protein, the translocation-associated membrane protein, which has the same acronym.

The results obtained for IRAK2 also suggest a duplication event specifically in the mammalian lineage (Fig. 3.2). The exact contribution of IRAK2 in TLR and IL-1R signaling has long remained elusive, but it was suggested that it serves as an accessory molecule in conjunction with IRAK1. Recent studies in mice have shown that IRAK2 is required to perpetuate the signal triggered by TLR4 or TLR9 (Kawagoe et al. 2008). Although the physiological role for IRAK2 in the signal cascade triggered by other TLRs has not been refined, it seems likely that IRAK2 arose in mammals to modulate specific signaling pathways.

The novel *Irf11*, on the other hand, was found only in fish. In the phylogenetic analysis *Irf11* appeared equally distantly related to IRF1 and IRF2 (Fig. 3.3). *Irf1* and *Irf2* are both found in fish, with two *irf2* genes present in zebrafish. Since *Irf11* is highly divergent in sequence but still resembles IRF1 and 2 more than the other IRFs, it seems likely that an ancestral gene was duplicated before the split of teleosts and tetrapods, and then lost in the latter. However, the phylogenetic analysis also shows that the IRF1 proteins found in the mammals and fish are rather divergent in sequence and it can therefore not be excluded that *Irf11* is a result of teleost-specific duplication.

Unambiguously identifiable gene duplications were more often found in fish than in mammals. For the protein groups with conserved orthology discussed here, duplication was observed in 12 fish genes compared to three duplicated genes in mammals. However, not all duplicated genes were found in all three fish species, arguing for duplication events within specific fish lineages rather than duplication of these genes in the entire fish lineage. Orthologous relationships between mammals and fish were analyzed for more than 50 different genes, thus the duplication of genes found in teleost, though more frequent than in mammals, does not support the third whole genome duplication postulated for the teleost lineage (Volf 2005).

But it cannot be excluded that the duplicated genes found in fish present remnants of a third genome duplication, as additional copies might have been lost or have become so divergent that they could not be identified with the search criteria applied. The analysis of the syntenic arrangement of the *STAT1-STAT4* containing region in human and zebrafish (Fig. 3.5) might support this, as it not only shows that the *Stat1* genes were duplicated in zebrafish but also that the adjacent *STAT4* had only been retained in one of the duplicated arrangements in zebrafish. Nevertheless, based on this finding it

cannot be concluded that, firstly, this duplication event has happened in all fish lineages and secondly, that this is also the case for all of the analyzed genes.

The conservation of the intracellular components of innate immune signaling pathways might also be attributed to the involvement of several of these proteins in non-immune signaling pathways, e.g. that of STAT members in Fgf signaling, which is already present in invertebrates. Conversely, not all members of the analyzed protein families have a function in innate immunity. However, for some, like TRAF3, such a function has only recently been reported (Oganessian et al. 2006).

4.1.2. Divergent protein families

The family of the class II cytokine receptors is neither highly conserved, nor does it exhibit species-specific expansions. All analyzed species have approximately the same number of receptor chain genes, but the divergence is so great that for most of the genes no reliable orthologies can be established. A similar lack of orthology is seen for the ligands, besides for IL10 and IFN γ , for which clear orthologs were found. Apart from the lineage specific expansions of the type I IFNs, there are similar numbers of class II cytokine genes in the five species. A group of fish interferons was identified, that clustered together on a clade without mammalian cytokines (Fig. 3.7). However, the strong divergence also prohibits speculations on which ligand might bind to which receptor in the zebrafish. Thus far, functional receptors have been identified for Ifn ϕ 1 and Ifn ϕ 2, consisting of either Crfb1 or Crfb2, respectively, in combination with Crfb5, and which both are involved in activating an antiviral response upon ligand binding (Aggad et al. 2009; Levraud et al. 2007). The studies presented in this work regarding potential Ifn γ receptor genes will be discussed below.

The rapid evolution of the gene families for the class II cytokines and their receptors probably reflects the fact that the IFN system is frequently subverted by pathogens, resulting in the need for compensatory mutations to escape inactivation. Significantly, the receptor family member that is not primarily associated with pathogen defense, TF, does not exhibit this high level of divergence.

The greatest divergence was found in the NLR protein family, with lineage-specific expansions in each organism, as has also been observed for this protein family in echinoderms (Hibino et al. 2006; Rast et al. 2006). Lineage-specific expansions have also been observed for the TLRs (Jault et al. 2004; Meijer et al. 2004), and for the tripartite motif (TRIM) protein family (van der Aa et al. 2009). In addition to the fish-specific expansions, these protein families have also sets of orthologous receptors in

fish and mammals. The gene family encoding non-rearranging receptors, the NITRs, however, have been found exclusively in fish and present an extraordinarily divergent and rapidly evolving gene family (Hawke et al. 2001; Yoder et al. 2004; Yoder et al. 2001).

Thus, it appears that those molecules that are directly involved in interactions with pathogen components are those that are most likely to diversify by undergoing lineage-specific expansions. Indeed, a study that specifically tested the role of lineage-specific gene families in five eukaryotic species found that the genes that were particularly prone to such expansions included those involved in responses to pathogens (Lespinet et al. 2002). Furthermore, the results presented in this work are in concordance with recent findings from a comparison of three insect genomes that showed the following (Waterhouse et al. 2007): first, the genes associated with immune functions are on average more divergent than the rest of the genome; and second, that the divergence occurs primarily in those genes whose products interact with the pathogen. The authors found that in addition to pathogen recognition proteins, this was also the case for the effectors, which were not analyzed in the study presented here.

The expansion of gene families involved in pathogen recognition is likely to reflect adaptations of the species to the specific pathogen environments. The C-terminal LRRs of the novel NLRs differ enormously in their repeat number and arrangements and also the N-terminal parts of these proteins are variable in sequence. In their NACHT and Fisna domains, however, the fish-specific NLRs exhibit high sequence conservation. It will be interesting to determine whether the Fisna domain fulfills a physiological function within the NLR protein and whether the different motifs and repeats identified in the N-terminal region interact with as yet unknown targets. Particularly for the group 1 and 2 members that harbor PYD-like motifs, it will be a question for further studies whether they would interact with the adaptor protein ASC (PYCARD), which was also identified during this analysis (Fig. 3.11) but was not included in the further investigations. In respect to the oligomerization of the NACHT-domains as shown in the inflammasomes, it will be exciting to analyze whether the different group members interact with each other via their NACHT-domains and whether there is a preference for either intra- or inter-group association.

4.2 *In vivo* analysis of innate immune genes

4.2.1. Infection assays

Initially, infection assays were tested for their capacity to induce lethal infections in embryos or larvae. With the co-incubation method this could not be achieved, as the bacteria accumulated in the gastro-intestinal tract but did not raise the mortality in the course of the experiments. Although the co-incubation method presents a natural route of infection, it appeared that the bacteria were not able to penetrate the mucosa and thereby to induce a systemic infection. Using adult Pacific salmon it was shown that *V. anguillarum* induces necrosis in the host intestinal mucosa, and it has been suggested that this presents a likely mode of excretion and transmission (Ransom et al. 1996). Both pathogens are most abundant in blood and blood-producing tissues where they are causing haemorrhagic septicaemia to which the infected host will succumb. This suggests that zebrafish larvae are more resistant to the infection, and that this might be caused by different modes of defense strategies employed during the developmental stages. Both TLRs and NLRs are expressed in mouse intestinal epithelium. Mutations in the NLRs have been associated with autoinflammatory disorders like Morbus Crohn and other bowel diseases, which are characterized by acute inflammation of the intestinal epithelium. It will be a question of further studies to analyze the contribution of the TLR, the canonical NLRs, and the novel fish-specific NLRs during infection of the gastro-intestinal tract in zebrafish larvae and adult fish.

Injection of *Y.ruckeri* into the blood system did cause a lethal infection in otherwise untreated embryos and was therefore used in the further infection assays.

4.2.2. Functional characterization of *ifny* genes and potential target genes

In support to the functional characterization of the *ifny* genes in zebrafish by Dirk Sieger, it was shown that the IFN- γ signaling system can be activated in the early zebrafish embryo and is able to upregulate several target genes.

Many of these potential target genes that are inducible by IFN γ in mammals were not inducible by the zebrafish Ifns. However, members of the *irg* family were clearly induced by both zebrafish Ifny. In particular, the members of the *irge* and *irgf* group showed responsiveness to Ifny.

This was unexpected for the members of the *irgf* group. The *irge* and *irgf* genes are most likely a result of a species-specific expansion (Bekpen et al. 2005), but they also resemble the *Irgc* genes in mammals in that they have an intron in the same place in the middle of the main exon that encodes the GTPase-domain. The mammalian *Irgc* genes are not inducible by IFN γ and their expression is restricted to the testis. Most of

the *irge* and *irgf1* genes were also found to be expressed in the testes of zebrafish (Fig. 3.25). However, their functional roles during innate immune responses as well as their function in the testis have not been analyzed yet.

The two *ifny* genes did not exhibit differences in their activation of the tested target genes, which suggests that they act at least in a partially redundant manner. This was also observed during the knockdown experiments in combination with infection. Knockdown of each *ifny* resulted in a similar reduction in survival rates, showing that, in each case, the remaining *ifny* is equally effective at inducing a low-level defence.

However, the sequences of the *ifny* genes show only a low degree of identity to each other (18.8% amino acid identity between zebrafish *ifny1* and *ifny2*). Furthermore, only *Ifny2* contains a nuclear localisation signal (NLS), whereas *Ifny1* does not. The NLS of *Ifny2* is found in the same position as in mouse and human IFN γ . Nuclear localisation of mammalian IFN γ by its NLS has been shown to be necessary for full biological activity (Subramaniam et al. 2001a). Uptake of IFN γ is a receptor-mediated endocytic process. It has been reported that plasma membrane lipid microdomains are the primary sites for the endocytic events leading to nuclear translocation of IFN γ , IFN γ 1, as well as STAT1 α (Subramaniam and Johnson 2002).

In the zebrafish embryo, however, IFN γ 1 is also without an NLS able to trigger a signaling cascade as efficiently as the NLS-containing IFN γ 2, indicating that the NLS might not be a general prerequisite for IFN γ signaling in the zebrafish. Furthermore, only downregulation of both *ifny* genes resulted in a dramatic increase of mortality due to infection. This further supports the hypothesis that *Ifny1* and *Ifny2* act redundantly in the embryos' response to bacterial infection.

4.2.3. Putative *Ifny* receptor genes

Knockdown of *crfb13* showed that *Ifny2* target gene activation is impaired and that the survival of infected embryos is dramatically decreased, when both *crfb13* and *ifny1* are downregulated. This strongly suggests that *Crfb13* is the functional ligand-binding chain in the receptor complex transducing the *Ifny2* signal. Furthermore, it indicates that the *Ifny* proteins differ in the composition of their cognate receptors.

The infection studies gave no indication that *Crfb13* is also necessary to transduce the *Ifny1* signal, as the embryos in which *ifny2* and *crfb13* were blocked showed the same survival rates as the untreated embryos. The RT-PCR analysis of the target gene induction showed a partial reduction in *irgf1* expression. Since *irgf1* is specifically induced by overexpression of either *ifny*, an influence of the basal *Ifny2* levels should

not lead to this observation, although a potential positive feedback loop for *ifny2* can not be excluded. This is supported by the finding that *ifny1* overexpression activated *ifny2* expression (Fig. 3.24), albeit the observed effect was relatively weak.

The general paradigm for the interaction of mammalian IFN γ with its receptor is that an IFN γ dimer interacts with a tetrameric receptor complex, consisting of two IFNGR1 and two IFNGR2 chains. Based on the *crfb13* knockdown experiments it appears not very likely that *lfny1* and *lfny2* constitute a heterodimer *in vivo*. On the other hand it could be theoretically possible that *Crfb13* is one of two IFNGR1 equivalents for *lfny1*, and that the other receptor chain, not affected by the knockdown of *crfb13*, is sufficient to transduce the *lfny1* signal.

Georges Lutfalla and Dina Aggad showed by Q-RT-PCR that a knockdown of *crfb17* reduces the expression of the target gene *irgf1*, when this was induced by either *lfny1* or *lfny2* (personal communication, shared manuscript in preparation). However, the decrease of *irgf1* expression levels was not as strong as that observed for knockdown of *crfb13* or *crfb6* in combination with overexpression of *lfny2*. Their finding suggests that *crfb17* is involved in the transduction of the *lfny1* signal, but it also indicates that *crfb17* might function as a receptor chain for IFN γ 2 as well. In preliminary infection assays an increase in mortality was not observed for embryos injected with *crfb17*-Mo in combination with either *ifny*-Mo. When the concentration of *Y. ruckeri* was raised to 300cfu, all embryos which were injected with either *ifny1*- and *ifny2*-Mo, or with *crfb17*-Mo in combination with *ifny1*-Mo or *ifny2*-Mo, died within 24 hours after the infection (data not shown). Further experiments will be undertaken, to determine the role of *Crfb17* in IFN γ signaling.

The finding that knockdown of *crfb6* did not alter the expression of *irgf1*, suggested that *Crfb6* might not be involved in *lfny* signaling. However, a weak reduction was sometimes observed when *irgf1* expression was induced by *lfny2*. Q-RT-PCR conducted by Georges Lutfalla and Dina Aggad showed that injection of a *crfb6* splice-Mo led to a decrease in *lfny2*-induced *irgf1* expression. This suggests that *Crfb6* might be the IFNGR2 chain equivalent for the *lfny2* receptor complex in the zebrafish.

The discrepancies of the *crfb6* knockdown effect are most likely due to the different methods applied. The semi-quantitative RT-PCR used in the present study is not as sensitive and quantifiable as the Q-RT-PCR and changes in expression levels might therefore not have been detected. However, the *crfb13* knockdown effect on *irgf1* expression was detectable by RT-PCR. The observed fold changes in *irgf1* expression were similar in the Q-RT-PCRs for *crfb13*-Mo and *crfb6*-Mo. Another explanation might be that the *crfb6*-AUG-Mo did not target the *crfb6* transcript, although successful

knockdown of the *crfb6* 5'UTR-GFP-RNA could be demonstrated or that a different translational start site was used.

In mammalian models it has been shown that the *IFNGR2* expression is tightly regulated and that in certain cell types downregulation of *IFNGR2* was induced upon exposure to IFN γ (Bach et al. 1995). The probable contribution of *Crfb6* in the *lfn2* receptor will be tested using infection assays.

In summary, these findings suggest that the *lfn2* receptor is composed of *Crfb13* as the ligand-binding and signal transducing chain and *Crfb6* as the second signal transducing chain. In the view that a functional receptor complex is potentially tetrameric, a combination of *Crfb13* and *Crfb17* appears possible. For the *lfn1* receptor only *Crfb17* is a likely candidate for the ligand binding chain. Which of the *crfb* genes encodes the second signal transducing chain could not be determined.

4.2.4. The *nwd1/NACHT-P1* gene

The *NWD1/NACHT-P1* gene was found during the phylogenetic analysis of the NLR genes as a new member of the canonical NLRs. In contrast to other NLRs, the *NWD1* protein contains WD40 repeats at its C-terminus. The *NACHT* domain shares the domain architecture of the other NLRs, but exhibits a modified P-loop. Although related to the canonical NLRs and *APAF1*, the *NWD1* protein lacks an identifiable N-terminal domain. The potential physiological role of *NWD1* has, so far, not been determined.

The initial prediction for the *nwd1* gene was based on a GenScan annotation. To validate the *nwd1* sequence and to examine splice variants and polymorphisms, transcripts of the gene were sequenced. Additional exons were found as well as internal alternative splice sites. The *nwd1* gene in zebrafish has 19 exons and encodes a protein of 1620 amino acid residues.

However, the functional analysis of *nwd1* was hampered by the fact that a knockdown was not achieved. In situ hybridization revealed expression of *nwd1* in the neuromasts. Neuromasts or the lateral line system in general, has not been linked to immune defense mechanisms. However due to the presence of the WD40 domains, *NWD1* could possibly be linked to apoptosis. It has been shown that the hair cells of the neuromast undergo cell death, whereas the surrounding mantle cells proliferate (Williams and Holder 2000). Analysis of a potential role for *NWD1* in apoptosis will be an exciting question for further studies.

5 Abstract

The zebrafish embryo offers the in vertebrates so far unparalleled opportunity to study innate immune responses without the influence of an acquired response, which starts to operate much later in development. In the recent past the zebrafish has proven to be a versatile tool to study host-pathogen interactions and an excellent model for the study of human diseases. However, it has been unclear whether the defense mechanisms employed in the embryo are comparable to that known from mammals.

In order to determine the extent of conservation between mammalian and fish innate immune pathways, a phylogenetic analysis was conducted to search the zebrafish genome and those of two pufferfish for putative orthologs of known mammalian innate immune genes. This revealed that those components of the intracellular signaling cascades, that transduce the signal downstream of the receptors, are conserved between fish and mammals. However, for the class II cytokines and their receptors the assembled data showed that orthologous relationships cannot easily be established. Within the class II cytokines it could be shown that fish have their own set of interferons (named interferon- ϕ), which are more closely related to each other than to the mammalian class II cytokine genes or to those shared by mammals and fish, suggesting that interferon genes expanded independently in zebrafish and mammals. The class II cytokine receptor genes are highly divergent. Mammals and fish have approximately the same number of receptor genes. Since syntenic relationships were found only between pufferfish and mammals and appeared to have been lost in the zebrafish, no reliable orthologies could be established.

IFN γ is a key regulator of immune responses in mammals, but a possible role of the two zebrafish *ifn γ* genes during innate immunity is not well established. Infection studies in zebrafish embryos showed that both genes mediate responses to protect the embryo against pathogenic bacterial infection, but seem to function in a redundant manner. Analysis of putative interferon receptor genes revealed that zebrafish *Ifn γ 1* and *Ifn γ 2* use distinct receptor chains to transduce the signal to the conserved intracellular signaling pathway. By conducting knockdown experiments in combination with infection assays it was shown that *ifn γ 2* depends on *crfb13* to protect the embryo against infection with *Yersinia ruckeri*.

Among the NLR protein family, a large fish-specific expansion was found. The NLRs are intracellular pathogen sensors that have only recently been described in mammals. They react to various pathogens and are implicated in several human autoimmune disorders, such as Morbus Crohn. More than 200 novel zebrafish genes encoding

NLRs were identified in this study. They were found to be closely related to each other but lack the identifiable effector domains that mediate the downstream events in mammals. A new conserved domain was identified, which is present in all fish NLRs and which was termed Fisna. Its functional role is however unknown.

Taken together the results from the phylogentic analyses suggest that the signaling mediators are conserved in fish, whereas those proteins that possibly respond to or interact with pathogens appear to have diverged.

In addition to the fish-specific NLRs, *Nwd1*/NACHT-P1 was identified as a novel NLR gene in fish and mammals. Analysis of the genomic organization and transcript structure of zebrafish *nwd1* revealed that it encodes a predicted protein of 1620 amino acids that does not contain any known N-terminal effector domain. In situ hybridization in zebrafish showed that it is specifically expressed in neuromasts, which are mechanosensory organs found only in fish and amphibians. In RT-PCR studies, mouse *Nwd1* was found expressed in tissues such as brain, thymus, or testis. These data suggest a functional role for this gene, which awaits further analysis.

6 Zusammenfassung

Der Zebrafisch Embryo bietet die Möglichkeit das angeborene Immunsystem in Vertebraten unabhängig von dem Einfluss einer adaptiven Immunantwort zu untersuchen, was in Säugertiermodellen nicht durchzuführen ist. In den letzten Jahren hat sich der Zebrafisch als geeignetes Modellsystem zur Untersuchung von Interaktionen zwischen Wirt und Pathogenen herausgestellt und wird als Modell zur Untersuchung von Krankheiten des Menschen verwendet. Es war bislang jedoch nicht geklärt, inwieweit die Verteidigungsstrategien des angeborenen Immunsystems in Fischembryonen mit den in Säugern bekannten Mechanismen vergleichbar sind.

Um das Ausmaß der Konservierung zwischen den angeborenen Immunmechanismen in Fischen und Säugern zu bestimmen, wurde eine phylogenetische Analyse durchgeführt. Dazu wurden das Genom des Zebrafisches und die Genome zweier Kugelfischarten auf mögliche Orthologe der aus Säugern bekannten Komponenten durchsucht und die gefundenen Proteine hinsichtlich ihrer Verwandtschaftsbeziehungen zu den entsprechenden Säugerproteinen analysiert.

Dies zeigte, dass die meisten Komponenten der intrazellulären Signaltransduktionskaskaden, die an einer Signalweiterleitung beteiligt sind, in Säugern und Fischen konserviert sind.

Die Ergebnisse für die Mitglieder der Klasse II Cytokine und ihrer Rezeptoren ergaben, dass die phylogenetischen Verwandtschaftsbeziehungen in dieser Gruppe schwierig zu bestimmen sind. Es wurde gezeigt, dass Fische innerhalb der Klasse II Cytokine eine eigene Gruppe von Interferonen besitzen (bezeichnet als Interferon- ϕ), die untereinander engere Verwandtschaft aufweisen als mit Klasse II Cytokinen die in Fischen und Säugern oder nur in Säugern vorkommen. Daher scheinen die Interferongene in Zebrafischen und Säugern unabhängig voneinander expandiert zu sein. Die Rezeptoren der Klasse II Cytokine sind hochgradig divergent. Säuger und Fische besitzen ungefähr die gleiche Anzahl an Genen für die Rezeptoren. Da Syntenieverhältnisse nur zwischen Säugern und Kugelfischen gefunden wurden, aber in Zebrafischen anscheinend verloren gegangen sind, konnten keine verlässlichen Orthologien bestimmt werden.

Interferon- γ ist ein bedeutsamer Regulator vieler Immunreaktionen in Säugetieren, eine Rolle der beiden Zebrafisch *Interferon- γ* Gene bei der angeborenen Immunität wurde bis vor kurzem jedoch nicht untersucht. Infektionsexperimente in Zebrafischembryonen ergaben, dass die beiden *ifn γ* Gene im Zebrafisch am Schutz des Embryos gegenüber pathogenen bakteriellen Infektionen beteiligt sind, dabei aber anscheinend redundante

Funktionen ausüben. Die Untersuchung möglicher Gene für Interferonrezeptorketten ergab, dass *Ifny1* und *Ifny2* unterschiedliche Rezeptorketten nutzen, um das Signal an den konservierten intrazellulären Signalweg weiterzuleiten. Durch sogenannte *knockdown* Experimente in Kombination mit Infektionsansätzen wurde bestimmt, dass *Ifny2* von *Crfb13* abhängt, um den Embryo vor einer Infektion mit *Yersinia ruckeri* zu schützen.

In der NLR Proteinfamilie konnte eine große, Fisch-spezifische Expansion festgestellt werden. Die NLRs sind intrazelluläre Pathogensensoren, die erst vor kurzem in Säugern beschrieben wurden. Sie reagieren auf verschiedene Pathogene und sind an Autoimmunkrankheiten beteiligt wie etwa Morbus Crohn. In dieser Arbeit konnten über 200 neue Zebrafisch Gene für NLRs identifiziert werden, die zwar sehr eng miteinander verwandt sind, jedoch keine der aus Säugern bekannten Effektor-domänen zur Signalweiterleitung enthalten. Eine neue, in allen Fisch-NLRs konservierte Domäne wurde identifiziert, die *Fisna* genannt wurde. Ihre physiologische Funktion ist allerdings noch ungeklärt. Zusammengefaßt deuten die Ergebnisse der phylogenetischen Analyse darauf hin, dass die Signalmediatoren in Wirbeltieren konserviert sind, während Proteine, die auf Pathogene reagieren oder mit ihnen interagieren, anscheinend divergiert sind.

Zusätzlich zu den Fisch-spezifischen NLRs wurde ein neues NLR Protein, *NWD1/NACHT-P1*, in Fischen und Säugern identifiziert. Eine Analyse der genomischen Organisation von *nwd1* und der Struktur von dessen Transkripten zeigte, dass es für ein Protein von 1620 Aminosäureresten kodiert welches keine der bekannten Effektor-domänen im N-terminalen Bereich enthält. *In situ* Hybridisierung zeigte, dass das Gen in der Zebrafischlarve in Neuromasten exprimiert ist. Dies sind mechanosensorische Organe in Fischen und Amphibien, die in Säugern nicht vorkommen. RT-PCR Analysen von murinem *Nwd1* ergaben, dass es in unterschiedlichen Geweben exprimiert wird, wie etwa im Gehirn, im Thymus oder im Testis. Dies deutet darauf hin, dass das Genprodukt eine funktionale Rolle besitzt, die in zukünftigen Studien noch zu ermitteln ist.

7 References

- Abi Rached, L., McDermott, M. F., and Pontarotti, P.: The MHC big bang. *Immunol Rev* 167: 33-44, 1999
- Acehan, D., Jiang, X., Morgan, D. G., Heuser, J. E., Wang, X., and Akey, C. W.: Three-dimensional structure of the apoptosome: implications for assembly, procaspase-9 binding, and activation. *Mol Cell* 9: 423-32, 2002
- Aderem, A. and Ulevitch, R. J.: Toll-like receptors in the induction of the innate immune response. *Nature* 406: 782-7, 2000
- Adkins, B.: T-cell function in newborn mice and humans. *Immunol Today* 20: 330-5, 1999
- Aggad, D., Mazel, M., Boudinot, P., Mogensen, K. E., Hamming, O. J., Hartmann, R., Kottenko, S., Herbomel, P., Lutfalla, G., and Levraud, J. P.: The two groups of zebrafish virus-induced interferons signal via distinct receptors with specific and shared chains. *J Immunol* 183: 3924-31, 2009
- Agius, C., Agbede, S.A: An electron microscopical study on the genesis of lipofuscin, melanin and haemopoietin in the haemopoietic tissues of fish. *J. Fish Biol.* 24: 471- 488, 1984
- Al-Adhami, M. A. and Kunz, Y. W.: Ontogenesis of haematopoietic sites in *Brachydanio Rerio*. *Development Growth & Differentiation* 19: 171-179, 1977
- Alder, M. N., Rogozin, I. B., Iyer, L. M., Glazko, G. V., Cooper, M. D., and Pancer, Z.: Diversity and function of adaptive immune receptors in a jawless vertebrate. *Science* 310: 1970-3, 2005
- Altmann, S. M., Mellon, M. T., Distel, D. L., and Kim, C. H.: Molecular and functional analysis of an interferon gene from the zebrafish, *Danio rerio*. *J Virol* 77: 1992-2002, 2003
- Altschul, S. F., Gish, W., Miller, W., Myers, E. W., and Lipman, D. J.: Basic local alignment search tool. *J Mol Biol* 215: 403-10, 1990
- Amatruda, J. F. and Zon, L. I.: Dissecting hematopoiesis and disease using the zebrafish. *Dev Biol* 216: 1-15, 1999
- Andrejeva, J., Childs, K. S., Young, D. F., Carlos, T. S., Stock, N., Goodbourn, S., and Randall, R. E.: The V proteins of paramyxoviruses bind the IFN-inducible RNA helicase, mda-5, and inhibit its activation of the IFN-beta promoter. *Proc Natl Acad Sci U S A* 101: 17264-9, 2004
- Arbouzova, N. I. and Zeidler, M. P.: JAK/STAT signalling in *Drosophila*: insights into conserved regulatory and cellular functions. *Development* 133: 2605-16, 2006
- Arch, R. H. and Thompson, C. B.: 4-1BB and Ox40 are members of a tumor necrosis factor (TNF)-nerve growth factor receptor subfamily that bind TNF receptor-associated factors and activate nuclear factor kappaB. *Mol Cell Biol* 18: 558-65, 1998
- Bach, E. A., Szabo, S. J., Dighe, A. S., Ashkenazi, A., Aguet, M., Murphy, K. M., and Schreiber, R. D.: Ligand-induced autoregulation of IFN-gamma receptor beta chain expression in T helper cell subsets. *Science* 270: 1215-8, 1995
- Bach, E. A., Tanner, J. W., Marsters, S., Ashkenazi, A., Aguet, M., Shaw, A. S., and Schreiber, R. D.: Ligand-induced assembly and activation of the gamma interferon receptor in intact cells. *Mol Cell Biol* 16: 3214-21, 1996
- Balachandran, S., Thomas, E., and Barber, G. N.: A FADD-dependent innate immune mechanism in mammalian cells. *Nature* 432: 401-5, 2004
- Barut, B. A. and Zon, L. I.: Realizing the potential of zebrafish as a model for human disease. *Physiol Genomics* 2: 49-51, 2000

- Bazan, J. F.: Structural design and molecular evolution of a cytokine receptor superfamily. *Proc Natl Acad Sci U S A* 87: 6934-8, 1990
- Bekpen, C., Hunn, J. P., Rohde, C., Parvanova, I., Guethlein, L., Dunn, D. M., Glowalla, E., Leptin, M., and Howard, J. C.: The interferon-inducible p47 (IRG) GTPases in vertebrates: loss of the cell autonomous resistance mechanism in the human lineage. *Genome Biol* 6: R92, 2005
- Berman, J. N., Kanki, J. P., and Look, A. T.: Zebrafish as a model for myelopoiesis during embryogenesis. *Exp Hematol* 33: 997-1006, 2005
- Bertrand, J. Y., Kim, A. D., Teng, S., and Traver, D.: CD41+ cmyb+ precursors colonize the zebrafish pronephros by a novel migration route to initiate adult hematopoiesis. *Development* 135: 1853-62, 2008
- Bertrand, J. Y., Kim, A. D., Violette, E. P., Stachura, D. L., Cisson, J. L., and Traver, D.: Definitive hematopoiesis initiates through a committed erythromyeloid progenitor in the zebrafish embryo. *Development* 134: 4147-56, 2007
- Beutler, B. A.: TLRs and innate immunity. *Blood* 113: 1399-1407, 2009
- Bin, L. H., Xu, L. G., and Shu, H. B.: TIRP, a novel Toll/interleukin-1 receptor (TIR) domain-containing adapter protein involved in TIR signaling. *J Biol Chem* 278: 24526-32, 2003
- Birnboim, H. C. and Doly, J.: A rapid alkaline extraction procedure for screening recombinant plasmid DNA. *Nucleic Acids Res* 7: 1513-23, 1979
- Boeckmann, B., Bairoch, A., Apweiler, R., Blatter, M. C., Estreicher, A., Gasteiger, E., Martin, M. J., Michoud, K., O'Donovan, C., Phan, I., Pilbout, S., and Schneider, M.: The SWISS-PROT protein knowledgebase and its supplement TrEMBL in 2003. *Nucleic Acids Res* 31: 365-70, 2003
- Boehm, U., Guethlein, L., Klamp, T., Ozbek, K., Schaub, A., Futterer, A., Pfeffer, K., and Howard, J. C.: Two families of GTPases dominate the complex cellular response to IFN-gamma. *J Immunol* 161: 6715-23, 1998
- Boyden, E. D. and Dietrich, W. F.: Nalp1b controls mouse macrophage susceptibility to anthrax lethal toxin. *Nat Genet* 38: 240, 2006
- Brenot, A., King, K. Y., Janowiak, B., Griffith, O., and Caparon, M. G.: Contribution of glutathione peroxidase to the virulence of *Streptococcus pyogenes*. *Infect Immun* 72: 408-13, 2004
- Burns, C. E., DeBlasio, T., Zhou, Y., Zhang, J., Zon, L., and Nimer, S. D.: Isolation and characterization of runxa and runxb, zebrafish members of the runt family of transcriptional regulators. *Exp Hematol* 30: 1381-9, 2002
- Burns, C. E., Traver, D., Mayhall, E., Shepard, J. L., and Zon, L. I.: Hematopoietic stem cell fate is established by the Notch-Runx pathway. *Genes Dev* 19: 2331-42, 2005
- Cervantes, J., Nagata, T., Uchijima, M., Shibata, K., and Koide, Y.: Intracytosolic *Listeria monocytogenes* induces cell death through caspase-1 activation in murine macrophages. *Cell Microbiol* 10: 41-52, 2008
- Chamaillard, M., Hashimoto, M., Horie, Y., Masumoto, J., Qiu, S., Saab, L., Ogura, Y., Kawasaki, A., Fukase, K., Kusumoto, S., Valvano, M. A., Foster, S. J., Mak, T. W., Nunez, G., and Inohara, N.: An essential role for NOD1 in host recognition of bacterial peptidoglycan containing diaminopimelic acid. *Nat Immunol* 4: 702-7, 2003
- Chen, J. Y., You, Y. K., Chen, J. C., Huang, T. C., and Kuo, C. M.: Organization and promoter analysis of the zebrafish (*Danio rerio*) interferon gene. *DNA Cell Biol* 24: 641-50, 2005
- Chen, W. Q., Xu, Q. Q., Chang, M. X., Zou, J., Secombes, C. J., Peng, K. M., and Nie, P.: Molecular characterization and expression analysis of the IFN-gamma related gene (IFN-gammarel) in grass carp *Ctenopharyngodon idella*. *Vet Immunol Immunopathol*, 2009

- Chung, J. Y., Park, Y. C., Ye, H., and Wu, H.: All TRAFs are not created equal: common and distinct molecular mechanisms of TRAF-mediated signal transduction. *J Cell Sci* 115: 679-88, 2002
- Clamp, M., Cuff, J., Searle, S. M., and Barton, G. J.: The Jalview Java alignment editor. *Bioinformatics* 20: 426-7, 2004
- Collazo, A., Fraser, S. E., and Mabee, P. M.: A dual embryonic origin for vertebrate mechanoreceptors. *Science* 264: 426-30, 1994
- Cooper, M. D. and Alder, M. N.: The evolution of adaptive immune systems. *Cell* 124: 815-22, 2006
- Crowhurst, M. O., Layton, J. E., and Lieschke, G. J.: Developmental biology of zebrafish myeloid cells. *Int J Dev Biol* 46: 483-92, 2002
- Cui, S., Eisenacher, K., Kirchhofer, A., Brzozka, K., Lammens, A., Lammens, K., Fujita, T., Conzelmann, K. K., Krug, A., and Hopfner, K. P.: The C-terminal regulatory domain is the RNA 5'-triphosphate sensor of RIG-I. *Mol Cell* 29: 169-79, 2008
- Cumano, A., Ferraz, J. C., Klaine, M., Di Santo, J. P., and Godin, I.: Intraembryonic, but not yolk sac hematopoietic precursors, isolated before circulation, provide long-term multilineage reconstitution. *Immunity* 15: 477-85, 2001
- Damiano, J. S., Oliveira, V., Welsh, K., and Reed, J. C.: Heterotypic interactions among NACHT domains: implications for regulation of innate immune responses. *Biochem J* 381: 213-9, 2004
- Danilova, N., Hohman, V. S., Sacher, F., Ota, T., Willett, C. E., and Steiner, L. A.: T cells and the thymus in developing zebrafish. *Dev Comp Immunol* 28: 755-67, 2004
- Danilova, N. and Steiner, L. A.: B cells develop in the zebrafish pancreas. *Proc Natl Acad Sci U S A* 99: 13711-6, 2002
- Darnell, J. E., Jr.: STATs and gene regulation. *Science* 277: 1630-5, 1997
- Davis, J. M., Clay, H., Lewis, J. L., Ghori, N., Herbomel, P., and Ramakrishnan, L.: Real-time visualization of mycobacterium-macrophage interactions leading to initiation of granuloma formation in zebrafish embryos. *Immunity* 17: 693-702, 2002
- Deng, L., Wang, C., Spencer, E., Yang, L., Braun, A., You, J., Slaughter, C., Pickart, C., and Chen, Z. J.: Activation of the I κ B kinase complex by TRAF6 requires a dimeric ubiquitin-conjugating enzyme complex and a unique polyubiquitin chain. *Cell* 103: 351-61, 2000
- Der, S. D., Zhou, A., Williams, B. R., and Silverman, R. H.: Identification of genes differentially regulated by interferon alpha, beta, or gamma using oligonucleotide arrays. *Proc Natl Acad Sci U S A* 95: 15623-8, 1998
- DeSandro, A., Nagarajan, U. M., and Boss, J. M.: The bare lymphocyte syndrome: molecular clues to the transcriptional regulation of major histocompatibility complex class II genes. *Am J Hum Genet* 65: 279-86, 1999
- Detrich, H. W., 3rd, Kieran, M. W., Chan, F. Y., Barone, L. M., Yee, K., Rundstadler, J. A., Pratt, S., Ransom, D., and Zon, L. I.: Intraembryonic hematopoietic cell migration during vertebrate development. *Proc Natl Acad Sci U S A* 92: 10713-7, 1995
- DeYoung, B. J. and Innes, R. W.: Plant NBS-LRR proteins in pathogen sensing and host defense. *Nat Immunol* 7: 1243-9, 2006
- Diaz, M. O., Pomykala, H. M., Bohlander, S. K., Maltepe, E., Malik, K., Brownstein, B., and Olopade, O. I.: Structure of the human type-I interferon gene cluster determined from a YAC clone contig. *Genomics* 22: 540-52, 1994
- Dobson, J. T., Seibert, J., Teh, E. M., Da'as, S., Fraser, R. B., Paw, B. H., Lin, T. J., and Berman, J. N.: Carboxypeptidase A5 identifies a novel mast cell lineage in the zebrafish providing new insight into mast cell fate determination. *Blood* 112: 2969-72, 2008

- Dodds, P. N., Lawrence, G. J., Catanzariti, A. M., Teh, T., Wang, C. I., Ayliffe, M. A., Kobe, B., and Ellis, J. G.: Direct protein interaction underlies gene-for-gene specificity and coevolution of the flax resistance genes and flax rust avirulence genes. *Proc Natl Acad Sci U S A* 103: 8888-93, 2006
- Du Pasquier, L.: The immune system of invertebrates and vertebrates. *Comp Biochem Physiol B Biochem Mol Biol* 129: 1-15, 2001
- Eddy, S. R.: Profile hidden Markov models. *Bioinformatics* 14: 755-63, 1998
- Efron, B.: The Jackknife, the Bootstrap and Other Resampling Plans. *CBMS-NSF Regional Conference Series in Applied Mathematics*, SIAM, Philadelphia, 1982
- Ehrt, S., Schnappinger, D., Bekiranov, S., Drenkow, J., Shi, S., Gingeras, T. R., Gaasterland, T., Schoolnik, G., and Nathan, C.: Reprogramming of the macrophage transcriptome in response to interferon-gamma and Mycobacterium tuberculosis: signaling roles of nitric oxide synthase-2 and phagocyte oxidase. *J Exp Med* 194: 1123-40, 2001
- Evans, D. L., Carlson, R. L., Graves, S. S., and Hogan, K. T.: Nonspecific cytotoxic cells in fish (*Ictalurus punctatus*). IV. Target cell binding and recycling capacity. *Dev Comp Immunol* 8: 823-33, 1984a
- Evans, D. L., Graves, S. S., Cobb, D., and Dawe, D. L.: Nonspecific cytotoxic cells in fish (*Ictalurus punctatus*). II. Parameters of target cell lysis and specificity. *Dev Comp Immunol* 8: 303-12, 1984b
- Evans, D. L., Hogan, K. T., Graves, S. S., Carlson, R. L., Jr., Floyd, E., and Dawe, D. L.: Nonspecific cytotoxic cells in fish (*Ictalurus punctatus*). III. Biophysical and biochemical properties affecting cytolysis. *Dev Comp Immunol* 8: 599-610, 1984c
- Evans, D. L., Smith, E. E., Jr., and Brown, F. E.: Nonspecific cytotoxic cells in fish (*Ictalurus punctatus*). VI. Flow cytometric analysis. *Dev Comp Immunol* 11: 95-104, 1987
- Farrar, M. A., Campbell, J. D., and Schreiber, R. D.: Identification of a functionally important sequence in the C terminus of the interferon-gamma receptor. *Proc Natl Acad Sci U S A* 89: 11706-10, 1992
- Farrar, M. A., Fernandez-Luna, J., and Schreiber, R. D.: Identification of two regions within the cytoplasmic domain of the human interferon-gamma receptor required for function. *J Biol Chem* 266: 19626-35, 1991
- Faustin, B., Lartigue, L., Bruey, J.-M., Luciano, F., Sergienko, E., Bailly-Maitre, B., Volkmann, N., Hanein, D., Rouiller, I., and Reed, J. C.: Reconstituted NALP1 Inflammasome Reveals Two-Step Mechanism of Caspase-1 Activation. *Molecular Cell* 25: 713, 2007
- Feldmeyer, L., Keller, M., Niklaus, G., Hohl, D., Werner, S., and Beer, H. D.: The inflammasome mediates UVB-induced activation and secretion of interleukin-1beta by keratinocytes. *Curr Biol* 17: 1140-5, 2007
- Felsenstein, J.: Confidence limits on phylogenies: An approach using the bootstrap. *Evolution* 39: 783-791, 1985
- Ferguson, H. W.: The relationship between ellipsoids and melano-macrophage centres in the spleen of turbot (*Scophthalmus maximus*). *Journal of Comparative Pathology* 86: 377, 1976
- Fernandes-Alnemri, T., Wu, J., Yu, J. W., Datta, P., Miller, B., Jankowski, W., Rosenberg, S., Zhang, J., and Alnemri, E. S.: The pyroptosome: a supramolecular assembly of ASC dimers mediating inflammatory cell death via caspase-1 activation. *Cell Death Differ* 14: 1590-604, 2007
- Field, H. A., Ober, E. A., Roeser, T., and Stainier, D. Y. R.: Formation of the digestive system in zebrafish. I. liver morphogenesis. *Developmental Biology* 253: 279, 2003
- Finn, R. D., Tate, J., Misty, J., Coghill, P. C., Sammut, S. J., Hotz, H.-R., Ceric, G., Forslund, K., Eddy, S. R., Sonnhammer, E. L. L., and Bateman, A.: The Pfam protein families database. *Nucl. Acids Res.* 36: D281-288, 2008

- Finstad, J. and Good, R. A.: The Evolution Of The Immune Response. 3. Immunologic Responses In The Lamprey. *J Exp Med* 120: 1151-68, 1964
- Fitzgerald, K. A., Palsson-McDermott, E. M., Bowie, A. G., Jefferies, C. A., Mansell, A. S., Brady, G., Brint, E., Dunne, A., Gray, P., Harte, M. T., McMurray, D., Smith, D. E., Sims, J. E., Bird, T. A., and O'Neill, L. A.: Mal (MyD88-adaptor-like) is required for Toll-like receptor-4 signal transduction. *Nature* 413: 78-83, 2001
- Franchi, L., Amer, A., Body-Malapel, M., Kanneganti, T. D., Ozoren, N., Jagirdar, R., Inohara, N., Vandenabeele, P., Bertin, J., Coyle, A., Grant, E. P., and Nunez, G.: Cytosolic flagellin requires Ipaf for activation of caspase-1 and interleukin 1beta in salmonella-infected macrophages. *Nat Immunol* 7: 576-82, 2006
- Franchi, L., Kanneganti, T. D., Dubyak, G. R., and Nunez, G.: Differential requirement of P2X7 receptor and intracellular K⁺ for caspase-1 activation induced by intracellular and extracellular bacteria. *J Biol Chem* 282: 18810-8, 2007
- Fujii, T., Nakagawa, H., and Murakawa, S.: Immunity in lamprey. I. Production of haemolytic and haemagglutinating antibody to sheep red blood cells in Japanese lampreys. *Dev Comp Immunol* 3: 441-51, 1979a
- Fujii, T., Nakagawa, H., and Murakawa, S.: Immunity in lamprey. II. Antigen-binding responses to sheep erythrocytes and hapten in the ammocoete. *Dev Comp Immunol* 3: 609-20, 1979b
- Fujisawa, A., Kambe, N., Saito, M., Nishikomori, R., Tanizaki, H., Kanazawa, N., Adachi, S., Heike, T., Sagara, J., Suda, T., Nakahata, T., and Miyachi, Y.: Disease-associated mutations in CIAS1 induce cathepsin B-dependent rapid cell death of human THP-1 monocytic cells. *Blood* 109: 2903-11, 2007
- Furnes, C., Seppola, M., and Robertsen, B.: Molecular characterisation and expression analysis of interferon gamma in Atlantic cod (*Gadus morhua*). *Fish & Shellfish Immunology* 26: 285, 2009
- Gack, M. U., Shin, Y. C., Joo, C.-H., Urano, T., Liang, C., Sun, L., Takeuchi, O., Akira, S., Chen, Z., Inoue, S., and Jung, J. U.: TRIM25 RING-finger E3 ubiquitin ligase is essential for RIG-I-mediated antiviral activity. *Nature* 446: 916, 2007
- Geddes, K., Magalhaes, J. G., and Girardin, S. E.: Unleashing the therapeutic potential of NOD-like receptors. *Nat Rev Drug Discov* 8: 465-79, 2009
- Gering, M. and Patient, R.: Hedgehog signaling is required for adult blood stem cell formation in zebrafish embryos. *Dev Cell* 8: 389-400, 2005
- Girardin, S. E., Boneca, I. G., Carneiro, L. A., Antignac, A., Jehanno, M., Viala, J., Tedin, K., Taha, M. K., Labigne, A., Zahringer, U., Coyle, A. J., DiStefano, P. S., Bertin, J., Sansonetti, P. J., and Philpott, D. J.: Nod1 detects a unique muropeptide from gram-negative bacterial peptidoglycan. *Science* 300: 1584-7, 2003a
- Girardin, S. E., Boneca, I. G., Viala, J., Chamaillard, M., Labigne, A., Thomas, G., Philpott, D. J., and Sansonetti, P. J.: Nod2 is a general sensor of peptidoglycan through muramyl dipeptide (MDP) detection. *J Biol Chem* 278: 8869-72, 2003b
- Girardin, S. E., Travassos, L. H., Herve, M., Blanot, D., Boneca, I. G., Philpott, D. J., Sansonetti, P. J., and Mengin-Lecreux, D.: Peptidoglycan molecular requirements allowing detection by Nod1 and Nod2. *J Biol Chem* 278: 41702-8, 2003c
- Gitlin, L., Barchet, W., Gilfillan, S., Cella, M., Beutler, B., Flavell, R. A., Diamond, M. S., and Colonna, M.: Essential role of mda-5 in type I IFN responses to polyriboinosinic:polyribocytidylic acid and encephalomyocarditis picornavirus. *Proceedings of the National Academy of Sciences* 103: 8459-8464, 2006

- Gongora, R., Figueroa, F., and Klein, J.: Independent duplications of Bf and C3 complement genes in the zebrafish. *Scand J Immunol* 48: 651-8, 1998
- Grayfer, L. and Belosevic, M.: Molecular characterization, expression and functional analysis of goldfish (*Carassius auratus* L.) interferon gamma. *Dev Comp Immunol* 33: 235-46, 2009
- Grech, A., Quinn, R., Srinivasan, D., Badoux, X., and Brink, R.: Complete structural characterisation of the mammalian and *Drosophila* TRAF genes: implications for TRAF evolution and the role of RING finger splice variants. *Mol Immunol* 37: 721-34, 2000
- Greenlee, A. R., Brown, R. A., and Ristow, S. S.: Nonspecific cytotoxic cells of rainbow trout (*Oncorhynchus mykiss*) kill YAC-1 targets by both necrotic and apoptic mechanisms. *Dev Comp Immunol* 15: 153-64, 1991
- Greenlund, A. C., Farrar, M. A., Viviano, B. L., and Schreiber, R. D.: Ligand-induced IFN gamma receptor tyrosine phosphorylation couples the receptor to its signal transduction system (p91). *Embo J* 13: 1591-600, 1994
- Greenlund, A. C., Morales, M. O., Viviano, B. L., Yan, H., Krolewski, J., and Schreiber, R. D.: Stat recruitment by tyrosine-phosphorylated cytokine receptors: an ordered reversible affinity-driven process. *Immunity* 2: 677-87, 1995
- Haller, O. and Kochs, G.: Interferon-induced mx proteins: dynamin-like GTPases with antiviral activity. *Traffic* 3: 710-7, 2002
- Hawke, N. A., Yoder, J. A., Haire, R. N., Mueller, M. G., Litman, R. T., Miracle, A. L., Stuge, T., Shen, L., Miller, N., and Litman, G. W.: Extraordinary variation in a diversified family of immune-type receptor genes. *Proc Natl Acad Sci U S A* 98: 13832-7, 2001
- Herbomel, P., Thisse, B., and Thisse, C.: Ontogeny and behaviour of early macrophages in the zebrafish embryo. *Development* 126: 3735-45, 1999
- Herraez, M. P. and Zapata, A. G.: Structural characterization of the melano-macrophage centres (MMC) of goldfish *Carassius auratus*. *Eur J Morphol* 29: 89-102, 1991
- Hibino, T., Loza-Coll, M., Messier, C., Majeske, A. J., Cohen, A. H., Terwilliger, D. P., Buckley, K. M., Brockton, V., Nair, S. V., Berney, K., Fugmann, S. D., Anderson, M. K., Pancer, Z., Cameron, R. A., Smith, L. C., and Rast, J. P.: The immune gene repertoire encoded in the purple sea urchin genome. *Dev Biol* 300: 349-65, 2006
- Hildemann, W. H.: Transplantation immunity in fishes: Agnatha, Chondrichthyes and Osteichthyes. *Transplant Proc* 2: 253-9, 1970
- Hornig, T., Barton, G. M., and Medzhitov, R.: TIRAP: an adapter molecule in the Toll signaling pathway. *Nat Immunol* 2: 835-41, 2001
- Hou, S. X., Zheng, Z., Chen, X., and Perrimon, N.: The JAK/STAT Pathway in Model Organisms: Emerging Roles in Cell Movement. *Developmental Cell* 3: 765, 2002
- Hsu, L. C., Ali, S. R., McGillivray, S., Tseng, P. H., Mariathasan, S., Humke, E. W., Eckmann, L., Powell, J. J., Nizet, V., Dixit, V. M., and Karin, M.: A NOD2-NALP1 complex mediates caspase-1-dependent IL-1beta secretion in response to *Bacillus anthracis* infection and muramyl dipeptide. *Proc Natl Acad Sci U S A* 105: 7803-8, 2008
- Huang, M. T.-H., Taxman, D. J., Holley-Guthrie, E. A., Moore, C. B., Willingham, S. B., Madden, V., Parsons, R. K., Featherstone, G. L., Arnold, R. R., O'Connor, B. P., and Ting, J. P.-Y.: Critical Role of Apoptotic Speck Protein Containing a Caspase Recruitment Domain (ASC) and NLRP3 in Causing Necrosis and ASC Speck Formation Induced by *Porphyromonas gingivalis* in Human Cells. *J Immunol* 182: 2395-2404, 2009

- Hubbard, T. J. P., Aken, B. L., Ayling, S., Ballester, B., Beal, K., Bragin, E., Brent, S., Chen, Y., Clapham, P., Clarke, L., Coates, G., Fairley, S., Fitzgerald, S., Fernandez-Banet, J., Gordon, L., Graf, S., Haider, S., Hammond, M., Holland, R., Howe, K., Jenkinson, A., Johnson, N., Kahari, A., Keefe, D., Keenan, S., Kinsella, R., Kokocinski, F., Kulesha, E., Lawson, D., Longden, I., Megy, K., Meidl, P., Overduin, B., Parker, A., Pritchard, B., Rios, D., Schuster, M., Slater, G., Smedley, D., Spooner, W., Spudich, G., Trevanion, S., Vilella, A., Vogel, J., White, S., Wilder, S., Zadissa, A., Birney, E., Cunningham, F., Curwen, V., Durbin, R., Fernandez-Suarez, X. M., Herrero, J., Kasprzyk, A., Proctor, G., Smith, J., Searle, S., and Flicek, P.: Ensembl 2009. *Nucl. Acids Res.* 37: D690-697, 2009
- Hughes, A. L.: The evolution of the type I interferon gene family in mammals. *J Mol Evol* 41: 539-48, 1995
- Igawa, D., Sakai, M., and Savan, R.: An unexpected discovery of two interferon gamma-like genes along with interleukin (IL)-22 and -26 from teleost: IL-22 and -26 genes have been described for the first time outside mammals. *Molecular Immunology* 43: 999, 2006
- Inohara, N., Ogura, Y., Chen, F. F., Muto, A., and Nuñez, G.: Human Nod1 Confers Responsiveness to Bacterial Lipopolysaccharides. *Journal of Biological Chemistry* 276: 2551-2554, 2001
- Inohara, N., Ogura, Y., Fontalba, A., Gutierrez, O., Pons, F., Crespo, J., Fukase, K., Inamura, S., Kusumoto, S., Hashimoto, M., Foster, S. J., Moran, A. P., Fernandez-Luna, J. L., and Nuñez, G.: Host Recognition of Bacterial Muramyl Dipeptide Mediated through NOD2. *Journal of Biological Chemistry* 278: 5509-5512, 2003
- Ishikawa, H. and Barber, G. N.: STING is an endoplasmic reticulum adaptor that facilitates innate immune signalling. *Nature* 455: 674-8, 2008
- Janssens, S. and Beyaert, R.: Functional diversity and regulation of different interleukin-1 receptor-associated kinase (IRAK) family members. *Mol Cell* 11: 293-302, 2003
- Jaso-Friedmann, L., Leary, J. H., 3rd, and Evans, D. L.: The non-specific cytotoxic cell receptor (NCCRP-1): molecular organization and signaling properties. *Dev Comp Immunol* 25: 701-11, 2001
- Jault, C., Pichon, L., and Chluba, J.: Toll-like receptor gene family and TIR-domain adapters in *Danio rerio*. *Mol Immunol* 40: 759-71, 2004
- Jin, M. S., Kim, S. E., Heo, J. Y., Lee, M. E., Kim, H. M., Paik, S. G., Lee, H., and Lee, J. O.: Crystal structure of the TLR1-TLR2 heterodimer induced by binding of a tri-acylated lipopeptide. *Cell* 130: 1071-82, 2007
- Jones, J. D. G. and Dangl, J. L.: The plant immune system. *Nature* 444: 323, 2006
- Kalev-Zylinska, M. L., Horsfield, J. A., Flores, M. V., Postlethwait, J. H., Vitas, M. R., Baas, A. M., Crosier, P. S., and Crosier, K. E.: Runx1 is required for zebrafish blood and vessel development and expression of a human RUNX1-CBF2T1 transgene advances a model for studies of leukemogenesis. *Development* 129: 2015-30, 2002
- Kang, D. C., Gopalkrishnan, R. V., Wu, Q., Jankowsky, E., Pyle, A. M., and Fisher, P. B.: mda-5: An interferon-inducible putative RNA helicase with double-stranded RNA-dependent ATPase activity and melanoma growth-suppressive properties. *Proc Natl Acad Sci U S A* 99: 637-42, 2002
- Kanneganti, T. D., Lamkanfi, M., Kim, Y. G., Chen, G., Park, J. H., Franchi, L., Vandenabeele, P., and Nunez, G.: Pannexin-1-mediated recognition of bacterial molecules activates the cryopyrin inflammasome independent of Toll-like receptor signaling. *Immunity* 26: 433-43, 2007
- Kaplan, D. H., Greenlund, A. C., Tanner, J. W., Shaw, A. S., and Schreiber, R. D.: Identification of an interferon-gamma receptor alpha chain sequence required for JAK-1 binding. *J Biol Chem* 271: 9-12, 1996

- Kato, H., Takeuchi, O., Mikamo-Satoh, E., Hirai, R., Kawai, T., Matsushita, K., Hiiragi, A., Dermody, T. S., Fujita, T., and Akira, S.: Length-dependent recognition of double-stranded ribonucleic acids by retinoic acid-inducible gene-I and melanoma differentiation-associated gene 5. *J Exp Med* 205: 1601-10, 2008
- Kato, H., Takeuchi, O., Sato, S., Yoneyama, M., Yamamoto, M., Matsui, K., Uematsu, S., Jung, A., Kawai, T., Ishii, K. J., Yamaguchi, O., Otsu, K., Tsujimura, T., Koh, C. S., Reis e Sousa, C., Matsuura, Y., Fujita, T., and Akira, S.: Differential roles of MDA5 and RIG-I helicases in the recognition of RNA viruses. *Nature* 441: 101-5, 2006
- Kawagoe, T., Sato, S., Matsushita, K., Kato, H., Matsui, K., Kumagai, Y., Saitoh, T., Kawai, T., Takeuchi, O., and Akira, S.: Sequential control of Toll-like receptor-dependent responses by IRAK1 and IRAK2. *Nat Immunol* 9: 684, 2008
- Kawai, T. and Akira, S.: The roles of TLRs, RLRs and NLRs in pathogen recognition. *Int Immunol* 21: 317-37, 2009
- Kawai, T., Takahashi, K., Sato, S., Coban, C., Kumar, H., Kato, H., Ishii, K. J., Takeuchi, O., and Akira, S.: IPS-1, an adaptor triggering RIG-I- and Mda5-mediated type I interferon induction. *Nat Immunol* 6: 981-8, 2005
- Kedinger, V., Alpy, F., Tomasetto, C., Thisse, C., Thisse, B., and Rio, M. C.: Spatial and temporal distribution of the traf4 genes during zebrafish development. *Gene Expr Patterns* 5: 545-52, 2005
- Kim, H. M., Park, B. S., Kim, J.-I., Kim, S. E., Lee, J., Oh, S. C., Enkhbayar, P., Matsushima, N., Lee, H., Yoo, O. J., and Lee, J.-O.: Crystal Structure of the TLR4-MD-2 Complex with Bound Endotoxin Antagonist Eritoran. *130*: 906, 2007
- Kim, Y. G., Park, J. H., Shaw, M. H., Franchi, L., Inohara, N., and Nunez, G.: The cytosolic sensors Nod1 and Nod2 are critical for bacterial recognition and host defense after exposure to Toll-like receptor ligands. *Immunity* 28: 246-57, 2008
- Kimmel, C. B., Ballard, W. W., Kimmel, S. R., Ullmann, B., and Schilling, T. F.: Stages of embryonic development of the zebrafish. *Dev Dyn* 203: 253-310, 1995
- Kissa, K., Murayama, E., Zapata, A., Cortes, A., Perret, E., Machu, C., and Herbomel, P.: Live imaging of emerging hematopoietic stem cells and early thymus colonization. *Blood* 111: 1147-56, 2008
- Klamp, T., Boehm, U., Schenk, D., Pfeffer, K., and Howard, J. C.: A giant GTPase, very large inducible GTPase-1, is inducible by IFNs. *J Immunol* 171: 1255-65, 2003
- Klein, J. and Nikolaidis, N.: The descent of the antibody-based immune system by gradual evolution. *Proc Natl Acad Sci U S A* 102: 169-74, 2005
- Kobayashi, K., Hernandez, L. D., Galan, J. E., Janeway, C. A., Jr., Medzhitov, R., and Flavell, R. A.: IRAK-M is a negative regulator of Toll-like receptor signaling. *Cell* 110: 191-202, 2002
- Koonin, E. V. and Aravind, L.: The NACHT family - a new group of predicted NTPases implicated in apoptosis and MHC transcription activation. *Trends Biochem Sci* 25: 223-4, 2000
- Korz, S., Emelyanov, A., and Korzh, V.: Developmental analysis of ceruloplasmin gene and liver formation in zebrafish. *Mech Dev* 103: 137-9, 2001
- Kovacsovics, M., Martinon, F., Micheau, O., Bodmer, J. L., Hofmann, K., and Tschopp, J.: Overexpression of Helicard, a CARD-containing helicase cleaved during apoptosis, accelerates DNA degradation. *Curr Biol* 12: 838-43, 2002
- Krause, C. D. and Pestka, S.: Evolution of the Class 2 cytokines and receptors, and discovery of new friends and relatives. *Pharmacol Ther* 106: 299-346, 2005
- Kumar, H., Kawai, T., and Akira, S.: Toll-like receptors and innate immunity. *Biochemical and Biophysical Research Communications* 388: 621, 2009

- Kumar, S., Tamura, K., and Nei, M.: MEGA3: Integrated software for Molecular Evolutionary Genetics Analysis and sequence alignment. *Brief Bioinform* 5: 150-63, 2004
- Lam, S. H., Chua, H. L., Gong, Z., Lam, T. J., and Sin, Y. M.: Development and maturation of the immune system in zebrafish, *Danio rerio*: a gene expression profiling, in situ hybridization and immunological study. *Developmental & Comparative Immunology* 28: 9, 2004
- Lam, S. H., Chua, H. L., Gong, Z., Wen, Z., Lam, T. J., and Sin, Y. M.: Morphologic transformation of the thymus in developing zebrafish. *Developmental Dynamics* 225: 87-94, 2002
- Lamkanfi, M., Amer, A., Kanneganti, T. D., Munoz-Planillo, R., Chen, G., Vandenabeele, P., Fortier, A., Gros, P., and Nunez, G.: The Nod-like receptor family member Naip5/Birc1e restricts *Legionella pneumophila* growth independently of caspase-1 activation. *J Immunol* 178: 8022-7, 2007
- Langenau, D. M., Ferrando, A. A., Traver, D., Kutok, J. L., Hezel, J. P., Kanki, J. P., Zon, L. I., Look, A. T., and Trede, N. S.: In vivo tracking of T cell development, ablation, and engraftment in transgenic zebrafish. *Proc Natl Acad Sci U S A* 101: 7369-74, 2004
- Le Morvan, C., Deschaux, P., and Troutaud, D.: Effects and mechanisms of environmental temperature on carp (*Cyprinus carpio*) anti-DNP antibody response and non-specific cytotoxic cell activity: a kinetic study. *Dev Comp Immunol* 20: 331-40, 1996
- Leipe, D. D., Koonin, E. V., and Aravind, L.: STAND, a class of P-loop NTPases including animal and plant regulators of programmed cell death: multiple, complex domain architectures, unusual phyletic patterns, and evolution by horizontal gene transfer. *J Mol Biol* 343: 1-28, 2004
- Lemaitre, B., Meister, M., Govind, S., Georgel, P., Steward, R., Reichhart, J. M., and Hoffmann, J. A.: Functional analysis and regulation of nuclear import of dorsal during the immune response in *Drosophila*. *Embo J* 14: 536-45, 1995
- Lemaitre, B., Nicolas, E., Michaut, L., Reichhart, J.-M., and Hoffmann, J. A.: The Dorsoventral Regulatory Gene Cassette *spätzle/Toll/cactus* Controls the Potent Antifungal Response in *Drosophila* Adults. *Cell* 86: 973, 1996
- Lespinet, O., Wolf, Y. I., Koonin, E. V., and Aravind, L.: The role of lineage-specific gene family expansion in the evolution of eukaryotes. *Genome Res* 12: 1048-59, 2002
- Letunic, I., Doerks, T., and Bork, P.: SMART 6: recent updates and new developments. *Nucl. Acids Res.* 37: D229-232, 2009
- Levraud, J. P., Boudinot, P., Colin, I., Benmansour, A., Peyrieras, N., Herbomel, P., and Lutfalla, G.: Identification of the zebrafish IFN receptor: implications for the origin of the vertebrate IFN system. *J Immunol* 178: 4385-94, 2007
- Lewis, R. S. and Ward, A. C.: Conservation, duplication and divergence of the zebrafish *stat5* genes. *Gene* 338: 65-74, 2004
- Li, M., Liu, X., Zhou, Y., and Su, S. B.: Interferon-lambdas: the modulators of antiviral, antitumor, and immune responses. *J Leukoc Biol* 86: 23-32, 2009
- Lieschke, G. J., Oates, A. C., Crowhurst, M. O., Ward, A. C., and Layton, J. E.: Morphologic and functional characterization of granulocytes and macrophages in embryonic and adult zebrafish. *Blood* 98: 3087-3096, 2001
- Lightfield, K. L., Persson, J., Brubaker, S. W., Witte, C. E., von Moltke, J., Dunipace, E. A., Henry, T., Sun, Y. H., Cado, D., Dietrich, W. F., Monack, D. M., Tsolis, R. M., and Vance, R. E.: Critical function for Naip5 in inflammasome activation by a conserved carboxy-terminal domain of flagellin. *Nat Immunol* 9: 1171-8, 2008

- Lin, A. F., Xiang, L. X., Wang, Q. L., Dong, W. R., Gong, Y. F., and Shao, J. Z.: The DC-SIGN of Zebrafish: Insights into the Existence of a CD209 Homologue in a Lower Vertebrate and Its Involvement in Adaptive Immunity. *J Immunol* 183: 7398-7410, 2009
- Lin, H. F., Traver, D., Zhu, H., Dooley, K., Paw, B. H., Zon, L. I., and Handin, R. I.: Analysis of thrombocyte development in CD41-GFP transgenic zebrafish. *Blood* 106: 3803-10, 2005
- Linthicum, D. S. and Hildemann, W. H.: Immunologic responses of Pacific hagfish. 3. Serum antibodies to cellular antigens. *J Immunol* 105: 912-8, 1970
- Litman, G. W., Finstad, F. J., Howell, J., Pollara, B. W., and God, R. A.: The evolution of the immune response. 3. Structural studies of the lamprey immunoglobulin. *J Immunol* 105: 1278-85, 1970
- Litman, G. W., Hawke, N. A., and Yoder, J. A.: Novel immune-type receptor genes. *Immunol Rev* 181: 250-9, 2001
- Liu, H., Su, Y. C., Becker, E., Treisman, J., and Skolnik, E. Y.: A Drosophila TNF-receptor-associated factor (TRAF) binds the ste20 kinase Misshapen and activates Jun kinase. *Curr Biol* 9: 101-4, 1999
- Long, S., Milev-Milovanovic, I., Wilson, M., Bengten, E., Clem, L. W., Miller, N. W., and Chinchar, V. G.: Identification and expression analysis of cDNAs encoding channel catfish type I interferons. *Fish Shellfish Immunol* 21: 42-59, 2006
- Long, S., Wilson, M., Bengten, E., Bryan, L., Clem, L. W., Miller, N. W., and Chinchar, V. G.: Identification of a cDNA encoding channel catfish interferon. *Dev Comp Immunol* 28: 97-111, 2004
- Lord, K. A., Hoffman-Liebermann, B., and Liebermann, D. A.: Nucleotide sequence and expression of a cDNA encoding MyD88, a novel myeloid differentiation primary response gene induced by IL6. *Oncogene* 5: 1095-7, 1990
- Lutfalla, G., Roest Crollius, H., Stange-Thomann, N., Jaillon, O., Mogensen, K., and Monneron, D.: Comparative genomic analysis reveals independent expansion of a lineage-specific gene family in vertebrates: the class II cytokine receptors and their ligands in mammals and fish. *BMC Genomics* 4: 29, 2003
- Mamane, Y., Heylbroeck, C., Genin, P., Algarte, M., Servant, M. J., LePage, C., DeLuca, C., Kwon, H., Lin, R., and Hiscott, J.: Interferon regulatory factors: the next generation. *Gene* 237: 1-14, 1999
- Marchalonis, J. J. and Edelman, G. M.: Phylogenetic origins of antibody structure. 3. Antibodies in the primary immune response of the sea lamprey, *Petromyzon marinus*. *J Exp Med* 127: 891-914, 1968
- Mariathasan, S., Weiss, D. S., Newton, K., McBride, J., O'Rourke, K., Roose-Girma, M., Lee, W. P., Weinrauch, Y., Monack, D. M., and Dixit, V. M.: Cryopyrin activates the inflammasome in response to toxins and ATP. *Nature* 440: 228-32, 2006
- Martin, S. A. M., Taggart, J. B., Seear, P., Bron, J. E., Talbot, R., Teale, A. J., Sweeney, G. E., Hoyheim, B., Houlihan, D. F., Tocher, D. R., Zou, J., and Secombes, C. J.: Interferon type I and type II responses in an Atlantic salmon (*Salmo salar*) SHK-1 cell line by the salmon TRAITs/SGP microarray. *Physiol. Genomics* 32: 33-44, 2007
- Martinon, F., Burns, K., and Tschopp, J.: The inflammasome: a molecular platform triggering activation of inflammatory caspases and processing of proIL-beta. *Mol Cell* 10: 417-26, 2002
- Martinon, F., Petrilli, V., Mayor, A., Tardivel, A., and Tschopp, J.: Gout-associated uric acid crystals activate the NALP3 inflammasome. *Nature* 440: 237-41, 2006
- Matsunaga, T. and Rahman, A.: In Search of the Origin of the Thymus: the Thymus and GALT May Be Evolutionarily Related*. *Scandinavian Journal of Immunology* 53: 1-6, 2001

- McGonagle, D., Savic, S., and McDermott, M.: The NLR network and the immunological disease continuum of adaptive and innate immune-mediated inflammation against self. *Seminars in Immunopathology* 29: 303, 2007
- Medzhitov, R. and Janeway, C., Jr.: Innate immune recognition: mechanisms and pathways. *Immunol Rev* 173: 89-97, 2000
- Medzhitov, R., Preston-Hurlburt, P., and Janeway, C. A., Jr.: A human homologue of the Drosophila Toll protein signals activation of adaptive immunity. *Nature* 388: 394-7, 1997
- Meijer, A. H., Gabby Krens, S. F., Medina Rodriguez, I. A., He, S., Bitter, W., Ewa Snaar-Jagalska, B., and Spaink, H. P.: Expression analysis of the Toll-like receptor and TIR domain adaptor families of zebrafish. *Mol Immunol* 40: 773-83, 2004
- Meylan, E., Curran, J., Hofmann, K., Moradpour, D., Binder, M., Bartenschlager, R., and Tschopp, J.: Cardif is an adaptor protein in the RIG-I antiviral pathway and is targeted by hepatitis C virus. *Nature* 437: 1167-72, 2005
- Miao, E. A., Alpuche-Aranda, C. M., Dors, M., Clark, A. E., Bader, M. W., Miller, S. I., and Aderem, A.: Cytoplasmic flagellin activates caspase-1 and secretion of interleukin 1beta via Ipaf. *Nat Immunol* 7: 569-75, 2006
- Miao, E. A., Ernst, R. K., Dors, M., Mao, D. P., and Aderem, A.: Pseudomonas aeruginosa activates caspase 1 through Ipaf. *Proceedings of the National Academy of Sciences* 105: 2562-2567, 2008
- Michallet, M. C., Meylan, E., Ermolaeva, M. A., Vazquez, J., Rebsamen, M., Curran, J., Poeck, H., Bscheider, M., Hartmann, G., Konig, M., Kalinke, U., Pasparakis, M., and Tschopp, J.: TRADD protein is an essential component of the RIG-like helicase antiviral pathway. *Immunity* 28: 651-61, 2008
- Milev-Milovanovic, I., Long, S., Wilson, M., Bengten, E., Miller, N. W., and Chinchar, V. G.: Identification and expression analysis of interferon gamma genes in channel catfish. *Immunogenetics* 58: 70-80, 2006
- Miller, D. J., Hemmrich, G., Ball, E. E., Hayward, D. C., Khalturin, K., Funayama, N., Agata, K., and Bosch, T. C.: The innate immune repertoire in cnidaria--ancestral complexity and stochastic gene loss. *Genome Biol* 8: R59, 2007
- Mink, M., Fogelgren, B., Olszewski, K., Maroy, P., and Csiszar, K.: A novel human gene (SARM) at chromosome 17q11 encodes a protein with a SAM motif and structural similarity to Armadillo/beta-catenin that is conserved in mouse, Drosophila, and Caenorhabditis elegans. *Genomics* 74: 234-44, 2001
- Molofsky, A. B., Byrne, B. G., Whitfield, N. N., Madigan, C. A., Fuse, E. T., Tateda, K., and Swanson, M. S.: Cytosolic recognition of flagellin by mouse macrophages restricts Legionella pneumophila infection. *J Exp Med* 203: 1093-104, 2006
- Moore, C. B., Bergstralh, D. T., Duncan, J. A., Lei, Y., Morrison, T. E., Zimmermann, A. G., Accavitti-Loper, M. A., Madden, V. J., Sun, L., Ye, Z., Lich, J. D., Heise, M. T., Chen, Z., and Ting, J. P. Y.: NLRX1 is a regulator of mitochondrial antiviral immunity. *Nature* 451: 573, 2008
- Murayama, E., Kissa, K., Zapata, A., Mordelet, E., Briolat, V., Lin, H. F., Handin, R. I., and Herbomel, P.: Tracing hematopoietic precursor migration to successive hematopoietic organs during zebrafish development. *Immunity* 25: 963-75, 2006
- Neely, M. N., Pfeifer, J. D., and Caparon, M.: Streptococcus-zebrafish model of bacterial pathogenesis. *Infect Immun* 70: 3904-14, 2002
- O'Toole, R., Von Hofsten, J., Rosqvist, R., Olsson, P. E., and Wolf-Watz, H.: Visualisation of zebrafish infection by GFP-labelled Vibrio anguillarum. *Microb Pathog* 37: 41-6, 2004

- Oganesyan, G., Saha, S. K., Guo, B., He, J. Q., Shahangian, A., Zarnegar, B., Perry, A., and Cheng, G.: Critical role of TRAF3 in the Toll-like receptor-dependent and -independent antiviral response. *Nature* 439: 208-11, 2006
- Oshiumi, H., Matsumoto, M., Funami, K., Akazawa, T., and Seya, T.: TICAM-1, an adaptor molecule that participates in Toll-like receptor 3-mediated interferon-beta induction. *Nat Immunol* 4: 161-7, 2003a
- Oshiumi, H., Sasai, M., Shida, K., Fujita, T., Matsumoto, M., and Seya, T.: TIR-containing adapter molecule (TICAM)-2, a bridging adapter recruiting to toll-like receptor 4 TICAM-1 that induces interferon-beta. *J Biol Chem* 278: 49751-62, 2003b
- Palis, J., Chan, R. J., Koniski, A., Patel, R., Starr, M., and Yoder, M. C.: Spatial and temporal emergence of high proliferative potential hematopoietic precursors during murine embryogenesis. *Proc Natl Acad Sci U S A* 98: 4528-33, 2001
- Palis, J., Robertson, S., Kennedy, M., Wall, C., and Keller, G.: Development of erythroid and myeloid progenitors in the yolk sac and embryo proper of the mouse. *Development* 126: 5073-84, 1999
- Pan, Q., Mathison, J., Fearn, C., Kravchenko, V. V., Da Silva Correia, J., Hoffman, H. M., Kobayashi, K. S., Bertin, J., Grant, E. P., Coyle, A. J., Sutterwala, F. S., Ogura, Y., Flavell, R. A., and Ulevitch, R. J.: MDP-induced interleukin-1beta processing requires Nod2 and CIAS1/NALP3. *J Leukoc Biol* 82: 177-83, 2007
- Pancer, Z., Amemiya, C. T., Ehrhardt, G. R., Ceitlin, J., Gartland, G. L., and Cooper, M. D.: Somatic diversification of variable lymphocyte receptors in the agnathan sea lamprey. *Nature* 430: 174-80, 2004
- Pancer, Z. and Cooper, M. D.: The evolution of adaptive immunity. *Annu Rev Immunol* 24: 497-518, 2006
- Pelegri, P. and Surprenant, A.: Pannexin-1 couples to maitotoxin- and nigericin-induced interleukin-1beta release through a dye uptake-independent pathway. *J Biol Chem* 282: 2386-94, 2007
- Pestka, S., Krause, C. D., Sarkar, D., Walter, M. R., Shi, Y., and Fisher, P. B.: Interleukin-10 and related cytokines and receptors. *Annu Rev Immunol* 22: 929-79, 2004a
- Pestka, S., Krause, C. D., and Walter, M. R.: Interferons, interferon-like cytokines, and their receptors. *Immunol Rev* 202: 8-32, 2004b
- Petrilli, V., Papin, S., Dostert, C., Mayor, A., Martinon, F., and Tschopp, J.: Activation of the NALP3 inflammasome is triggered by low intracellular potassium concentration. *Cell Death Differ* 14: 1583-9, 2007
- Pollara, B., Litman, G. W., Finstad, J., Howell, J., and Good, R. A.: The evolution of the immune response. VII. Antibody to human "O" cells and properties of the immunoglobulin in lamprey. *J Immunol* 105: 738-45, 1970
- Prajsnar, T. K., Cunliffe, V. T., Foster, S. J., and Renshaw, S. A.: A novel vertebrate model of *Staphylococcus aureus* infection reveals phagocyte-dependent resistance of zebrafish to non-host specialized pathogens. *Cell Microbiol* 10: 2312-25, 2008
- Pruitt, K. D., Tatusova, T., and Maglott, D. R.: NCBI reference sequences (RefSeq): a curated non-redundant sequence database of genomes, transcripts and proteins. *Nucleic Acids Res* 35: D61-5, 2007
- Ransom, D. G., Haffter, P., Odenthal, J., Brownlie, A., Vogelsang, E., Kelsh, R. N., Brand, M., van Eeden, F. J., Furutani-Seiki, M., Granato, M., Hammerschmidt, M., Heisenberg, C. P., Jiang, Y. J., Kane, D. A., Mullins, M. C., and Nusslein-Volhard, C.: Characterization of zebrafish mutants with defects in embryonic hematopoiesis. *Development* 123: 311-319, 1996

- Rast, J. P., Smith, L. C., Loza-Coll, M., Hibino, T., and Litman, G. W.: Genomic insights into the immune system of the sea urchin. *Science* 314: 952-6, 2006
- Regnier, C. H., Tomasetto, C., Moog-Lutz, C., Chenard, M. P., Wendling, C., Basset, P., and Rio, M. C.: Presence of a new conserved domain in CART1, a novel member of the tumor necrosis factor receptor-associated protein family, which is expressed in breast carcinoma. *J Biol Chem* 270: 25715-21, 1995
- Reith, W. and Mach, B.: The bare lymphocyte syndrome and the regulation of MHC expression. *Annu Rev Immunol* 19: 331-73, 2001
- Ren, T., Zamboni, D. S., Roy, C. R., Dietrich, W. F., and Vance, R. E.: Flagellin-deficient Legionella mutants evade caspase-1- and Naip5-mediated macrophage immunity. *PLoS Pathog* 2: e18, 2006
- Renauld, J. C.: Class II cytokine receptors and their ligands: key antiviral and inflammatory modulators. *Nat Rev Immunol* 3: 667-76, 2003
- Rhodes, J., Hagen, A., Hsu, K., Deng, M., Liu, T. X., Look, A. T., and Kanki, J. P.: Interplay of Pu.1 and Gata1 Determines Myelo-Erythroid Progenitor Cell Fate in Zebrafish. *Developmental Cell* 8: 97, 2005
- Roberts, R. J.: Melanin-containing cells of the teleost fish and their relation to disease. In W. E. Ribelin, Migaki, G. (ed.): *The pathology of fishes*, pp. 399–428, University of Wisconsin Press, Madison, WI, 1975
- Robertson, B., Bergan, V., Rokenes, T., Larsen, R., and Albuquerque, A.: Atlantic salmon interferon genes: cloning, sequence analysis, expression, and biological activity. *J Interferon Cytokine Res* 23: 601-12, 2003
- Saito, T., Hirai, R., Loo, Y. M., Owen, D., Johnson, C. L., Sinha, S. C., Akira, S., Fujita, T., and Gale, M., Jr.: Regulation of innate antiviral defenses through a shared repressor domain in RIG-I and LGP2. *Proc Natl Acad Sci U S A* 104: 582-7, 2007
- Saitou, N. and Nei, M.: The neighbor-joining method: a new method for reconstructing phylogenetic trees. *Mol Biol Evol* 4: 406-25, 1987
- Sambrook, J., Russell, D. W., and Cold Spring Harbor, L.: Molecular cloning: a laboratory manual / Joseph Sambrook, David W. Russell. Cold Spring Harbor Laboratory, Cold Spring Harbor, N.Y., 2001
- Sapède, D., Gompel, N., Dambly-Chaudière, C., and Ghysen, A.: Cell migration in the postembryonic development of the fish lateral line. *Development* 129: 605-15, 2002
- Sato, A., Mayer, W. E., Overath, P., and Klein, J.: Genes encoding putative natural killer cell C-type lectin receptors in teleostean fishes. *Proc Natl Acad Sci U S A* 100: 7779-84, 2003
- Savan, R., Ravichandran, S., Collins, J. R., Sakai, M., and Young, H. A.: Structural conservation of interferon gamma among vertebrates. *Cytokine & Growth Factor Reviews* 20: 115, 2009
- Schroder, M., Baran, M., and Bowie, A. G.: Viral targeting of DEAD box protein 3 reveals its role in TBK1/IKKepsilon-mediated IRF activation. *Embo J* 27: 2147-57, 2008
- Schulte-Merker, S., Ho, R. K., Herrmann, B. G., and Nusslein-Volhard, C.: The protein product of the zebrafish homologue of the mouse T gene is expressed in nuclei of the germ ring and the notochord of the early embryo. *Development* 116: 1021-32, 1992
- Schuster-Bockler, B., Schultz, J., and Rahmann, S.: HMM Logos for visualization of protein families. *BMC Bioinformatics* 5: 7, 2004
- Sepulcre, M. P., Alcaraz-Perez, F., Lopez-Munoz, A., Roca, F. J., Meseguer, J., Cayuela, M. L., and Mulero, V.: Evolution of lipopolysaccharide (LPS) recognition and signaling: fish TLR4 does not recognize LPS and negatively regulates NF-kappaB activation. *J Immunol* 182: 1836-45, 2009

- Seth, R. B., Sun, L., Ea, C. K., and Chen, Z. J.: Identification and characterization of MAVS, a mitochondrial antiviral signaling protein that activates NF-kappaB and IRF 3. *Cell* 122: 669-82, 2005
- Shiozaki, E. N., Chai, J., and Shi, Y.: Oligomerization and activation of caspase-9, induced by Apaf-1 CARD. *Proc Natl Acad Sci U S A* 99: 4197-202, 2002
- Sieger, D., Stein, C., Neifer, D., van der Sar, A. M., and Leptin, M.: The role of gamma interferon in innate immunity in the zebrafish embryo. *Dis Model Mech* 2: 571-81, 2009
- Soulat, D., Burckstummer, T., Westermayer, S., Goncalves, A., Bauch, A., Stefanovic, A., Hantschel, O., Bennett, K. L., Decker, T., and Superti-Furga, G.: The DEAD-box helicase DDX3X is a critical component of the TANK-binding kinase 1-dependent innate immune response. *Embo J* 27: 2135-46, 2008
- Sprague, J., Bayraktaroglu, L., Clements, D., Conlin, T., Fashena, D., Frazer, K., Haendel, M., Howe, D. G., Mani, P., Ramachandran, S., Schaper, K., Segerdell, E., Song, P., Sprunger, B., Taylor, S., Van Slyke, C. E., and Westerfield, M.: The Zebrafish Information Network: the zebrafish model organism database. *Nucl. Acids Res.* 34: D581-585, 2006
- Steimle, V., Otten, L. A., Zufferey, M., and Mach, B.: Complementation cloning of an MHC class II transactivator mutated in hereditary MHC class II deficiency (or bare lymphocyte syndrome). *Cell* 75: 135-46, 1993
- Stetson, D. B. and Medzhitov, R.: Type I interferons in host defense. *Immunity* 25: 373-81, 2006
- Subramaniam, P. S., Green, M. M., Larkin, J., 3rd, Torres, B. A., and Johnson, H. M.: Nuclear translocation of IFN-gamma is an intrinsic requirement for its biologic activity and can be driven by a heterologous nuclear localization sequence. *J Interferon Cytokine Res* 21: 951-9, 2001a
- Subramaniam, P. S. and Johnson, H. M.: Lipid microdomains are required sites for the selective endocytosis and nuclear translocation of IFN-gamma, its receptor chain IFN-gamma receptor-1, and the phosphorylation and nuclear translocation of STAT1alpha. *J Immunol* 169: 1959-69, 2002
- Subramaniam, P. S., Torres, B. A., and Johnson, H. M.: So many ligands, so few transcription factors: a new paradigm for signaling through the STAT transcription factors. *Cytokine* 15: 175-87, 2001b
- Sullivan, C., Postlethwait, J. H., Lage, C. R., Millard, P. J., and Kim, C. H.: Evidence for evolving Toll-IL-1 receptor-containing adaptor molecule function in vertebrates. *J Immunol* 178: 4517-27, 2007
- Sutterwala, F. S., Mijares, L. A., Li, L., Ogura, Y., Kazmierczak, B. I., and Flavell, R. A.: Immune recognition of *Pseudomonas aeruginosa* mediated by the IPAF/NLRC4 inflammasome. *J Exp Med* 204: 3235-45, 2007
- Suzuki, N., Suzuki, S., Duncan, G. S., Millar, D. G., Wada, T., Mirtsos, C., Takada, H., Wakeham, A., Itie, A., Li, S., Penninger, J. M., Wesche, H., Ohashi, P. S., Mak, T. W., and Yeh, W. C.: Severe impairment of interleukin-1 and Toll-like receptor signalling in mice lacking IRAK-4. *Nature* 416: 750-6, 2002
- Swaim, L. E., Connolly, L. E., Volkman, H. E., Humbert, O., Born, D. E., and Ramakrishnan, L.: Mycobacterium marinum Infection of Adult Zebrafish Causes Caseating Granulomatous Tuberculosis and Is Moderated by Adaptive Immunity. *Infect. Immun.* 74: 6108-6117, 2006
- Takahashi, K., Kawai, T., Kumar, H., Sato, S., Yonehara, S., and Akira, S.: Roles of caspase-8 and caspase-10 in innate immune responses to double-stranded RNA. *J Immunol* 176: 4520-4, 2006
- Takahashi, K., Yoneyama, M., Nishihori, T., Hirai, R., Kumeta, H., Narita, R., Gale, M., Jr., Inagaki, F., and Fujita, T.: Nonself RNA-sensing mechanism of RIG-I helicase and activation of antiviral immune responses. *Mol Cell* 29: 428-40, 2008

- Tanabe, T., Chamailard, M., Ogura, Y., Zhu, L., Qiu, S., Masumoto, J., Ghosh, P., Moran, A., Predergast, M. M., Tromp, G., Williams, C. J., Inohara, N., and Nunez, G.: Regulatory regions and critical residues of NOD2 involved in muramyl dipeptide recognition. *Embo J* 23: 1587-97, 2004
- Taniguchi, T., Ogasawara, K., Takaoka, A., and Tanaka, N.: IRF family of transcription factors as regulators of host defense. *Annu Rev Immunol* 19: 623-55, 2001
- Tautz, D. and Pfeifle, C.: A non-radioactive in situ hybridization method for the localization of specific RNAs in *Drosophila* embryos reveals translational control of the segmentation gene hunchback. *Chromosoma* 98: 81-5, 1989
- Thompson, J. D., Higgins, D. G., and Gibson, T. J.: CLUSTAL W: improving the sensitivity of progressive multiple sequence alignment through sequence weighting, position-specific gap penalties and weight matrix choice. *Nucleic Acids Res* 22: 4673-80, 1994
- Thompson, M. A., Ransom, D. G., Pratt, S. J., MacLennan, H., Kieran, M. W., Detrich, H. W., 3rd, Vail, B., Huber, T. L., Paw, B., Brownlie, A. J., Oates, A. C., Fritz, A., Gates, M. A., Amores, A., Bahary, N., Talbot, W. S., Her, H., Beier, D. R., Postlethwait, J. H., and Zon, L. I.: The cloche and spadetail genes differentially affect hematopoiesis and vasculogenesis. *Dev Biol* 197: 248-69, 1998
- Thoreau, E., Petridou, B., Kelly, P. A., Djiane, J., and Mornon, J. P.: Structural symmetry of the extracellular domain of the cytokine/growth hormone/prolactin receptor family and interferon receptors revealed by hydrophobic cluster analysis. *FEBS Lett* 282: 26-31, 1991
- Ting, J. P., Lovering, R. C., Alnemri, E. S., Bertin, J., Boss, J. M., Davis, B. K., Flavell, R. A., Girardin, S. E., Godzik, A., Harton, J. A., Hoffman, H. M., Hugot, J. P., Inohara, N., Mackenzie, A., Maltais, L. J., Nunez, G., Ogura, Y., Otten, L. A., Philpott, D., Reed, J. C., Reith, W., Schreiber, S., Steimle, V., and Ward, P. A.: The NLR gene family: a standard nomenclature. *Immunity* 28: 285-7, 2008
- Traver, D.: Cellular dissection of zebrafish hematopoiesis. *Methods Cell Biol* 76: 127-49, 2004
- Traver, D., Herbomel, P., Patton, E. E., Murphey, R. D., Yoder, J. A., Litman, G. W., Catic, A., Amemiya, C. T., Zon, L. I., and Trede, N. S.: The zebrafish as a model organism to study development of the immune system. *Adv Immunol* 81: 253-330, 2003
- Trede, N. S., Langenau, D. M., Traver, D., Look, A. T., and Zon, L. I.: The use of zebrafish to understand immunity. *Immunity* 20: 367-79, 2004
- Trede, N. S., Zapata, A., and Zon, L. I.: Fishing for lymphoid genes. *Trends in Immunology* 22: 302, 2001
- Trede, N. S. and Zon, L. I.: Development of T-cells during fish embryogenesis. *Dev Comp Immunol* 22: 253-63, 1998
- Turner, D. L. and Weintraub, H.: Expression of achaete-scute homolog 3 in *Xenopus* embryos converts ectodermal cells to a neural fate. *Genes Dev* 8: 1434-47, 1994
- van der Aa, L. M., Levraud, J. P., Yahmi, M., Lauret, E., Briolat, V., Herbomel, P., Benmansour, A., and Boudinot, P.: A large new subset of TRIM genes highly diversified by duplication and positive selection in teleost fish. *BMC Biol* 7: 7, 2009
- van der Biezen, E. A. and Jones, J. D.: Plant disease-resistance proteins and the gene-for-gene concept. *Trends Biochem Sci* 23: 454-6, 1998a
- van der Biezen, E. A. and Jones, J. D. G.: The NB-ARC domain: a novel signalling motif shared by plant resistance gene products and regulators of cell death in animals. *Current Biology* 8: R226, 1998b
- van der Sar, A. M., Abdallah, A. M., Sparrius, M., Reinders, E., Vandenbroucke-Grauls, C. M., and Bitter, W.: *Mycobacterium marinum* strains can be divided into two distinct types based on genetic diversity and virulence. *Infect Immun* 72: 6306-12, 2004

- van der Sar, A. M., Musters, R. J., van Eeden, F. J., Appelmelk, B. J., Vandenbroucke-Grauls, C. M., and Bitter, W.: Zebrafish embryos as a model host for the real time analysis of Salmonella typhimurium infections. *Cell Microbiol* 5: 601-11, 2003
- van der Sar, A. M., Stockhammer, O. W., van der Laan, C., Spaink, H. P., Bitter, W., and Meijer, A. H.: MyD88 innate immune function in a zebrafish embryo infection model. *Infect Immun* 74: 2436-41, 2006
- van Heel, D. A., Ghosh, S., Butler, M., Hunt, K., Foxwell, B. M., Mengin-Lecreux, D., and Playford, R. J.: Synergistic enhancement of Toll-like receptor responses by NOD1 activation. *Eur J Immunol* 35: 2471-6, 2005
- Venkataraman, T., Valdes, M., Elsby, R., Kakuta, S., Caceres, G., Saijo, S., Iwakura, Y., and Barber, G. N.: Loss of DExD/H Box RNA Helicase LGP2 Manifests Disparate Antiviral Responses. *J Immunol* 178: 6444-6455, 2007
- Viala, J., Chaput, C., Boneca, I. G., Cardona, A., Girardin, S. E., Moran, A. P., Athman, R., Memet, S., Huerre, M. R., Coyle, A. J., DiStefano, P. S., Sansonetti, P. J., Labigne, A., Bertin, J., Philpott, D. J., and Ferrero, R. L.: Nod1 responds to peptidoglycan delivered by the Helicobacter pylori cag pathogenicity island. *Nat Immunol* 5: 1166-74, 2004
- Volff, J. N.: Genome evolution and biodiversity in teleost fish. *Heredity* 94: 280-94, 2005
- Wajant, H., Muhlenbeck, F., and Scheurich, P.: Identification of a TRAF (TNF receptor-associated factor) gene in Caenorhabditis elegans. *J Mol Evol* 47: 656-62, 1998
- Wang, Z., Zhang, S., Tong, Z., Li, L., and Wang, G.: Maternal Transfer and Protective Role of the Alternative Complement Components in Zebrafish *Danio rerio*. *PLoS ONE* 4: e4498, 2009
- Wang, Z., Zhang, S., Wang, G., and An, Y.: Complement Activity in the Egg Cytosol of Zebrafish *Danio rerio*: Evidence for the Defense Role of Maternal Complement Components. *PLoS ONE* 3: e1463, 2008
- Waterhouse, R. M., Kriventseva, E. V., Meister, S., Xi, Z., Alvarez, K. S., Bartholomay, L. C., Barillas-Mury, C., Bian, G., Blandin, S., Christensen, B. M., Dong, Y., Jiang, H., Kanost, M. R., Koutsos, A. C., Levashina, E. A., Li, J., Ligoxygakis, P., Maccallum, R. M., Mayhew, G. F., Mendes, A., Michel, K., Osta, M. A., Paskewitz, S., Shin, S. W., Vlachou, D., Wang, L., Wei, W., Zheng, L., Zou, Z., Severson, D. W., Raikhel, A. S., Kafatos, F. C., Dimopoulos, G., Zdobnov, E. M., and Christophides, G. K.: Evolutionary dynamics of immune-related genes and pathways in disease-vector mosquitoes. *Science* 316: 1738-43, 2007
- Wilkinson, R. N., Pouget, C., Gering, M., Russell, A. J., Davies, S. G., Kimelman, D., and Patient, R.: Hedgehog and Bmp polarize hematopoietic stem cell emergence in the zebrafish dorsal aorta. *Dev Cell* 16: 909-16, 2009
- Willett, C. E., Cortes, A., Zuasti, A., and Zapata, A. G.: Early hematopoiesis and developing lymphoid organs in the zebrafish. *Dev Dyn* 214: 323-36, 1999
- Willett, C. E., Zapata, A. G., Hopkins, N., and Steiner, L. A.: Expression of zebrafish rag genes during early development identifies the thymus. *Dev Biol* 182: 331-41, 1997
- Williams, J. A. and Holder, N.: Cell turnover in neuromasts of zebrafish larvae. *Hearing Research* 143: 171, 2000
- Willingham, S. B., Allen, I. C., Bergstralh, D. T., Brickey, W. J., Huang, M. T.-H., Taxman, D. J., Duncan, J. A., and Ting, J. P. Y.: NLRP3 (NALP3, Cryopyrin) Facilitates In Vivo Caspase-1 Activation, Necrosis, and HMGB1 Release via Inflammasome-Dependent and -Independent Pathways. *J Immunol* 183: 2008-2015, 2009

- Willingham, S. B., Bergstralh, D. T., O'Connor, W., Morrison, A. C., Taxman, D. J., Duncan, J. A., Barnoy, S., Venkatesan, M. M., Flavell, R. A., Deshmukh, M., Hoffman, H. M., and Ting, J. P.: Microbial pathogen-induced necrotic cell death mediated by the inflammasome components CIAS1/cryopyrin/NLRP3 and ASC. *Cell Host Microbe* 2: 147-59, 2007
- Woelk, C. H., Frost, S. D., Richman, D. D., Higley, P. E., and Kosakovsky Pond, S. L.: Evolution of the interferon alpha gene family in eutherian mammals. *Gene* 397: 38-50, 2007
- Wolke, R. E.: Piscine macrophage aggregates: A review. *Annual Review of Fish Diseases* 2: 91, 1992
- Wright, E. K., Goodart, S. A., Growney, J. D., Hadinoto, V., Endrizzi, M. G., Long, E. M., Sadigh, K., Abney, A. L., Bernstein-Hanley, I., and Dietrich, W. F.: Naip5 affects host susceptibility to the intracellular pathogen *Legionella pneumophila*. *Curr Biol* 13: 27-36, 2003
- Xu, L.-G., Wang, Y.-Y., Han, K.-J., Li, L.-Y., Zhai, Z., and Shu, H.-B.: VISA Is an Adapter Protein Required for Virus-Triggered IFN- β Signaling. *Molecular Cell* 19: 727, 2005
- Xu, L. G., Li, L. Y., and Shu, H. B.: TRAF7 potentiates MEKK3-induced AP1 and CHOP activation and induces apoptosis. *J Biol Chem* 279: 17278-82, 2004
- Yamamoto, M., Sato, S., Hemmi, H., Hoshino, K., Kaisho, T., Sanjo, H., Takeuchi, O., Sugiyama, M., Okabe, M., Takeda, K., and Akira, S.: Role of adaptor TRIF in the MyD88-independent toll-like receptor signaling pathway. *Science* 301: 640-3, 2003a
- Yamamoto, M., Sato, S., Hemmi, H., Uematsu, S., Hoshino, K., Kaisho, T., Takeuchi, O., Takeda, K., and Akira, S.: TRAM is specifically involved in the Toll-like receptor 4-mediated MyD88-independent signaling pathway. *Nat Immunol* 4: 1144-50, 2003b
- Yarovinsky, F., Hieny, S., and Sher, A.: Recognition of *Toxoplasma gondii* by TLR11 prevents parasite-induced immunopathology. *J Immunol* 181: 8478-84, 2008
- Yarovinsky, F., Zhang, D., Andersen, J. F., Bannenberg, G. L., Serhan, C. N., Hayden, M. S., Hieny, S., Sutterwala, F. S., Flavell, R. A., Ghosh, S., and Sher, A.: TLR11 activation of dendritic cells by a protozoan profilin-like protein. *Science* 308: 1626-9, 2005
- Yoder, J. A., Litman, R. T., Mueller, M. G., Desai, S., Dobrinski, K. P., Montgomery, J. S., Buzzeo, M. P., Ota, T., Amemiya, C. T., Trede, N. S., Wei, S., Djeu, J. Y., Humphray, S., Jekosch, K., Hernandez Prada, J. A., Ostrov, D. A., and Litman, G. W.: Resolution of the novel immune-type receptor gene cluster in zebrafish. *Proc Natl Acad Sci U S A* 101: 15706-11, 2004
- Yoder, J. A., Mueller, M. G., Wei, S., Corliss, B. C., Prather, D. M., Willis, T., Litman, R. T., Djeu, J. Y., and Litman, G. W.: Immune-type receptor genes in zebrafish share genetic and functional properties with genes encoded by the mammalian leukocyte receptor cluster. *Proc Natl Acad Sci U S A* 98: 6771-6, 2001
- Yoder, J. A., Orcutt, T. M., Traver, D., and Litman, G. W.: Structural characteristics of zebrafish orthologs of adaptor molecules that associate with transmembrane immune receptors. *Gene* 401: 154-64, 2007
- Yoneyama, M., Kikuchi, M., Matsumoto, K., Imaizumi, T., Miyagishi, M., Taira, K., Foy, E., Loo, Y. M., Gale, M., Jr., Akira, S., Yonehara, S., Kato, A., and Fujita, T.: Shared and unique functions of the DExD/H-box helicases RIG-I, MDA5, and LGP2 in antiviral innate immunity. *J Immunol* 175: 2851-8, 2005
- Yoneyama, M., Kikuchi, M., Natsukawa, T., Shinobu, N., Imaizumi, T., Miyagishi, M., Taira, K., Akira, S., and Fujita, T.: The RNA helicase RIG-I has an essential function in double-stranded RNA-induced innate antiviral responses. *Nat Immunol* 5: 730-7, 2004

- Yu, X., Acehan, D., Ménétret, J.-F., Booth, C. R., Ludtke, S. J., Riedl, S. J., Shi, Y., Wang, X., and Akey, C. W.: A Structure of the Human Apoptosome at 12.8 Å Resolution Provides Insights into This Cell Death Platform. *Structure* 13: 1725, 2005
- Yu, X., Wang, L., Acehan, D., Wang, X., and Akey, C. W.: Three-dimensional structure of a double apoptosome formed by the Drosophila Apaf-1 related killer. *J Mol Biol* 355: 577-89, 2006
- Zamboni, D. S., Kobayashi, K. S., Kohlsdorf, T., Ogura, Y., Long, E. M., Vance, R. E., Kuida, K., Mariathasan, S., Dixit, V. M., Flavell, R. A., Dietrich, W. F., and Roy, C. R.: The Birc1e cytosolic pattern-recognition receptor contributes to the detection and control of Legionella pneumophila infection. *Nat Immunol* 7: 318-25, 2006
- Zapata, A.: Ultrastructural study of the teleost fish kidney. *Dev Comp Immunol* 3: 55-65, 1979
- Zapata, J. M., Matsuzawa, S., Godzik, A., Leo, E., Wasserman, S. A., and Reed, J. C.: The Drosophila tumor necrosis factor receptor-associated factor-1 (DTRAF1) interacts with Pelle and regulates NFkappaB activity. *J Biol Chem* 275: 12102-7, 2000
- Zarkadis, I. K., Mastellos, D., and Lambris, J. D.: Phylogenetic aspects of the complement system. *Dev Comp Immunol* 25: 745-62, 2001a
- Zarkadis, I. K., Sarrias, M. R., Sfyroera, G., Sunyer, J. O., and Lambris, J. D.: Cloning and structure of three rainbow trout C3 molecules: a plausible explanation for their functional diversity. *Dev Comp Immunol* 25: 11-24, 2001b
- Zhang, D. C., Shao, Y. Q., Huang, Y. Q., and Jiang, S. G.: Cloning, characterization and expression analysis of interleukin-10 from the zebrafish (Danio rerio). *J Biochem Mol Biol* 38: 571-6, 2005
- Zhang, G. and Ghosh, S.: Negative regulation of toll-like receptor-mediated signaling by Tollip. *J Biol Chem* 277: 7059-65, 2002
- Zhong, B., Yang, Y., Li, S., Wang, Y. Y., Li, Y., Diao, F., Lei, C., He, X., Zhang, L., Tien, P., and Shu, H. B.: The adaptor protein MITA links virus-sensing receptors to IRF3 transcription factor activation. *Immunity* 29: 538-50, 2008
- Zika, E., Fauquier, L., Vandel, L., and Ting, J. P.: Interplay among coactivator-associated arginine methyltransferase 1, CBP, and CIITA in IFN-gamma-inducible MHC-II gene expression. *Proc Natl Acad Sci U S A* 102: 16321-6, 2005
- Zika, E. and Ting, J. P.: Epigenetic control of MHC-II: interplay between CIITA and histone-modifying enzymes. *Curr Opin Immunol* 17: 58-64, 2005
- Zou, J., Carrington, A., Collet, B., Dijkstra, J. M., Yoshiura, Y., Bols, N., and Secombes, C.: Identification and bioactivities of IFN-gamma in rainbow trout *Oncorhynchus mykiss*: the first Th1-type cytokine characterized functionally in fish. *J Immunol* 175: 2484-94, 2005
- Zou, J., Clark, M. S., and Secombes, C. J.: Characterisation, expression and promoter analysis of an interleukin 10 homologue in the puffer fish, *Fugu rubripes*. *Immunogenetics* 55: 325-35, 2003
- Zou, J., Tafalla, C., Truckle, J., and Secombes, C. J.: Identification of a second group of type I IFNs in fish sheds light on IFN evolution in vertebrates. *J Immunol* 179: 3859-71, 2007
- Zou, J., Yoshiura, Y., Dijkstra, J. M., Sakai, M., Ototake, M., and Secombes, C.: Identification of an interferon gamma homologue in *Fugu*, *Takifugu rubripes*. *Fish Shellfish Immunol* 17: 403-9, 2004

8 Appendix

Sequencing of the *nwd1* gene

To determine the *nwd1* sequence, the 'primer walk' method was used along the predicted transcript sequence. The initial Genescan prediction started within exon 5 (Fig. 8.01). RT-PCRs on cDNA were performed using the following primer pairs: SP1 + ASP1, yielding in a fragment of 507bp; SP2 + ASP2, fragment size 866bp; SP3 + ASP1, fragment size 664bp; SP4 + ASP4, fragment size 820bp; SP5 + ASP5, fragment size 432bp; SP6 + ASP6, fragment size 511bp; SP6 + ASP8, fragment size 1124bp; SP8 + ASP8, fragment size 633bp; SP9 + ASP9, fragment size 667bp; SP10 + ASP10, fragment size 577bp; SP7 + ASP11, fragment size 1140bp; SP11 + ASP11, fragment size 833bp; SP12 + ASP12, fragment size 808bp; SP13 + ASP13, fragment size 468bp; SP14 + ASP14, fragment size 519bp. Additionally, a 5 kb RT-PCR product (Fig. 3.39) of the *nwd1* transcript was generated using SP13 and ASP12 oligos. This product was cloned into the pCRII-TOPO vector, subsequently sequenced and compared to those sequences derived from the 'primer walk'. By comparing the generated sequences an internal alternative intron was identified. Whereas sequences generated by the 'primer walk' led to the identification of the sequence of exon 17, this exon was disrupted in the 5 kb transcript and no RT-PCR product could be generated using the SP11 and ASP11 oligos. Analysis of the missing sequence by comparison to the entire sequence of exon 17 showed that splice sites are present at the beginning and end (AG-GT) of this sequence within exon 17. The open reading frame of the 5 kb transcript was not affected by the absence of parts of the sequence of exon 17, suggesting that an alternative internal intron was spliced out in this transcript. The complete sequence of the *nwd1* transcript is listed below with the sequence of the internal intron of exon 17 presented in grey font colour. The genomic structure of the *nwd1* gene and a schematic of the mRNA are presented in Fig 3.40 and Fig. 8.01.

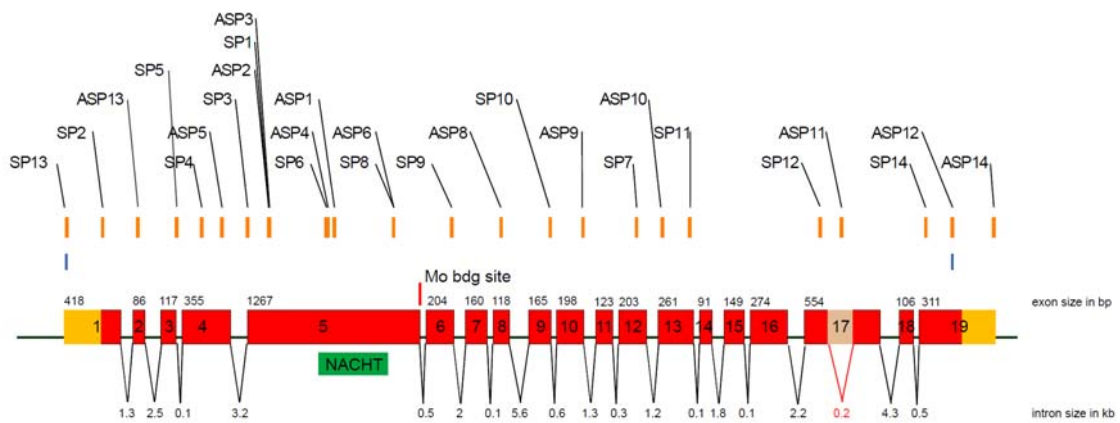


Fig. 8.01: Genomic organization of the *nwd1* gene.

Schematic of the genomic organization of the *nwd1* gene. The black horizontal line denotes the 33kb fragment of chromosome 11 containing the *nwd1* gene. The 19 exons are represented by red boxes. Above each box, the exon size is given in bp. The coding exons are labeled in red, the UTRs in orange. The intron size is given in kb. The splicable internal intron of exon 17 is shown in light red. The NACHT-domain encoding sequence is marked by a green box below exon 5. The morpholino-binding site at the exon 5 – intron 5 boundary is indicated by a vertical red line. Small blue vertical lines represent the start and end of the 5kb *nwd1* transcript. The position of the oligos used for amplification and sequencing of fragments are indicated by small orange vertical lines. The drawing is based on the sequencing results obtained.

>Dr *nwd1* cDNA

```

cgtaaacaccgggtctccctcggccttctgatctcagtgataaaatgacggcgctgaggagaacaacaaccgagc
tggagcgcctgcaacagagagctgtgtctttttgtataataggagacagctgaaaagctttaaacaattgtcaaattg
ctgatttacatttacttttaattataatttcatttctcaaaactagcagtgatgctcacagtgccaccgtagaactaccggatgt
cggtggttaataggactggaatattctggattaactgaggtgttggtcaggatggatgtggtggagatgagagaggcactt
gggttgagggttctgcggggacaaagcgctgatttctgcagcctactccagaatggtgcggggtgtcatcagctccactc
actcagacatgaaaaatgagagaaatgcatttctgggagaagacctattcggagctacagaccactgccaagttgg
gtctgtttttgaggtagtgattcaaatgtggaatgcgtgacatcactgcatctgatcatttaataactgaactgtgcattaa
gaaatcgaaacctgccagaggatatcagatgggccaactttatagctttgatcggtaatcagatggccatcgctgtcc
cgcgctcatalaccagaggcagagtttgagttgtgctatcaaaactttccaaagatccagagagtttaagctcctaacc
aatggttttacaaggacagtaactcaatcccaccacatatctcctgccaatcacgggtgactaccacattacaatg
agagagattctgagaacgcacagttgcgggataatgatgtcatatcctggaatctaacagagtcacggctgctgcaggtt
ctccgcagtcagctctacaggctgagagagacggggatttactgctgacagcaagcacaagttttcaaactgtttta
gaatatgagatggagcatggctttctcaggactcaaaggatgcatcggctgtgctgtttttccggaactgcctcgactta
gtaaaagagactgcaagaaaaactttgcaaagttctgctggacgtcacagccgacggcttctggacacacaagccc
gggagctcttgactgacctgaagcaacgcacatctgcaacaccggctgcctccaaccactctgtatggagctcagcaaagg
agccatggaccaagccgcaagaacacaaggaatacctgggtaagctgtgtgaacaggtaacatctcaattgaagg

```

aactgatcagcagaaatgctctgcaaacctcaggaactcagtagatccagtatggtcctggctaaaaacaggagatcttt
catcatgccaagttgagtgaggagaagtgtgctgtgtttaaagggagagacgacattctgggaaagatctccatcacct
gtgggaatccaatgatgtttctcatggacctcttagtccatggacctccaggagtggtaaacagctctgctttgcaaact
ggccaaggaaatgcgagcagttgtgacaatcggggagttgtctgctgaggttgctgggaacatctctgctcagttcagat
gtcgattctgttctcgagggtttgtctcaagtgtgtggagctctagggttgcagtcccatactcgcatatagcgtacacgc
atgaagggttagttcgattttccattccatgctggaagacgtgtcaaaacaaggagacactcttactcattctagactca
ttggagcagcttttagagacaaacaaactcataaactagactggatacctaaaaataattccaccaatgtgcaaatcgta
ttctcaacttcaatgagtgcttgacaaatgtaaatcttggttcagcggaaagaaaacatctttaaattggaacttctcacga
aagatcaaggagagacgctcattgatgcatatagtgagctgaacgcaagctgacggcagaacagcaagacgc
aatcttacgctactttgagcaaagtggaaacctttgcatctgaaactcatgctagacactgccaactgtggtcctctac
acccccatgtctagttcacctggacaagtcggcggagggaagtgatgacacagtttgcgagtcacttgaggatcat
gggaagaagctagtcagtcagctctgagcttcatcctgttatcaagatatggactttcagaggcagagttacaggatgccc
tatcattagataatgatgttctagctgagatctataatgctggcttctccgagccatacgtcatgcttcccacgtttcat
tggtcaagactcaggcatgacctgagtgctcatctgacggagagatgggaagccggcgttcttctgctgggttctactcac
aggcagtttcagaactggtaaggaggagatattgtcacgtgatgtgaaagctgacatgcacacgatcctcgccgagta
ttctccggacagtgagtaagggcagctcagacctccttctcccctcactgagcgcatttctcaatgctgacagaaa
ggtatcaccagccctgtggtttctgaagaactgccaattgctgaagattcatgaacttcttatcacctgctcacgca
ggaaaatgggacgagctacgacaatcagtgctgggagctggactggttgctgtaagactctgcagtggtgctgag
ctgtgttattcaggacctgacctttgactgacctcactgactgcctgagatacagttgctgaaggagacgttttcttct
aaacctcgctggattttagcgacggccgctggatccctcgctgttagtgacagagatcttggcaggctacagggcttctg
ctgatcattacccctccatgattggtcaactgtgttctcaatgatggactggttgaatcctattctgaccttactgtgcca
aatgcagctcttgaagccctggtggccactaaagagcacctcagaggattcactaaaggggtgaaggctgtgttc
tgtctcaaagaggaagctgctgttagcaggttcagaggatggactgatcatagctggagctaaacaatctgcagcctc
ttcacactcttctggacataaagccgggtgctgtccctgaagctgacggacaaaaccaataactgttctactgggct
cgatgggactctgagaaaatggtgtctgataagtggactgcagctttctgcatcactgatgccgttctgtccaaacacac
agccctacacacatccatatgaatgaagaaaggaagatcatcataaccaaccaagcagccaagttaaagcttggga
tttgactgacagagcctctgtttgagctgaccgagtgattggttctgttcttggcattgtggaagatgaaatagcgtgcat
atgcagtgaggcgatactctgctttatgacatatccaccggcactcagactcccagacctcctgacctactctgccgga
caccataacatcacctgctgtctcactcaccaaacactccaagatactcattgctttgggaaagccgtctacattcgg
tgtggagccatgaaatggagctgtgattgatcttccatctccagctctcttctcagaacatctgaggatgaaaaactgctg
cttgaggatgtgacagaacattgtgctgttctctgtgacattgactcaatgcacaaggttctggatctcaacatgatgc
atctatcctgtgcccgtgcaaacagcgaaggtagcgaatcatcacgagtgcccaggatcgataatacgggtatgg
agcgtlaaccacaggagccctgctggactggatcgggtgatggattcctctgtgtcctcattggctgtacatcagcgtttatt
atttccgctctgttattgtcaaccagcttaaagtatggcagcttgaccacaacaccacgcaggaacaagagtttcatc
cccgcatactgcccctggcagctctgtcgaagatggtgatactgtattctatgtcaaggagggaaataaaaccgaggtt
ttcacctggagctgttcggaaggctgcagttagacagcatggacgttccctcagagggtgctgtatggaattagcccagc
agaaacggctccttctgctgctgcacactggaaccttatttaccgcttgactttatcccagaaacctgtgctctac

cgctccggaaagcctaccaatggtacgcagcatggccatcagcccacgagaggacaaaatggccgtcgcatatga
ggatgccgtctgtctgtttgagattacagcgagggacagctcccttgcgtcgatggaccattgaaaggtactcgcttgacc
tgttacattcctcaatctccgcatggctttgttgcgactgcaggctgctgtatgggacgtttggcggcgaagtggatgata
cgactttaaagcgccacagcagcagagctggatcaccacggtgcagccataacctgcatcaccatgagcaactggg
atgcgcaggcactgattggctctcaggactgtgttcagaagctgtggaattgagtccttactgaatcacaccatgga
gtacaagggcttttatttgaaggagtctatgtgtgtcttcaataaatgataaacgtgttactggatccttgacaaa
accgtcaaagtctgggatgttcgagtggttctgtatataccagtagcttactctccggtcataaggatgatgccacac
aaggatggattttagctgtatccagcatggctcattcatcaaggaaggtttcgctgtccagacagcctcaagcctggat
ataaccccctccggaactccaagtacattacaaagtcacttcacgagacaaaagtctgaacgttccacacagcgtgatc
aatgagctgccagattacaaccctgctcagttcaactcattggcatcggctctgatcaaatccaaccatccaatacgtgc
gttctccttaagtacattctacatcgcaaacctttataactaggcccacactattctgcgtgagattactaaagctgct
cccaaattgcatacttatgactattctacgccattttgtagtataaatagtttaagtagtggttcacattggaaactctaaaa
taataagtgactttaattaccgggatgatgcactcattcagccgctaaaacgaagtgtgtgtgattgacactcacacact
caacgaccg

Danke

Mein ganz besonderer Dank gilt Maria Leptin für die Möglichkeit, meine Doktorarbeit in ihrer Arbeitsgruppe unter einer hervorragenden Betreuung durchführen zu können. Für die ständige Diskussions- und Hilfsbereitschaft und für alles, was ich in den letzten Jahren von ihr lernen konnte.

Weiterhin möchte ich Herrn Prof. Dr. Siegfried Roth und Herrn Prof. Dr. Matthias Hammerschmidt für die Begutachtung der Dissertation bzw. die Übernahme des Prüfungsvorsitzes danken.

Ein weiteres Dankeschön geht an Astrid van der Sar für die Bakterien, Georges Lutfalla für Morpholinos und an die Mitarbeiter des ehemaligen Campos-Ortega Labors für die Aufnahme in ihren Fischräumen und der Erstausrüstung mit Zebrafischen.

Ein ganz herzlicher Dank geht an Dirk, Jule, David und Sanjita, weil ihr mir immer mit Rat und Tat zur Seite gestanden habt und mir mit Euch nicht nur die Fischerarbeit sehr viel Freude bereitet hat und natürlich auch an Lisa, Juliane, Inge, Kevin, Martina, Fiona, Gritt, Heidi, Hannelore, Katarina, Jayan, und Renjith und alle anderen Kollegen für ein unvergleichliches Arbeitsklima, Freundschaft, Hilfe, Diskussion und Parties.

Mein letzter und wichtigster Dank geht an Harry für einfach alles, was wir zusammen erleben dürfen. Und an meine Mutter und meine Geschwister für Rückhalt und Unterstützung in allen Lagen.

Erklärung

Ich versichere, dass ich die von mir vorgelegte Dissertation selbstständig angefertigt, die benutzten Quellen und Hilfsmittel vollständig angegeben und die Stellen der Arbeit - einschließlich Tabellen, Karten und Abbildungen -, die anderen Werken im Wortlaut oder dem Sinn nach entnommen sind, in jedem Einzelfall als Entlehnung kenntlich gemacht habe; dass diese Dissertation noch keiner anderen Fakultät oder Universität zur Prüfung vorgelegen hat; dass sie - abgesehen von unten angeführten Teilpublikationen - noch nicht veröffentlicht worden ist sowie, dass ich eine solche Veröffentlichung vor Abschluss des Promotionsverfahrens nicht vornehmen werde.

Die Bestimmungen dieser Promotionsordnung sind mir bekannt. Die von mir vorgelegte Dissertation ist von Prof. Dr. Maria Leptin betreut worden.

Köln, den 17.12.2009

Teilpublikationen

Stein, C., Caccamo, M., Laird, G., and Leptin, M : Conservation and divergence of gene families encoding components of innate immune response systems in zebrafish. *Genome Biol* 8:R251, 2007

Sieger, D., Stein, C., Neifer, D., van der Sar, A.M., and Leptin, M.: The role of gamma interferon in innate immunity in the zebrafish embryo. *Dis Model Mech* 2: 571-81, 2009

Lebenslauf

Persönliche Angaben:

Name: Stein
Vornamen: Cornelia
Geburtsdatum / -ort: 08.02. 1977 in Köln
Anschrift: Bachemer Str. 241, 50935 Köln
Familienstand: ledig
Staatsangehörigkeit: Deutsch

Schulbildung:

1983-1987 Besuch der Gemeinschaftsgrundschule Spoerkelhof, Köln

1987-1996 Besuch des städt. Dreikönigsgymnasiums Köln
Abschluss: allgemeine Hochschulreife

Hochschulbildung:

01.10. 1996 – 11.05. 2005 Studium der Biologie an der Universität zu Köln
Diplomarbeit am Institut für Genetik, Universität zu Köln.
Thema: „Untersuchung genetischer Komponenten in Zebrafischen, die an einer Anfälligkeit für oder Resistenz gegen eine Infektion mit *Mycobacterium marinum* beteiligt sind“.
Abschluss: Diplom Biologin

Doktorarbeit

seit 12. 5. 2005 Doktorarbeit in Genetik an der Mathematisch-Naturwissenschaftlichen Fakultät der Universität zu Köln, durchgeführt bei Prof. Dr. M. Leptin, Institut für Genetik, Köln